SOLID STATE FERMENTATION OF SWITCHGRASS MIXTURES: EXPERIMENTATION, MODELING AND ANALYSIS

A Dissertation

Presented to the Faculty of the Graduate School

of Cornell University

In Partial Fulfillment of the Requirements for the Degree of

Doctor of Philosophy

by

Linelle T Fontenelle

January 2011

SOLID STATE FERMENTATION OF SWITCHGRASS MIXTURES: EXPERIMENTATION, MODELING AND ANALYSIS

Linelle T Fontenelle

Cornell University 2011

In this study, the aerobic microbial degradation of switchgrass mixtures was characterized based on biological, physical and chemical parameters both experimentally and via mathematical modeling. Highly-instrumented 50L reactors were designed to facilitate better process control, online measurements and robust sampling for high temporal and spatial resolution. Switchgrass was amended with dog food and nitrogen fertilizer in C/N ratios of 15 and 18, respectively with initial moisture contents of 60 to 75% and biodegraded for 64 to 96h. Temperature and effluent gas concentrations were monitored online during the process and collected samples were analyzed for pH, moisture content, organic acid concentration, substrate composition and microbial community dynamics. A rapid technique for the extraction and purification of DNA from compost samples was developed and optimized. Real time PCR and probe hybridization procedures were also optimized for monitoring microbial community dynamics. Probe hybridization was used to monitor changes in the bacteria, fungi and yeast populations; the data from which was used to derive empirical parameters for process modeling, and real time PCR was used to measure changes in the gene copy numbers of bacteria, fungi, lactic acid bacteria and *Aspergillus spp*. Reactors were run in triplicate to test for process reproducibility.

The results revealed that the reactors reproduced results well and that profiles obtained from different runs were similar to each other and to other generally accepted profiles. Of three moisture contents: 60, 65 and 75%, the highest level of activity was seen in the 75% reactor, suggesting that this system may have been

operating near optimal moisture levels. Reactor height had a significant impact on the temperature and moisture content profiles and the bacterial population was found to be the driving force for carbon degradation in the process. Modeling the process using empirically derived microbial growth kinetics, substrate degradation kinetics and traditional heat and mass transfer equations resulted in model predictions that were in good agreement with the experimental data. It was also determined that using nitrogen fertilizer increased the initial rate of substrate degradation and after 96h, an average of18% of lignin, 24% of cellulose and 26% of hemicellulose had degraded.

BIOGRAPHICAL SKETCH

Linelle Fontenelle was born and raised in the small community of Grace on the island of St. Lucia. After graduating from high school at the St. Joseph's Convent, she completed her A'Levels in St. Lucia. She came to the United States by way of Florida in 2000 to pursue a higher education. She completed her Associate's degree at the Central Florida Community College and then moved to New York City to complete her Bachelor of Engineering degree at the City College of New York. In 2005, she moved further north to Ithaca where she entered the Ph.D. program in chemical engineering. During her tenure at Cornell, Linelle has served as a graduate resident fellow in Carl Becker House, class representative and co-chair of the women's group in the chemical engineering department, and president of the Engineering Graduate Student Association. Linelle currently resides with her amazing husband, Niki in southern California.

To my parents: Jacinta & Felix Fontenelle

ACKNOWLEDGMENTS

I would like to first of all thank God for bringing me to this point in my life and for providing me with the guidance that I need. My husband Niki, my parents and the rest of my family also need to be thanked for their continued support and their unwavering belief in me. I am deeply appreciative of my advisor Larry Walker for taking me under his wing and nurturing me in my growth and development as a researcher. I also owe gratitude to the other members of my committee, Mike Shuler and Anthony Hay for their insights and their willingness to share their knowledge with me. Stephane Corgie also needs to be thanked for guiding me through the molecular biology aspects of this project and for being supportive. In need of great recognition is Doug Cavney who taught me how to use the tools in the machine shop and who willingly provided me with any other support that I needed. Sue Fredenburg always had the answers or knew how to get them and to her I am very thankful for making my tenure in Riley Robb Hall much easier. I would also like to thank the other members of the Walker Lab for their support and encouragement and the New York State Foundation for Science, Technology and Innovation (NYSTAR) for providing funding for my work. In addition to the people who helped me develop educationally at Cornell, there are a number of others who helped in my greater development as a person at Cornell. These include the staff at Carl Becker House, the staff of the diversity programs in engineering office and the many wonderful friends I have made here. I could not have done this alone and so to everyone who helped and supported me in ways big and small, I say a very heartfelt THANK YOU and may God bless you.

TABLE OF CONTENTS

LIST OF FIGURES

LIST OF TABLES

CHAPTER 1

INTRODUCTION

1.1 Background

Solid state fermentation (SSF) may be defined as the growth of microorganisms on a moistened substrate in the absence of free flowing water (Mitchell et al., 2000). SSF has been used for thousands of years in the production of food products such as soy sauce and holds many advantages over traditional submerged fermentation, including cheaper production, higher product yields and lower energy requirements (Holker & Lenz, 2005). SSF may be broadly divided into two categories: that which involves the production of value added products such as enzymes and food and that which involves the control of environmental processes such as bioremediation and composting. Composting was chosen as the focus of this study because it is an exemplary SSF process.

Composting is useful for the reduction of municipal solid wastes and for the destruction of potentially hazardous pathogenic organisms. In the United States where there is a growing research in the sustainable production of cellulosic biofuel, the proper disposal of cellulosic wastes is an essential step. Composting of the agricultural wastes produces a biologically stable humic substance that may be used as a soil additive, thereby efficiently reducing the amount of waste generated. In composting, microbial activity and growth lead to the degradation of organic material. This degradation occurs via the formation of complex microbial communities that work in a delicate balance to drive physical and chemical changes in the compost pile.

As the microbes grow on the moistened solid substrate, their demand for oxygen and other nutrients changes, producing concentration gradients that contribute to overall mass transfer in the system. In addition, heat, which is a byproduct of the

process is generated and must be properly managed for the best process efficiency. This leads to heat transfer aspects within the system which must be properly controlled. These engineering aspects greatly hinder the reproducibility, scale-up and standardization of composting processes.

Despite understanding the physical processes which occur in the process, the underlying microbial mechanisms that drive these changes are poorly understood and inadequately characterized. Advances in molecular biology methods such as real-time PCR and probe hybridizations methods provide the tools necessary for monitoring the dynamics of microbial communities. Statistical tools then provide a method for correlating these observations to changes in physical and chemical variables; but this relation of abiotic to biotic phenomena remains challenging in composting processes. For better process understanding, control and prediction, these challenges must be overcome and therefore drive the goals of this research for better process characterization via both experimentation and modeling.

1.2 Research Objectives

1.2.1 Objective 1

Design, instrument and operate 50L working volume reactors

From an engineering perspective, reactor design is a critical element of process control and so the objective of this design process was to minimize the number of parameters that were variable during the process. For this reason, highly-instrumented reactors need to be designed to contain the substrate bed. This design style facilitates the regulation of a number of factors during the process.

One of the first considerations in reactor design is the type of material that will be used to construct the reactors. This is critical in self-heating processes such as composting, because the temperatures may reach 70^{o}C (Cooperband, 2002) and the

reactor walls must be able to withstand such high temperatures. In addition to the walls of the reactor providing containment, a plate is also needed in vertical, packed bed reactors for the substrate bed to sit on. Also, the interior of the reactors also need to be fitted with instruments for measurements for online tracking of temperature and oxygen concentration because these are indications of the progress of the composting process.

External to the reactor, but a major factor in the set up is the regulation of air into the reactors. The rate at which air enters the reactor is important because very high flow rates can lead to substantial drying of the substrate bed whereas flow rates that are too low may result in insufficient oxygen being supplied to growing microorganisms (Raghavarao et al., 2003). Even when optimal aeration rates are used, drying of the substrate bed may occur over time and saturating the air with water before it enters the reactor is an important design factor that minimizes the amount of drying that occurs (VanderGheynst, 1994). In addition, the used of forced aeration reduces mass transfer gradients and helps in the removal of gaseous products formed during decomposition, so this factor is also incorporated into the reactor design (VanderGheynst, 1994). Also, the inclusion of flow meters to regulate a continuous flow of air, leads to better process efficiency (Gervais & Molin, 2003).

Reactor insulation is another important design aspect because it minimizes heat losses to the environment. It also reduces radial gradients in the reactors. In composting, this is particularly important because the heat generated by microbial activity is part of a feedback loop that selects for microorganisms based on the temperature of the system. Thus considerations for insulation design must be made in the process.

Of significant importance is the design of sampling ports in the reactor when samples will be collected during the process because sampling often alters the

structure of the substrate bed. For this reason, minimization of bed disturbance during sampling is an important design consideration.

1.2.2 Objective 2

Characterize and correlate the spatial and temporal dynamics of abiotic and biotic phenomena during the initial stages of biodegradation

The most dramatic changes in physical variables in the composting process occur in the initial stages, so this period represents an ideal environment for gaining more insight into the dynamics of the process. During this time period, rapid increases in temperature and pH are commensurate with rapid decreases in the oxygen concentration. These observations lead to the hypothesis that changes in the underlying microbial communities that drive the process must be equally dramatic.

Advances in molecular biology tools have provided tools that may be used to track succession in the microbial community both quantitatively and qualitatively. From an engineering point of view, quantitative data is more useful because it may be subjected to further mathematical and statistical analyses. Probe hybridization is one of the few techniques that allows for quantitative data to be obtained.

The goal of this study was to monitor changes in the abiotic and biotic phenomena during the initial stages of composting and relate changes in the different variables to each other. A secondary goal was to determine the impact of initial moisture content by varying the amount of water added to the substrates. Another secondary goal was to determine how reactor height affected the changes seen in the variables. The hypothesis of this study was that changes in abiotic variables would be highly correlated with changes in the biotic variable. The first objective of this study was to track changes in the temperature, pH, moisture content, carbon dioxide concentration, oxygen concentration and microbial populations at specific time and

height increments during the process. Tracking the microbial populations led to the second objective, which was to optimize a protocol for the extraction of DNA from compost samples. This is because the isolation of DNA from compost samples is complicated by the presence of humic acids which co-extract with DNA. Another objective was to optimize the detection of and quantify the presence of bacteria, yeast and fungal populations by using probe hybridization. The final objective was to correlate changes in microbial population dynamics to the observed abiotic data.

1.2.3 Objective 3

Integrate empirical data to develop a mathematical model to simulate reactor profiles

Mathematical modeling is a useful tool for optimizing reactor performance and design and provides some insight into the underlying forces that drive energy transfer in the system. Composting models have appeared in the literature since 1976 (Mason, 2006) and have varied drastically in the amount of information that is incorporated in the model. This is because of the large number of parameters and the complexity of the process. Most of the variation has centered on microbial growth and activity since this is the major driving force for energy transfer. Approaches for describing the effect of microbial growth have varied from using microbial indicators such as oxygen uptake rate, carbon dioxide evolution rate or substrate decomposition rate to empirical equations to mechanistic equations that describe microbial growth from a theoretical perspective.

The goal of this study was to integrate microbial growth kinetics and substrate degradation kinetics into traditional heat and mass transfer equations in order to simulate experimental findings in temperature and oxygen profiles. The hypothesis was that integrating empirically derived microbial growth kinetics into energy transfer

equations would produce profiles that were in very good agreement with experimental data. The first objective was to develop a set of equations describing microbial growth kinetics. This required the use of parameter estimations based on experimental data. Thus microbial growth equations were developed with empirically derived growth parameters. The next objective was to develop a set of equations describing substrate degradation kinetics based on the labile and recalcitrant parts of the substrate and the ability of various microbial populations to metabolize those substrate components. The final objective was to numerically solve a system of nonlinear equations that included microbial growth kinetics, substrate degradation kinetics, heat transfer and mass transfer.

1.2.4 Objective 4

Assess the impact of a using nitrogen fertilizer as the nitrogen source on compost process dynamics in the early stages

Nitrogen content is a key component in composting systems because it gives an indication of the nutrients available for microbial growth. On its own, switchgrass does not contain enough nitrogen to facilitate noticeable degradation within 96h, so a nitrogen source is necessary to accelerate the process which was critical for the time period of interest. Nitrogen fertilizer represents a good alternative to the dog food used in Objective 2 because its carbon content is much lower than that found in the dog food. This is important because it gives a better indication of microbial growth on switchgrass since the microorganisms will be metabolizing the carbon from switchgrass for growth.

The goal of this study was to increase the rate of substrate degradation in the early stages of composting by using a nitrogen fertilizer as the nitrogen source and to track succession in the microbial community using real time PCR. Another goal was

to investigate acidity in the early stages of composting and to track changes in the substrate components of cellulose, hemicelluloses and lignin. The hypothesis for this study was that there would be rapid degradation within the first 96h and that changes in the organic acid concentrations would be commensurate with changes in the microbial populations. The first objective was to develop and optimize a real time PCR protocol for the quantification of 16S rRNA genes of general bacteria and lactic acid bacteria and the 18S rRNA genes of general fungi and Aspergillus spp. The next objective was to optimize a protocol for the detection of volatile fatty acids using gas chromatography and the final objective was to assess the extent of substrate degradation and relate that to changes in the microbial community and other physical variables.

The aforementioned objectives are presented in more detail in Chapters 3, 4 and 5 of this dissertation as part of three major studies: (i) experimentation and analysis of the degradation of switchgrass amended with dog food, (ii) modeling of the degradation process when switchgrass and dog food are the substrates and (iii) experimentation and analysis of the decomposition of switchgrass amended with a nitrogen fertilizer.

REFERENCES

Cooperband, L. 2002. The Art and Science of Composting - A Resource for Farmers and Compost Producers. University of Wisconsin - Madison.

Gervais, P., Molin, P. 2003. The role of water in solid-state fermentation. *Biochemical Engineering Journal*, **13**(2-3), 85-101.

Holker, U., Lenz, J. 2005. Solid-state fermentation - are there any biotechnological advantages? *Current Opinion in Microbiology*, **8**(3), 301-306.

Mason, I.G. 2006. Mathematical modelling of the composting process: A review. *Waste Management*, **26**(1), 3-21.

Mitchell, D., Berovic, M., Kriegerm, N. 2000. Biochemical Engineering Aspects of Solid State Bioprocessing. *Advances in Biochemical Engineering/Biotechnology*, **68**.

Raghavarao, K.S.M.S., Ranganathan, T.V., Karanth, N.G. 2003. Some engineering aspects of solid-state fermentation. *Biochemical Engineering Journal*, **13**(2-3), 127-135.

VanderGheynst, J.S. 1994. Design and Process Ananlysis of a High-Solids Aerated Static Bed. in: *Biological and Environmental Engineering*, Vol. Masters of Science, Cornell University. Ithaca, pp. 167.

CHAPTER 2

LITERATURE REVIEW

2.1 Solid state fermentation

2.1.1 Definition and uses

The growth of microorganisms on a moistened solid substrate in the absence of free flowing water describes the technological process known as solid state fermentation (SSF). It is an old and familiar technology that dates back to the year 1000 BC when it was used to produce soy sauce (Cannel & Mooyoung, 1980) and since then, SSF has evolved as a reputable method for a broad range of applications particularly in Asian countries(Holker & Lenz, 2005). SSF is characterized by moisture contents in the range of 40% to 80% (Shuler & Kargi, 2002), with the water being held within the substrate particles where it supports microbial growth.

Design and operating SSF systems is challenging given the high coupling of physical state variables; such as, temperature, moisture content, and the complex biochemical activities associated with the microbial ecology of the organic matrix. Thus, SSF technology faces many engineering challenges including heat and mass transfer limitations, reproducibility and standardization. These challenges must be overcome before SSF may be viewed as a leading technology in the western world (Holker & Lenz, 2005).

SSF has been used in numerous applications; such as, the production of enzymes, bio-control agents, organic acids, antibiotics, biopesticides, biofuels and a broad range of food products (Mitchell et al., 2000; Pryor, 2005). SSF is also being used for the development of bioprocesses such as biopulping, bioremediation and biodegradation of hazardous compounds (Pandey et al., 2000). Furthermore, highly

aerated SSF processes are employed around the world today in the composting of organic wastes to yield stabilized soil amendments. More broadly speaking, the areas of application of SSF may be divided into two categories (Raghavarao et al., 2003). The first category deals with applications that are value added such as the production of enzymes, fermented foods, biopesticides, organic acids, antibiotics and pigments. The other category deals with applications for environmental control such as composting, bioremediation and biodegradation. This literature review will provide general information about SSF but will mainly focus on the environmental control application of composting.

2.1.2 Advantages over submerged fermentations

In the Western world, submerged liquid fermentations have surpassed the use of SSF as a viable technology; in part, because of the lack of reproducibility of results (Holker & Lenz, 2005). Submerged fermentations are easier to control and thus result in a standardization of products fermented under very controlled conditions. Poor process control (temperature, pH, oxygen concentration) and longer process times characterize SSF reactors due to the heterogeneity of the substrate and the reaction environment (Cen & Xia, 1999). Furthermore, this leads to major difficulties in reactor scale up.

Despite the challenges associated with SSF, this technology offers several advantages over submerged fermentation. For example, the estimated cost of production of cellulases via SSF is US \$0.20 kg^{-1}, whereas the cost rises to US\$20 kg^{-1} when using submerged fermentations (Holker et al., 2004). In another study, tannase enzyme activity, using *A. niger* Aa-20 as the microorganism, increased from 2,500 IU L^{-1} in submerged fermentation to 12,000 IU L^{-1} in SSF (Holker et al., 2004). More specifically, the advantages of SSF over submerged fermentations include:

(a) Lower capital investments and operating costs as a result of the simplicity of the required equipment with regard to design and spatial requirements (Cen & Xia, 1999).

(b) Higher product yields per unit reactor volume (Cen & Xia, 1999). In the case of exo-pectinase, its production was found to be 50 times higher in SSF when compared to submerged fermentation, using *A.niger* CH4 as the microorganism (Holker et al., 2004).

(c) Lower risk of contamination from bacteria and yeast due to the low moisture content (Perez-Guerra et al., 2003). It has been found that the degradation of enzymes by contaminating proteases is 8 times higher in submerged fermentation than in SSF (Holker et al., 2004).

(d) Lower energy demands because of the lower requirements for aeration, water and mechanical agitation (Cen & Xia, 1999)

(e) Required carbon sources are less expensive and more abundant - agricultural residues are often used as raw materials (Cen & Xia, 1999).

(f) Production of enzymes that are more stable at higher temperature and extreme pH (Viniegra-Gonzalez et al., 2003)

(g) The use of mixed cultures to take advantage of synergistic effects during growth (Holker et al., 2004)

2.2 Composting – An exemplary SSF process

Composting may be defined as the aerobic microbial biodegradation of organic matter. This degradation occurs as a result of the activity of a community of bacteria, actinomycetes and fungi present in the system. Composting is used to reduce the volume of many municipal solid wastes that are biodegradeable, while ridding them of

plant and human pathogens. Agricultural and animal residues are also composted to reduce their volume and biologically convert them to more usable materials. The end result of a composting process is a stable, usable product that is free of pathogens and plant seeds (Haug, 1993).

In forested areas, this process takes place naturally when leaves, trees and possibly animal remains pile up on the forest floor. Eventually this pile of organic material is decomposed via microbial activity and returns to the soil as a source of nutrients. In nature, this process may take several years and maybe even decades, so composting is often done in controlled environments to speed up the process. Similar to what occurs in nature, in controlled aerobic composting systems, air is employed in the degradation of organic substrates to produce a stable humic substance while giving off carbon dioxide, water and heat:

$$\text{Organic waste} + \text{Oxygen} \xrightarrow[\text{activity}]{\text{microbial}} \text{Stable humic substance} + \text{Carbon dioxide} + \text{Water} + \text{Heat}$$

Anaerobic composting processes can be carried out and this is accomplished in the absence of oxygen yielding methane, carbon dioxide, organic acids and alcohols (Haug, 1993). The nature of these products increases the ejection of strong odors – a problem that is minimized in aerobic composting; for this reason, most composting processes are carried out under aerobic conditions. The extent of degradation and the rate at which it occurs is dependent on the type of substrate used and the process conditions under which composting is carried out.

2.2.1 Progression of a typical composting process

A temperature-dependent generalized model of the composting process is shown in Figure 2.1 and shows that the process occurs in three different phases. The

first stage is the mesophilic phase. At this stage, temperatures are moderate in the range of 10^{o}C to 45^{o}C (50^{o}F to 113^{o}F) (Cooperband, 2002) and mesophilic organisms commence the composting process by breaking down readily soluble and degradable components. These mesophilic organisms include yeasts, mesophilic fungi, lactic acid bacteria and Gram-negative bacteria (Steger et al., 2005). During this phase, there is also typically a drop in pH due to the formation of volatile fatty acids, particularly lactic and acetic acids (Sundberg & Jonsson, 2008). The next stage, termed the thermophilic phase or the active phase is characterized by elevated temperatures in the range of 54^{o}C to 66^{o}C (130^{o}F to 150^{o}F) (Cooperband, 2002) and possibly higher temperatures. In this active phase, thermophiles break down more complex compounds such as proteins, fats, cellulose and hemicellulose and in the process, kill off pathogens. This phase is typically marked by the presence of *Bacillus spp*. and *Thermus thermophilus* and basic pH conditions. The final stage of composting, known as the curing phase, undergoes a two-part process where first, the temperature cools back down to mesophilic conditions and then the compost enters the maturation phase where organic substrates continue to degrade and are converted into biologically stable humic substances (Cooperband, 2002). A new mesophilic microbial community replaces the thermophiles and complex substrates such as lignin are degraded (Steger et al., 2005).

The amount of time taken for each phase is dependent on the size and conditions of the compost pile. Some compost piles may go through all 3 phases within several hours while others may take up to several months to get to the maturation phase.

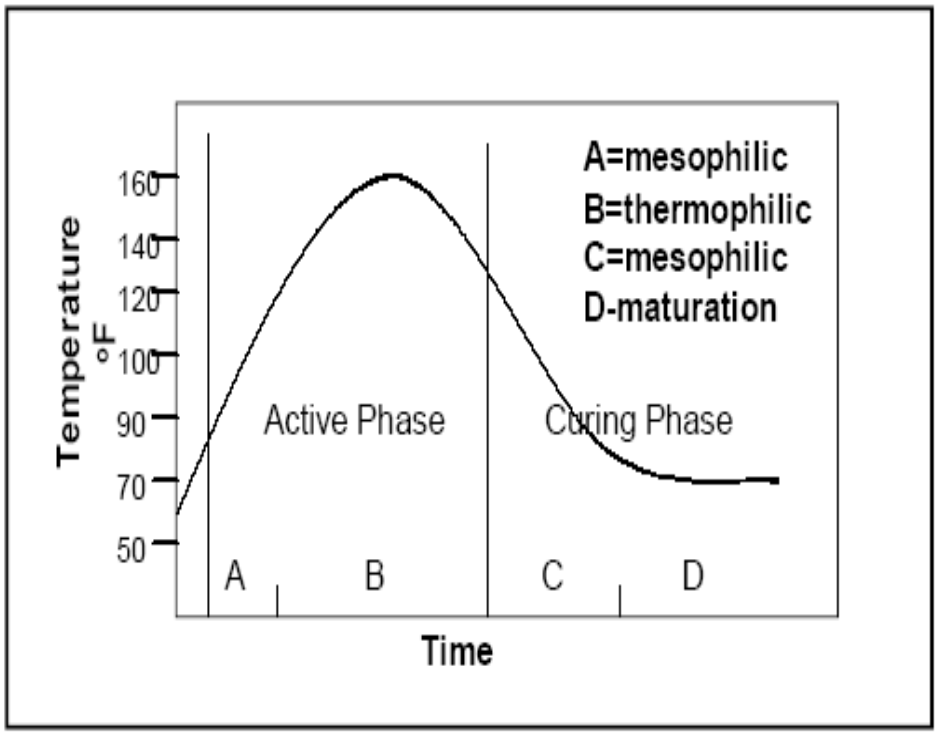

Figure 2.1 The phases of composting

2.3 Compost Microbial Community

The process of composting is driven by the microbial activity of organisms that lead to the degradation of the substrate. The shift in environmental conditions in compost piles from mesophilic to thermophilic also represents a shift in the microbial community structure from mesophilic to thermophilic organisms. The main organisms responsible for composting are bacteria and fungi, while all other microbes play minor roles in the decomposition process (Haug, 1993).

2.3.1 Bacteria

Bacteria dominate most compost piles throughout all the phases of composting. As the smallest known free-living organisms, they account for 80 - 90% of the microorganisms typically found in a gram of compost, and are responsible for the majority of the heat generation and degradation during the process (Trautmann & Olynciw, 2002). The domain, bacteria, encompasses a large number of prokaryotic microorganisms which come in different shapes and sizes and at different points during the composting process (Madigan et al., 2002). Mesophilic bacteria predominate during the first and last stages of composting, while thermophilic bacteria dominate during the active phase where the pathogenic prokaryotes are killed. A number of studies have been done to track the temporal population dynamics of bacteria in compost systems (Blanc et al., 1999; Dees & Ghiorse, 2001; Ishii et al., 2000; Pedro et al., 2001; Pedro et al., 2003; Schloss et al., 2005; Schloss et al., 2003; Strom, 1985a; Strom, 1985b). Notable bacteria within the compost pile include actinomycetes, which are filamentous bacteria responsible for degrading complex compounds like cellulose, lignin, chitin and proteins (Trautmann & Olynciw, 2002). Also notable is the *Bacillus* genera which dominates during the thermophilic phase

(Hatsu et al., 2002). In this group of microorganisms, *Bacillus subtilis* has been studied (Pryor, 2005) for use in numerous applications.

One of the first studies completed to quantify bacterial population dynamics in compost did so via the use of 16S rRNA probes (Schloss et al., 2005). This study built upon previous work (Schloss et al., 2003) that qualitatively profiled changes in the bacterial community using genetic fingerprinting (Schloss et al., 2005). For this investigation, the researchers designed small sub-unit rRNA probes to quantify the relative abundance of bacterial populations and found a trend in the bacterial population, which, for the most part, tracked the temperature profile. The researchers also found a shift in the dominant species, with Pseudomonas-type genes being most prevalent up to 72 hours and then domination by low G+C Gram-positive bacteria by 84 hours. This shift in population complemented changes observed for the temperature and carbon dioxide production profiles. The information gained from this study is extremely relevant to compost microbial community studies because it gives significant credence to the important role that bacteria play in composting processes and it also gives an indication of what groups have a major presence. Moreover, this assessment was accomplished through probe hybridization – one of the few methods that give quantitative data about the make-up of the community. Due to the highly sensitive nature of rRNA, working with it could prove difficult, and the researchers may have lost quite a bit of information while carrying out their protocol. The quantification of bacterial population dynamics could have been completed with rDNA probes that are less sensitive to work with. Although many of the genes in this study were unidentified, the study sets the stage for the need to explore the role of other microorganisms, such as fungi, in the composting process.

2.3.2 Fungi

Fungi work with bacteria to degrade organic material during composting. This group of microorganisms is highly adaptable and can grow under a vast variety of conditions, thereby facilitating their presence during all phases of composting. Fungi are ubiquitous in nature and have low moisture and nitrogen requirements (Haug, 1993); thus, making them ideal organisms for cellulosic compost piles, which tend to be low in nitrogen. Fungi are broadly classified as molds (aerobic) and yeasts (both aerobic and anaerobic) and can withstand a broad range of pH conditions (Haug, 1993). During composting, fungi facilitate substrate degradation by bacteria, by breaking down tough debris such as plant polymers (Trautmann & Olynciw, 2002).

The mode of growth of filamentous fungi (molds) puts them at a distinct advantage in competitive-nutrient environments (Madigan et al., 2002). The filaments (*hyphae*) grow by extending at the tip and by branching out (Madigan et al., 2002). In so doing, the tips are able to extend to areas that are more nutrient rich; thus, enabling filamentous fungi the ability to colonize solid substrates better than unicellular organisms (Raimbault, 1998). In addition, the rate at which branching occurs produces an exponential kinetic growth pattern of biomass (Raimbault, 1998). This is because the growth pattern allows the hyphal tips to excrete concentrated hydrolytic enzymes at the solid surface that break through the solid substrate, providing the fungi with access to nutrients available within the substrate particles (Raimbault, 1998). Fungi may be divided into five phylogenetically similar groups (Table 2.1) but most of these fungi feed off of dead organic material and are known as saprophytic fungi. Saprophytic fungi possess the ability to degrade complex polymers such as hemicelluloses, lignin, cellulose and protein via the secretion of enzymes. Of the classified groups, basidiomycetes are best known for the decomposition of

Table 2.1 Fungi Classifications (Madigan et al., 2002)

Group	Common Name	Hyphae	Typical Representatives	Habitats
Ascomycetes	Sac fungi	Septate	*Neurospora, Saccharomyces, Morchella*	Soil, decaying plant material
Basidiomycetes	Club fungi, mushrooms	septate	*Amanita, Qgaricus*	Soil, decaying plant material
Deuteromycetes	Fungi imperfecti	Septate	*Penicillium, Aspergillus, Candida*	Soil, decaying plant material, surfaces of animal bodies
Oomycetes	Water molds	Coenocytic	*Allomyces*	Aquatic
Zygomycetes	Bread molds	Coenocytic	*Mucor, Rhizopus*	Soil, decaying plant material

lignocellulosic substrates, with brown rot fungi metabolizing cellulose and white rot fungi utilizing both cellulose and lignin (Adney et al., 2008).

It is difficult to extract fungal DNA because of its branched mode of growth so many composting studies monitoring fungal growth continue to utilize quinone profiling or culture-dependent techniques (Chroni et al., 2009; Huang et al., 2010; Kornillowicz-Kowalska & Bohacz, 2010; Yu et al., 2007). A few researchers have been able to overcome the difficulties associated with extracting fungal DNA and have tracked the succession of fungal communities in compost using nucleic acid based techniques (Bonito et al., 2010; Dees & Ghiorse, 2001; Hansgate et al., 2005; Peters et al., 2000). The study by Dees and Ghiorse (Dees & Ghiorse, 2001) investigated the microbial diversity of thermophilic compost by using both culture-based and cultivation-independent techniques. This was accomplished by isolating 16S rRNA sequences from compost samples through extraction, PCR amplification, cloning, sequencing, and ARDRA (Amplified rDNA Restriction Analysis) screening. The researchers were able to PCR- amplify the bacteria and actinomycetes isolates from their samples at 50^{o}C, 60^{o}C and 74^{o}C; whereas the fungal isolates were only amplified at 50^{o}C and archaea resulted in no amplifications. These amplifications led to the result that gram positive bacteria governed the thermophilic phase of composting and that fungal growth disappeared at temperatures of 60^{o}C and higher (Dees & Ghiorse, 2001). Interestingly, the results from the culture-based techniques did not overlap with those from the cultivation-independent techniques, but rather the results complemented each other. Provided that their ARDRA analysis was done correctly, the lack of complete congruency between the two different methods used highlights some of the flaws of using culture based methods; namely, the preferential growth of certain bacterial groups coupled with the selected growth suppression of others as a result of the culture conditions and environment (Peters et al., 2000). The use of a

culture-based method could also account for the researchers' observations that their most abundant isolates were from groups not typically associated with compost piles. In addition, the findings of the study were limited by the availability of library clone sequences to which the isolates could be compared for identification. Although the results of this study agree with previous culture-based findings, advances in molecular biology tools and techniques have reduced the frequency of use of biased culture-based methods.

Another study (Hansgate et al., 2005) on fungal community dynamics, employed F-ARISA (Fungal-Automated rRNA Intergenic Spacer Analysis) and 18S rRNA gene cloning and sequencing to explore fungal populations in the initial stages of composting. The combination of these methods allowed the researchers to identify more fungal sequences than the previous study by Dees et al., and thus led to the observance of a shift in the fungal community structure between 48 and 60 hours, despite the small size of the A-OTUs (ARISA Operation Taxonomic Units). The researchers also verified the effect of fungi on the system pH by identifying the presence of *Rhizopus* and *Amylomyces* which are lactic acid producing fungi. This study provides much needed insight into the role of fungi in composting systems. This is extremely useful because it documents the temporal changes in the fungal community during the initial stages of composting. This information; although qualitative, provides a foundation upon which further fungal dynamics may be established; such as the use of fungal probes to quantify major fungal species. The use of the ARISA method also allows for high throughput analysis – a critical asset in managing numerous samples for temporal studies.

2.4 Molecular Biology Tools for Characterizing Compost Microbial Communities

Several methods have been developed to satisfy the need for microbial community information in compost samples. The choice of method depends on the level of detail desired, the sample size, and the time available for sample processing. Molecular biology techniques have surpassed the use of classical microbiological methods and biochemical methods in the identification of microbial groups because of the higher efficiencies and more accurate results. Microbiological methods employ culture-based protocols that may be laborious and biochemical methods, such as quinone profiling (Tang et al., 2004), DNA reassociation kinetics and Bisbenzimidazole-Cs-Cl-gradient fractionation, do not have broad applications because 99% of microorganisms have not been isolated (Muyzer, 1999), so databases for comparative purposes are of limited availability. For this reason, molecular biology techniques are leading the way towards obtaining microbial data.

2.4.1 Conventional and real time PCR

Most molecular biology techniques employ Polymerase Chain Reaction (PCR) as an essential step in the process of genetic fingerprinting. PCR is defined as the exponential amplification of a DNA fragment (Spiegelman et al., 2005). This amplified product can then be separated based on nucleic acid content to produce a pattern of bands on a gel that will provide an indication of the diversity of the microbial community (Spiegelman et al., 2005). These fingerprinting methods which lead to characterization of microbial communities include Amplified ribosomal DNA restriction analysis (ARDRA), denaturing gradient gel electrophoresis (DGGE), temperature gradient gel electrophoresis (TGGE), terminal-restriction fragment length polymorphism (T-RFLP), length heterogeneity polymerase chain reaction (LH-PCR), ribosomal intergenic spacer analysis (RISA), single-strand conformation

polymorphism (SSCP), randomly amplified polymorphic DNA (RAPD), functional PCR and direct cloning and sequencing. Of these methods, several have been used to evaluate compost microbial communities, and will be discussed in later paragraphs.

Despite the broad application of these molecular biology methods, the results are inherently biased because of the use of PCR during the process. PCR has several limitations that may hinder the accuracy of the results. Firstly, PCR is highly sensitive to environmental conditions and tiny amounts of contamination can lead to quantitatively different results (Spiegelman et al., 2005). In addition, polymerases, which are used to elongate the DNA strands, may incorrectly insert or delete nucleotides, producing incorrect sequences that go unnoticed because the polymerases are unable to proofread the strands (Spiegelman et al., 2005). Errors such as these become exponential because of the numerous repeated cycles that characterize PCR. Furthermore, PCRs of longer products are less efficient and less accurate (Spiegelman et al., 2005) – a particularly troubling issue in intricate microbial communities because of the differences in size and copy number of the various organisms. Additionally, PCR introduces many chimeric sequences, which occur when a foreign DNA strand is annealed to a prematurely terminated amplicon and is copied to completion in subsequent PCR cycles (Spiegelman et al., 2005).

Recent developments in molecular biology techniques have resulted in using PCR as a quantitative measure of microbial growth via the techniques of real-time (quantitative) PCR. In real-time PCR, amplification of the gene of interest is monitored by online detectors which capture the amount of fluorescence emitted during the extension step (Malinen et al., 2003). The emitted fluorescence is proportional to the amount of PCR product which in turn is related to the initial amount of DNA, cDNA or RNA targets present in the sample. To quantify the amount of DNA or RNA present in an unknown sample, samples of known

concentration must be amplified to produce a standard curve to which unknown samples are compared. A great advantage of real time PCR is that the slope of the standard curve may be used to calculate the efficiency of the reaction by the following equation: Efficiency = $10^{-1/slope}$ (Pfaffl, 2001). One of the most commonly used fluorescent dyes is SYBR Green because it is simple to use and relatively inexpensive. SYBR Green is an intercalating dye that binds to all double stranded DNA and emits a fluorescent signal at 521nm upon binding (Qiagen, 2010) (Figure 2.2). The non-specificity of this dye makes it broadly appropriate for a number of different targets, so this requires that the PCR primers be highly specific to the target DNA or RNA. One of the disadvantages of using SYBR Green is the possible contribution of primer-dimers and non specific PCR products to the fluorescent signal (Qiagen, 2010). For this reason, highly specific fluorescent probes have been designed for use in real time PCR. These probes are labeled with fluorescent dyes and contain pieces of DNA that are complimentary to the gene of interest. The most commonly used type of probe is the TaqMan probe which is designed with a fluorophore at the 5'end of the probe and a quencher molecule at the 3' end of the probe (Malinen et al., 2003). Using this technique, the quencher molecule and the fluorophore are separated by the action of Taq DNA polymerase during the annealing and extension phases, resulting in fluorescence emissions that are proportional to the amount of PCR product (Figure 2.3a). FRET (fluorescence resonance energy transfer) probes are also used, but less common. Real time PCR with FRET probes requires the use of 2 labeled probes which bind to the PCR product in a head to tail approach (Qiagen, 2010). One of the probes is labeled with a donor fluorophore while the other is labeled with an acceptor fluorophore. These two fluorophores come into close proximity with each other when the probes bind to the PCR product, allowing for the transfer of energy from the donor

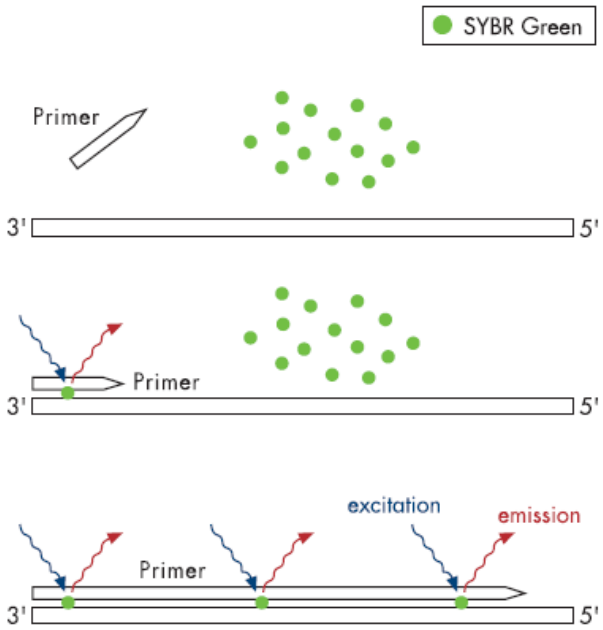

Figure 2.2 Schematic of detection of SYBR Green based fluorescence in real time PCR

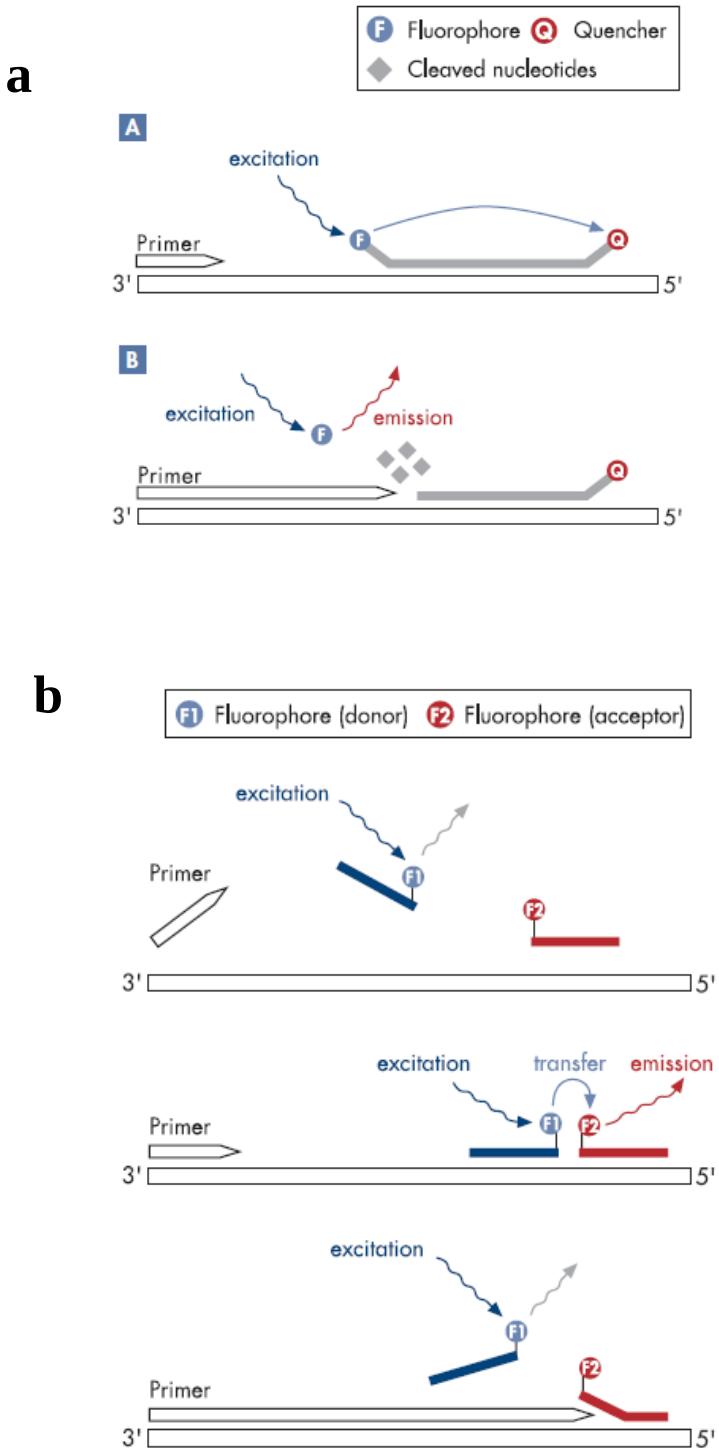

Figure 2.3 Mechanism of action of fluorescent probe s in real time PCR using (a) TaqMan probes and (b) FRET probes (Qiagen, 2010)

to the acceptor fluorophores (Figure 2.3b). This energy transfer is detected as fluorescence during the annealing phase of PCR and is proportional to the amount of PCR product. Although the use of fluorescent probes results in detection of only the desired PCR product, these highly specific probes are difficult to generate and often require lengthy validations.

To date, the number of studies utilizing real time PCR to monitor microbial community changes in composting environments is very limited. One of the few studies in this area looked at the decomposition of bovine and plant DNA in a composting environment based on changes in genes encoding for bovine mitochondrial DNA and plant chloroplast DNA (Xu et al., 2009). The researchers found significant changes in the target genes which reflected overall degradation and were able to show how useful real time PCR was as a tool for assessing biodegradation during composting.

2.4.2 DGGE

DGGE (Denaturing Gradient Gel Electrophoresis) is used to separate rDNA in a polyacrylamide gel containing a linear gradient of DNA denaturing compounds based on differences in G-C content of the sequences (Muyzer, 1999). As the DNA moves along the gel, the increased concentration gradient forces it to become single stranded, but it does not become completely denatured because of the presence of a GC clamp that is incorporated into one of the primers for the PCR amplification. Compost research completed using DGGE has produced microbial diversity data and identification when coupled with 16S rDNA sequencing (Ishii et al., 2000; Kowalchuk et al., 1999; Pedro et al., 2001). The most recent of these studies (Pedro et al., 2001) sought to characterize the microbial community of a composting process in a Hazaka system. Surprisingly, the study showed no significant changes in the microflora

during the composting process based on the DGGE profile even though the material had composted for 30 days. This unusual result may be due to the use of the Hazaka system which regulated the temperature at 60 – 76^{o}C during the thermophilic phase and at 45^{o}C during the mesophilic phase. Such regulation of the temperature during composting would not allow for the natural selection of microorganisms which are necessary for the degradation process. Amazingly, the authors did not present any explanations for the lack of community shifts, but overshadowed this by presenting the bacterial genera that comprised their samples. Another indication that composting conditions may not have been ideal for microorganism differentiation was that the lack of any noticeable change in the pH for the entire 30 day period. Although, this study did a good job of identifying species in the bacterial community that were present in their samples, the overall result provided no new insight into the changing roles of microorganisms during composting.

A major advantage of the DGGE method is that bands can be cut out from the gel and then sequenced to obtain phylogenetic information (Muyzer, 1999). Also, it is relatively easy to determine the changes in the microbial community through the absence or presence of bands on the gel (Pedro et al., 2001). The downsides associated with DGGE include laborious calibrations to ensure optimal separation conditions and DNA fragment lengths are limited to 500bp (Spiegelman et al., 2005). In addition, large amounts of DNA – as much as 500ng - are needed for good resolution with DGGE. Furthermore, PCR biases can lead to incorrect conclusions about the components of a given sample by either under or over- representing certain groups (Spiegelman et al., 2005).

2.4.3 TGGE

Similar to DGGE is TGGE (Temperature Gradient Gel Electrophoresis) which separates rDNA in the exact manner as DGGE, but uses temperature at the denaturing gradient as opposed to chemical denaturants (Spiegelman et al., 2005). The advantages and limitations of TGGE are the same as that of DGGE (Muyzer, 1999). To this author's knowledge, no microbial community analyses have been completed on compost samples using TGGE, but several have been done on soil samples (Smit et al., 1999).

2.4.4 SSCP

In the SSCP (Single Strand Conformation Polymorphism) method, PCR-amplified DNA fragments are denatured and separated on non-denaturing gels based on the folded structures of the single strands of DNA (Muyzer, 1999). Although SSCP is used primarily to identify polymorphisms and mutations in human genes, it has found application in microbial community studies (Spiegelman et al., 2005). SSCP has also been used to track microorganism community dynamics in compost samples (Alfreider et al., 2002; Peters et al., 2000). The more recent of these works (Alfreider et al., 2002) used SSCP in combination with 16S rRNA sequencing to determine the microbial complexity of a compost system consisting of domestic organic wastes, wood chips and yard trimmings. Seven samples were collected over a period of 23 days and after analysis revealed that a significant shift occurred in the community profile in the initial curing period. Considering that composting goes through three different stages, it is somewhat surprising that this study only found one change in the community profile. Also strange was the initial temperature of 41^{o}C the compost reactor. The proximity of this value to thermophilic temperatures could explain why the authors did not observe a shift from the mesophilic phase to the active

phase. Furthermore, the authors did not present the dynamics of physical state variables such as temperature and pH and so it was not possible to correlate the observed shift in the microbial community to those variables. Despite the inability of the authors to sequence their most abundant clones, they have presented SSCP as a viable alternative to DGGE to monitor microbial community dynamics during composting.

A major disadvantage of using SSCP is the re-annealing of DNA strands during electrophoresis, after being initially denatured (Spiegelman et al., 2005). This can lead to complex structures that can produce more than one band on a gel in addition to other possible bands added through PCR biases (Spiegelman et al., 2005). Furthermore, the sensitivity of the SSCP method is affected by electrophoretic conditions such as temperature and the gel matrix and SSCP only works optimally for short DNA fragments in the range of 150-400bp (Muyzer, 1999). Also, SSCP requires very high specificity for rRNA genes because the folded conformations of these genes are very similar (Spiegelman et al., 2005). SSCP is advantageous because it is simpler to carry out than DGGE (Spiegelman et al., 2005) and more samples can be processed at once through the creation of larger gels (Alfreider et al., 2002).

2.4.5 RISA

The RISA (Ribosomal Intergenic Spacer Analysis) method creates a community profile of the PCR-amplified genetic region between 16S rRNA and 23S rRNA on the basis of species-specific length polymorphisms in the region (Spiegelman et al., 2005). RISA has been automated (Automated Ribosomal Intergenic Spacer Analysis, ARISA) to increase resolution and analytic power (Ranjard et al., 2001). This technique was employed in a study (Schloss et al., 2003) to develop bacterial community fingerprints during the initial stages of composting.

Nine samples were taken over a period of 96 hours for each reactor and through subsequent analysis, the authors observed 2 major shifts in the community population – one between 12 and 24 hours and the other between 60 and 72 hours. The first shift corresponded with an increase in temperature and a drop in pH while the second shift corresponded with increases in both temperature and pH. Through the phylogenetic identification of the most common groups, the authors were able to correlate the species of bacteria to the observed physical phenomenon. This study, although qualitative, provides a glimpse of the intricate relationship between biotic and abiotic phenomena. The information obtained from this study is critical towards further understanding the dynamics responsible for changes observed in the initial stages of composting. Similar to that study, another investigation (Hansgate et al., 2005) (discussed in the previous section) used a variation of ARISA to characterize fungal communities. This variation, called fungal ARISA (F-ARISA) focuses on the rDNA region that contains the two internal transcribed spacers (ITS) and the 5.8S rRNA gene (Ranjard et al., 2001).

One of the major limitations of using RSIA and its variations is that it only provides a general assessment of the microbial community through the community fingerprint (Ranjard et al., 2001). RISA must be used in conjunction with other methods to identify major species of interest which may not be identifiable due to the limited information available in intergenic spacer databases (Spiegelman et al., 2005). Furthermore, PCR biases particularly affect RISA because shorter fragments may be preferentially amplified even though intergenic spacer regions are of varying lengths (Spiegelman et al., 2005).

The flexibility of RISA in terms of the number of variations of the method (Ranjard et al., 2001) that can be used, make it an attractive option. In addition, this method, once automated leads to rapid, high-throughput analysis (Spiegelman et al.,

2005) which makes it ideal for obtaining high resolution data in complex systems that require numerous sampling points. ARISA also produces highly specific profiles that are readily comparable at different time points (Spiegelman et al., 2005). Moreover, ARISA may be used with other high-throughput technologies, such as capillary electrophoresis systems that increase the rapidity and reproducibility of the method (Ranjard et al., 2001).

2.4.6 ARDRA

ARDRA (Amplified rDNA Restriction Analysis), also known as restriction fragment length polymorphism (RFLP) is a method in which PCR-amplified DNA is subjected to restriction digestion analysis based on the theory that differences in gene sequences will create unique binding sites for various restriction enzymes (Spiegelman et al., 2005). A community profile is created after the digested fragments are run on a gel (Muyzer, 1999). This method was employed in one composting study (Dees & Ghiorse, 2001) (discussed in previous section) to determine the microbial diversity during the thermophilic phase. One of the major limitations of using this method is that the members of the microbial community may be overestimated through the presence of more bands on the gel than the number of amplified DNA sequences (Muyzer, 1999). Also, similar to ARISA, ARDRA must be used in conjunction with another technique to detect and identify the specific groups present in the profile (Spiegelman et al., 2005). Furthermore, ARDRA may become very time consuming because each experiment needs to be optimized to find the best combination of restriction enzymes that work for the system of interest (Spiegelman et al., 2005). Despite these limitations, ARDRA is advantageous because it is rapid once optimized, cost-effective and it uses two parameters to separate rDNA genes: size and sequence (Spiegelman et al., 2005).

2.4.7 Sequencing

The aforementioned methods provide excellent qualitative results about the genetic fingerprints of microbial groups in composting systems and Table 2.2 summarizes the significance of these and other PCR based methods. While all of these methods provide insightful snapshots of the microbial community, the information they provide is limited because they must be used in conjunction with another technique for species identification. Usually this other method is DNA sequencing and until recently, Sanger sequencing was the key method used to generate sequences. The need for faster, cheaper and higher throughput has resulted in the development of pyrosequencing, which has a 100-fold increase in throughput over Sanger sequencing (Margulies et al., 2005). This technique is continuously being improved for higher throughput and lower cost because of the promise it holds for revolutionizing microbial characterization, with 454 pyrosequencing being the most commonly used method currently. Through pyrosequencing, DNA sequences of all microorganisms present in a sample may be obtained and analyzed from the phylum level all the way down to the genus and species levels using analytical software. Even entire genomes may be sequenced using this technique. To date, pyrosequencing has been used to study diverse environments such as the human gut (Andersson et al., 2008) and marine samples (Goldberg et al., 2006) but there are hardly any published studies on compost microbial communities using pyrosequencing techniques. One of the only studies available presently that analyzed composting samples using pyrosequencing showed that the number of sequences obtained from compost samples paled in comparison to soil and anaerobic digester samples (Bibby et al., 2010). The composting sample contained 16, 474 sequences whereas the anaerobic digester sample contained 44, 108 sequences and the soil sample 43, 670 sequences. All samples were in the final stages of treatment and had been designated as pathogen

free; so this data suggests that the composting process was the most efficient at eliminating pathogens and producing a stable microbial product. This was further evidenced in the analysis of known pathogens present in the samples, which showed that the compost sample contained 5 sequences of known pathogens whereas the anaerobic digester and soil samples contained 43 and 48 sequences of known pathogens, respectively.

2.4.8 Probe hybridization

Probe hybridization is a molecular biological method that does not require the use of PCR, and is available for providing information about the microbial community in a compost sample. In probe hybridizations, a labeled fragment of a known DNA sequence is hybridized to its complimentary strand in an environmental sample. The labeling may be done via radioactivity or chemiluminescence to detect and visualize the presence of specific species in the microbial community. According to Spiegelman et al. (Spiegelman et al., 2005), there are 3 main reasons for using oligonucleotide probes: (i) to investigate the presence of various taxonomic groups in the community, (ii) to measure the relative abundance of specific taxa, and (iii) to determine the spatial distribution of species or groups present. Probe hybridizations may be used (i) with clone libraries in the identification of groups of interest (Schloss, 2002), (ii) along with other fingerprinting techniques (Schloss, 2002) and (iii) directly in order to investigate the presence of taxonomic groups.

To obtain quantitative information from probe hybridization, the environmental sample must first be denatured and immobilized onto a positively charged membrane. In addition to the sample, a known amount of a standard must

Table 2.2 Summary of PCR-based molecular biological methods (Spiegelman et al., 2005)

Method	Description	Community Profile	Taxonomic Identification	Quantitative	Limitations	Advantages
ARDRA	Separates amplified 16S molecules by restriction patterns	yes	possible	no	Optimization required	Rapid; minimal requirements
DGGE	Separates amplified 16S molecules by % G-C content	yes	possible	no	Labor intensive; complex profiles possible	Single base pair resolution
TGGE	Separates amplified 16S molecules by % G-C content	yes	possible	no	Labor intensive; complex profiles possible	Single base pair resolution
T-RFLP	Separates amplified 16S molecules by restriction patterns	yes	yes	yes	Optimization required	High throughput; immediate, digital analysis
LH-PCR	Separates amplified 16S molecules by length	yes	possible	no	Some ambiguity in results	Great simplicity and speed

Table 2.2 (Continued)

RISA	Separates amplified 16S-23S intergenic region by length	yes	possible	possible	Small database; especially sensitive to PCR artefacts	Great simplicity and speed; automation possible
SSCP	Separates amplified 16S ssDNA by sequence-dependent higher order structure	yes	no	possible	Can be a delicate procedure	Great simplicity and speed; automation possible
RAPD	Sequence-independent profiling based on random PCR priming	yes	no	no	Non-generalizable profiles	Fast, easy and inexpensive; high statistical power possible
Functional PCR	Several PCR-based analyses using amplified catabolic genes; indirect functional assay	n/a	n/a	no	Limited taxonomic information; limited databases	Better-suited to specialized investigations

also be blotted onto the membrane. The probe is then hybridized to this membrane and the intensities of the signals obtained from the samples, either through radioactivity or chemiluminescence, are compared to those of the standards to provide relative abundance data.

Probe hybridizations provide flexibility in obtaining taxonomic information because of the breadth of information that may be gleaned from the data. In addition, the high specificity of the probes greatly minimizes the possibility of mismatch errors and the probes are relatively easy and cheap to produce. The greatest limitation of probe hybridization is the possibility of errors during the probe synthesis. The probing will only be as efficient as the probe design for which there may be limited amounts of sequence data available in databases. In addition, probing is limited by the difficulty in detecting lesser known organisms (Spiegelman et al., 2005). Furthermore, in compost samples, probe hybridizations are complicated by the presence of humic acids, which are often co-extracted with nucleic acids through the extraction procedure (Ishii et al., 2000). The presence of humic acids affects the quantification of DNA, the performance of DNA in PCR amplification and DNA-DNA hybridizations (Bachoon et al., 2001). A study (Bachoon et al., 2001) done to determine the effects of humic substances on DNA quantification and hybridization found that the Hoechst dye gave more reliable results when using a fluorescence detection procedure. The study; however, concluded that treating the samples with PVPP (polyvinylpolypyrrodidone), reduced the amount of humic substances present, thereby allowing for the use of the samples in hybridizations with little interference from humic contaminants (Bachoon et al., 2001).

2.5 Composting Operating Conditions

Environmental variables such as temperature, moisture and pH dictate the conditions under which any compost pile is operating and thus, play an essential role in determining microbial growth and the nature of the product formed. The effects of these operating conditions will be discussed in this section.

2.5.1 Moisture Content

Understanding and managing the transport of moisture during composting and within any solid state fermentation process is essential for the manipulation of that process. The moisture content of the substrate is a key factor in determining the synthesis and secretion of desired products via enzymatic action, biomass growth, and nutrient and gas transport (Bellon-Maurel et al., 2003). If the moisture content is too low, some microorganisms will not have enough water to sustain growth. In addition, substrate swelling, which is necessary for microbial activity on the substrate, will not occur. On the other hand, if the moisture content is too high, the void spaces within the solid matrix will be filled with water that will inhibit the transfer of oxygen to the substrate particles and the transfer of metabolic products such as carbon dioxide away from the substrate particle and could also foster contamination of the solid matrix. Thus, an optimum moisture content must be found to maximize the output of a given SSF application such as enzyme production (Montiel-Gonzalez et al., 2004) or microorganism growth. While many microorganisms are able to grow on solid substrates, bacteria and yeasts grow on solid substrates containing 40 – 70% moisture, whereas filamentous fungi can grow extensively in low moisture environments.

The effect of moisture content in many SSF systems is best described using the term, water activity (Bellon-Maurel et al., 2003; Gervais & Molin, 2003; Oriol et al., 1988; Perez-Guerra et al., 2003). Water activity, a_w, is defined at a given temperature

using the following relationship: $a_w = P_s / P_o$, where P_s is the vapor pressure of water in equilibrium with the substrate and P_o is the vapor pressure of pure water (Cen & Xia, 1999; Perez-Guerra et al., 2003). For a microorganism, the water activity is the amount of water available to it in its immediate surroundings for microbial activity (Bellon-Maurel et al., 2003). This parameter is difficult to measure in composting environments and is typically not used, but values in the range of 0.95 to 0.98 are typical in other SSF processes (Mitchell et al., 2000). Studies have shown that small changes in the value of the water activity of a given system can noticeably affect the growth and activity of microorganisms (Montiel-Gonzalez et al., 2004; Oriol et al., 1988). Water activity is; however, challenging to measure and is seldom reported in the literature; so moisture content values are typically used.

Managing the amount of moisture in a compost pile is critical because of variations in water transport as a result of water evaporation through mass transfer and water production via metabolism. Most compost piles typically start with initial moistures in the range of 60 to70% as this is considered an ideal range for the most commonly used substrates (Gajalakshmi & Abbasi, 2008). Significant drying may occur during composting leading to reduced microbial activity, so compost piles are typically turned to minimize this risk or water may be added periodically to the substrate bed (Nakasaki et al., 1998; Walker et al., 1999). In systems employing forced aeration, the risk for drying of the organic matrix is especially high; thus, to minimize drying, reactors are often aerated with saturated air (Hogan et al., 1989; Oriol et al., 1988; VanderGheynst et al., 1997).

2.5.2 Temperature

Temperature is arguably the most critical factor in any SSF process. It influences the type of metabolic product formed, the rate and extent of substrate

degradation and product formation, the growth and metabolism of microorganisms, and the extent of heat and mass transfer processes (Cen & Xia, 1999; Mitchell et al., 2000; Pandey, 2003; Perez-Guerra et al., 2003). Based on the generalized composting model shown in Figure 2.1, one can use the temperature to determine the progress of degradation processes because it provides a measure of the rate and extent of the process.

Temperature variations occur within SSF reactors as a result of the buildup of heat produced from the metabolic activity of microorganisms. The heat accumulates because of the challenges associated with heat removal. One of the most common difficulties is that of uneven heating of the substrate matrix, resulting in the development of radial and axial temperature gradients (Raghavarao et al., 2003). Radial temperature gradients may be overcome by enclosing the vessels in insulation and axial gradients are commonly combated through the forced aeration of saturated air through the substrate bed (Cen & Xia, 1999; Perez-Guerra et al., 2003; Raghavarao et al., 2003; Raimbault, 1998). In composting processes, one of the most commonly used strategies to combat uneven heating is the turning of the compost pile in an effort to make the substrate bed more homogeneous (Chroni et al., 2009; Walker et al., 1999).

Temperature is the easiest variable to monitor online and is arguably the most controllable. In SSF studies where the goal is to produce a specific bio-substance, temperature was manipulated to optimize product growth or activity (Dalsenter et al., 2005; dos Santos et al., 2004; Prakasham et al., 2005). In these studies, the isothermal approach was used whereby several fermentations were carried out at a range of temperatures, with each reactor being held at a constant temperature throughout. In addition, other studies have been done to model the temporal and spatial temperature patterns for a given reactor system (Dalsenter et al., 2005; dos Santos et al., 2004;

Saucedocastaneda et al., 1990; Stuart & Mitchell, 2003; VanderGheynst et al., 1997), in order to make the system more predictable for scale up. In typical composting systems, the opposite effect is often desired, where temperatures increase as much as possible in order to kill off known pathogens from the system.

2.5.3 Aeration

The necessity of oxygen (O_2) for high-rate microbe growth and activity dictates that the substrate bed must be continuously and uniformly oxygenated for optimal results. One way of achieving this is to periodically mix the substrate bed; however, it has been found that a continuous air supply is a more efficient way of providing oxygen to the solid matrix (Gervais & Molin, 2003; Raghavarao et al., 2003). Forced aeration of saturated air not only provides O_2 to the reactor bed, but also helps to sustain humidity requirements and to evenly dissipate some of the metabolic heat and gaseous metabolites generated. This is in comparison to natural composting processes where the much less efficient method of diffusion is the main transport mechanism for O_2 into the pile.

As with the moisture content, an optimal aeration rate must be maintained to optimize microbial growth and activity. When the aeration rate is too low, mass transfer processes become limited and consequently either: slows down the growth of microorganisms if the flow rate is really low or generates more heat if the low flow rate is still able to sustain metabolic activity (Raghavarao et al., 2003). On the other hand, if the rate of aeration is too high, the substrate bed will become dry as a result of rapid evaporation of water from the bed. This desiccation can lead to lower metabolic activity and dramatic changes in the microbial population and composition of the substrate bed. Aeration values vary in the literature from low values of 8L/min (200-L bioreactor) (Bari et al., 2000) to high values of 100L/min (770-L bioreactor)

(VanderGheynst et al., 1997). One way of maximizing the effects of extreme aeration rates is by using discontinuous flow rates (Nakasaki et al., 2000). In this method, the aeration rate is kept to a minimum at the beginning of the process when the temperature is low and a high flow rate is applied later on in the process when the temperature has risen to a given set point.

2.5.4 pH

Changes in pH during biodegradation provide another indication of the activity of microorganisms within the system. Bacteria prefer a pH in the range of 6-7.5, whereas fungi prefer to operate in the pH range of 5.5-8.0 (Gajalakshmi & Abbasi, 2008). Overall, a pH range of 5.5-8.0 has been found to be optimal for many composting processes (Fogarty & Tuovinen, 1991). These changes in pH are associated with the hydrolysis of proteins in the substrate and the production of ammonia and organic acids at different stages in the process (Bellon-Maurel et al., 2003; Lu et al., 2004). Although pH is difficult to measure online because of the lack of free water, it is an important factor in determining the optimum conditions for product growth, particularly for enzymes. Buffers and other pH correcting agents, such as urea and ammonia, may be added to the solid substrate in an attempt to control the pH, but this is still not very effective at eradicating pH gradients from the system (Perez-Guerra et al., 2003).

Typically, when cellulosic substrates are used, the initial pH is in the range of 4.5 – 6.5 (Cen & Xia, 1999). This low pH in the initial phase is typically attributed to the formation of organic acids and carbon dioxide (Gajalakshmi & Abbasi, 2008). Some studies have found that as organic decomposition proceeds, pH values quickly become basic as a result of the production of ammonia (NH_3) (Lu et al., 2004); while other work has found that the pH becomes more acidic for a brief period of time

before it rapidly becomes basic (Beltz, 2000). At that point, the pH either stabilizes at a basic pH value around 9.1 (Lu et al., 2004) or the pH may become more basic as a result of utilization of the organic acids and a shift from bicarbonate alkalinity to hydroxide alkalinity due to carbon dioxide stripping (Beltz, 2000). These studies do agree; however, that different initial treatments such as different aeration rates have little effect on the pH trends (Beltz, 2000; Lu et al., 2004).

Two studies by the same investigator found that low pH inhibits the transition from mesophilic to thermophilic conditions during composting, while higher pH leads to faster decomposition with higher aeration rates when water is frequently added to the substrate to compensate for drying (Sundberg & Jonsson, 2008; Sundberg et al., 2004). In both of these studies, the author notes that organic acids are a key factor in regulating pH because of their presence under acidic conditions and absence under alkaline conditions. The production and subsequent utilization of organic acids in composting environments is microbially driven and as such depends on temperature and oxygen levels. Lower rates of formation and faster decomposition rates of organic acids have been correlated to higher oxygen concentrations and thus more rapid rises in pH (Beck-Friis et al., 2003). Changing the initial microflora also resulted in increases in the initial rates of degradation by first increasing the pH. Nakasaki et al. (1996) showed that inoculating compost with acid-tolerant bacteria produced a marked increase in the degradation rate while Choi and Park (1998) demonstrated that inhibition of the growth of thermophilic bacteria caused by the presence of organic acids could be overcome by adding yeasts to metabolize organic acids.

2.5.5 Substrate

The desired result of a given SSF process is the determining factor in the choice of substrate used. This selection is critical because the substrate will be the

provider of nutrients and physical support for the growth of microorganisms. Listed in Table 2.3 are some substrates that have been used with various microorganisms and the products formed, while in Table 2.4, the chemical composition of some frequently used substrates are listed.

From Table 2.3, it is seen that different substrates can make the same product and that the same substrate can make different products. This is due to the effect of the nature of the inoculum added to the fermentation process. Inoculation provides the seed organism or organisms that will initiate substrate decomposition and *Aspergillus niger* is one of the most common organisms used to act on a variety of substrates in SSF. Table 2.3 again illustrates one of the advantages of this process – that waste material may be used to produce pure products of high value.

The chemical composition of substrates, as shown in Table 2.4 is important because it shows what inorganic nutrients are available to support microbial growth. One of the most important factors for composting from this table is the carbon/nitrogen (C/N) ratio because it gives an indication of the level of degradability of the substrate. In composting processes C/N ratios in the range of 15 to 30 are typically used because this facilitates a good balance between microbial growth and substrate decomposition (Haug, 1993). Comparing soy meal to wheat straw, one would expect that soy meal is much easier to degrade because the C/N ratio of wheat straw is 12 times that of soy meal. Wheat straw has a particularly high C/N ratio and this suggests that on its own, this substrate may take several decades to degrade. For this reason, many substrates are amended with nitrogen sources to put them in a range where degradation can occur more quickly. Nitrogen is a critical nutrient because it is needed in high concentrations for cellular synthesis (Haug, 1993). If the amount of nitrogen present is limiting, then microbial population growth will also be limited, causing the degradation process to take much longer. On the other hand, if nitrogen is

Table 2.3 Substrates associated with various SSF products or processes

Substrate	**Microorganism**	**Product or Process**
Alkali-treated sugar cane	*Trichoderma reesei* & *A. niger*	Cellulases
Composted chicken manure	*Trichoderma vierns*	Bioherbicide
Corn cob	*Phanerachaete chrysosporium*	Lignolytic enzymes
Dry coffee husks	*Aspergillus niger*	Citric acid
Eucalypt wood	*Phlebia radiate or Funalia trogii*	Biopulping pretreatment
Ground soybeans	*Bacillus subtilis*	Pyrazines
Impregnated hemp	*Coniothyrium minitans*	Bioinsecticide
Impregnated spent malt grains	*Xanthomonas campestris*	Xanthan gum
Impregnated sugar cane bagasse	*Aspergillus tamarii*	Caffeine removal
Municipal solid waste	*natural consortia*	Methane
Pineapple waste	*Aspergillus niger*	Citric acid
Rice bran	*Aspergillus niger*	Glucoamylase
Rice flour	*Colletotrichum truncatum*	Bioinsecticide
Sawdust	*Lentinula edodes*	Shiitake
Soy bran and wheat bran	*Aspergillus niger*	Pectinases
Steamed rice	*Aspergillus oryzae*	Kojic acid
Sugar cane bagasse pith	*Phanerochaete chrysosporium*	Bioremediation

Table 2.3 (Continued)

Sugar beet pulp or citrus waste	*Neurospoa sitophila*	Protein enrichment
Various fruit peel	*Saccharomyces cerevisiae*	Fermented food
Wheat bran	*Aspergillus oryzae*	Iturin

Table 2.4 Nutritional composition of common agricultural wastes used as substrates in SSF (Pryor, 2005)

Substrate	C:N	Ca (%)	P (%)	Mg (%)	K (%)	S (%)	Na (%)	Cl (%)	Protein (%)	Fat (%)	Fiber (%)
Corn flour	34.0	0.02	0.31	0.09	0.26	0.12	0.03	0.05	8.8	3.6	2.3
Millet	26.1	0	0.3								
Rice bran	24.0	0.08	1.4	0.95	1.74	0.18	0.03	0.07	12.9	1.5	12.9
Rice husk	92.6										
Sorghum	27.4	0.03	0.3						8.9	2.8	2.2
Soy Hulls	27.3	0.4	0.15	0.14	0.72	0.09	0.04	0			
Soy meal	6.6	0.2	0.6	0.25	1.8	0.33	0.03	0.07	48	0.9	3.4
Wheat bran	18.9	0.07	1.01	0.61	1.18		0.002		15.7	4	10
Wheat middlings	18.4	0.15	0.9	0.5	1.2	0.15	0.17	0.03	16	4.3	7.8
Wheat straw	88.7										

Table 2.5 Main groups of microorganisms involved in SSF processes

Microflora	**SSF Process**
Bacteria	
Bacillus spp.	Composting, Natto, amylase
Pseudomonas spp.	Composting
Lactobacillus spp.	Ensiling, Food
Yeast	
Endomicopsis burtonil	Tape, cassava, rice
Saccharomyces cerevisiae	Food, Ethanol
Fungi	
Aspergillus spp.	Composting, Industrial, Food
Monilia	Composting
Beauveria spp.	Biological control, Bioinsecticide
Aspergillus oryzae	Koji, Food, citric acid
Aspergillus niger	Feed, Proteins, Amylase, citric acid
Penicilium notatum, roqueffortii	Penicillin, Cheese

in excess, it will be given off as ammonia gas. This is problematic for composts which will be used as soil additives because nitrogen is needed in the compost as a nutrient for growing plants. The carbon content of the substrate is also important because it provides the substrate for microbial metabolism once the cells are synthesized. Research has also shown that the amount of time required for composting, increases with increasing C/N ratios; however, if the nitrogen present is part of a nondegradable organic molecule, it would not be available for degradation regardless of the C/N ratio (Haug, 1993).

Lignocellulosic material is of particular importance as substrates because of their prominent abundance and their potential to serve as energy crops for biofuel production. In fact, SSF technology provides promise of cheaper production and better hydrolytic efficiencies (Tengerdy & Szakacs, 2003) of substrates for the production of biofuels. These substrates are typically composed of 40-50% cellulose, 25-35% hemicellulose and 15-20% lignin (Wyman et al., 2005). Cellulose is a glucose polymer, whereas hemicullulose is a pentose-sugar heteropolymer and lignin is an aromatic network polymer that binds together cellulose and hemicellulose (Chandra et al., 2007). As a result of their structures, cellulose and hemicelluloses are easier to decompose than lignin. Lignin is particularly recalcitrant to microbial degradation but succumbs to metabolism by white rot fungi (Tuomela et al., 2000). Under composting conditions, simple carbohydrates such as sugars and polymers are decomposed to carbon dioxide, heat and water and nitrogenous compounds produce ammonia (Gajalakshmi & Abbasi, 2008). Cellulose and hemicelluloses are then metabolized and lastly lignin is decomposed.

2.6 Engineering aspects of composting

One of the goals of many SSF systems is to make them more predictable and controllable so that reactor scale up would be possible without destroying the reliability of the process or hindering the formation of the a stable humic product. This section discusses the major engineering aspects which play a role in the design of large scale composting and other SSF processes.

2.6.1 Mass Transfer Aspects

The transfer of mass in solid state reactors plays a critical role in determining the growth of microorganisms. The materials being transferred include nutrients, gases and enzymes which are transported at two scales – the mirco-scale and macro-scale (Raghavarao et al., 2003). The macro-scale phenomena include the bulk flow of air into and out of the reactors, natural conduction, convection and diffusion in systems not employing forced aeration, cooling of the reactors by conduction and convection, and the effects of agitation on the substrate bed. At the micro-scale, transfer is dependent on the growth mechanism of the microorganisms and is further subdivided at the particular level.

In aerated reactors, the bulk flow of air serves to cool the solid matrix via evaporative cooling and to provide oxygen to growing microorganisms. The process of transferring oxygen from the bulk air flow to the cells of the microorganism takes place both at the inter- and intra-particular level. Other gases and nutrients in the system also undergo a similar mass transfer mechanism. At the inter-particular level, substances are transferred from the air-filled pores in the solid matrix to the growing microorganism whilst at the intra-particular level, substance are transferred within the solid matrix (Raghavarao et al., 2003).

The effectiveness of mass transfer in any SSF system is dependent on the nature of the substrates and the materials being transferred. This is because concentration gradients of oxygen, enzymes, nutrients and products are developed as microorganisms grow on the substrate. Any change in these concentration gradients is a potential source for limiting mass transfer. For instance, if the void spaces within the solid matrix are mostly filled with water, as opposed to air, growth of the microorganisms will be hindered and thus the rate of product formation will be greatly decreased. Thus, the porosity/void fraction of the substrate bed is extremely important in SSF applications because it allows for the exchange of gases and nutrients in order for aerobic metabolism to be dominant. To evaluate intra-particular mass transfer limitations, the effectiveness factor, η, may be used (Shuler & Kargi, 2002). This factor, which has a maximum value of 1 is defined as $\eta = r_{obs} / r$ where r_{obs} is the observed reaction rate with diffusion limitations and r is the reaction rate in the absence of any diffusion limitations.

2.6.2 Heat Transfer Aspects

The removal of waste metabolic heat is perhaps the most critical factor in large scale value added SSF processes and is limited by the heat capacity of the substrate (Raimbault, 1998). In addition, the porosity and size of the substrate bed decreases as fermentation progresses (Oppenheimer et al., 1997), further limiting heat transfer. Traditional methods of conduction and convection provide limited heat removal capability for packed beds over 15cm in diameter (Mitchell et al., 2000) due to the poor thermal conductivity of most substrates. In aerated packed beds, axial convection and evaporation are the main heat transfer mechanisms, but need to be highly regulated to avoid drying the substrate bed. Periodic mixing, which distributes

the generated heat more evenly across the substrate bed, would also need to be highly regulated to minimize mechanical damage to the microorganisms present.

The major difficulty associated with heat transfer is that it occurs at two different levels within the bioreactor – intra- and inter-particularly. The result of this is non-uniform localized heating that increases the temperature gradients in the system. Thus the rate of heat transfer is hampered by both local and global heat transfer rates and the rate at which heat is transferred between phases, for example, transfer from the particle surface to the gas phase (Raimbault, 1998). Many studies done to model heat transfer aspects of SSF systems have assumed thermal equilibrium between phases in order to simplify the models (VanderGheynst et al., 1997).

2.6.3 Heat Generation

Microbial growth and activity in SSF reactors produces significant amounts of heat that must be properly managed. In composting, this heat generation, which leads to rapid increases in temperature is favorable for material degradation, but in other value added SSF processes such as enzyme production, huge amounts of heat are lethal (dos Santos et al., 2004). Heat generation is a direct result of microorganism metabolic activity, which cannot be directly measured, but may be indicated by a number of different factors (Saucedocastaneda et al., 1990). Some authors; however, doubt the direct proportionality between heat production and microbial growth (Mitchell et al., 2004), but provide no alternatives to this relationship.

The factors which have been used to estimate heat generation are all indicators of microbial activity including oxygen consumption rate (VanderGheynst et al., 1997) carbon dioxide depletion rate (Nakasaki et al., 2000; Saucedocastaneda et al., 1990), and biomass growth rate (Dalsenter et al., 2005; von Meien & Mitchell, 2002). There are assumptions incorporated in the use of any of these components and so the

selected indicator of metabolic activity depends on the desired outcome of the researcher (Mitchell et al., 2004). Due to the complexity of theoretically balancing the intricate components in metabolic heat production, many studies have developed empirical sub-models to represent this phenomenon (Lenz et al., 2004; Mitchell et al., 2004).

Alkoaik et al. (Alkoaik & Ghaly, 2006) determined the amount of heat generated by the composting of greenhouse tomato plant residues in bench scale batch reactors by performing energy balances on the entire system and calculating heat transfer equations based on estimated and theoretical parameters. The authors determined that a cumulative total of 2131.6 KJ of heat was produced from a reactor that was approximately 0.02 m^3 in volume over a period of about 40 hours at a heat production rate of 16.4 KJ/g DM, which falls within the median range of other literature values (Alkoaik & Ghaly, 2006). Of the heat produced, the authors found that the majority of it (62.57%) was lost via convection as exhaust gas since the system was aerated. Compared to this, the amount of heat gained by the organic matrix and the bioreactor materials was minimal (0.9%) and very small losses were seen through the reactor walls (2%) but this is not surprising because the reactors were insulated.

2.6.4 Reactor Design

Reactors designed for SSF systems are built to overcome as many of the challenges associated with heat and mass transfer as possible. For this reason, there exist a number of different designs, each of which focuses on minimizing the effect of a known process constraint or limitation. Since these complications have been well documented, there are certain criteria that must be met by a well-designed SSF reactor.

These requirements (Cen & Xia, 1999; Mitchell et al., 2000; Perez-Guerra et al., 2003; Raghavarao et al., 2003) are to:

(a) Contain the substrate bed – Of importance is the nature of the material used to build the reactors. It must be durable enough to withstand increases in temperature, pressure drops across static piles, and corrosion. The material must also be of low cost and harmless to the process.

(b) Prevent unwanted contamination from entering the reactor – This is of particular importance where sterile environments are required for product growth, such as in the food industry, but is difficult to achieve as a result of solids handling. In addition, the conditions for organism optimal growth, such as pH, flow rate and moisture content may be affected via this contamination.

(c) Have control systems for temperature, heat removal, air flow rate and humidity – The ability to regulate all of these factors that affect the growth of microorganisms is essential for proper product formation. This is perhaps the most difficult aspect of the bioreactor design because gradients (temperature, heat, concentration) can still develop even with control mechanisms in place.

(d) Prevent the uncontrolled release of process microorganisms – Many SSF processes produce pathogens from fungal spores (Raghavarao et al., 2003) and thus need to be exhausted properly to prevent the release of these organisms into the atmosphere.

(e) Maintain uniformity in the substrate bed – This is most commonly achieved via mixing during the process and serves as a deterrent for the formation of local temperature zones and thus leads to fewer and narrower thermal gradients.

(f) Scale up easily – The design employed on the bench scale must also be readily applicable on the large scale for the industrial production of the materials whilst maintaining low cost and low labor intensity.

Once an SSF reactor is built it may be run continuously, in batch, or in fed-batch mode, with batch reactors being the most common. In batch reactors, the solid substrates are mixed and then fermented without the addition of any new material, whereas in continuous reactors, new material is added regularly to the fermenters while fermented material is constantly removed. In fed-batch operations, new material is added periodically to the initial raw material, mixed and allowed to ferment for a given time period. In comparing fed-batch operations to batch operations for the composting of mixed organic substrates, Nakasaki et al. (Nakasaki et al., 1998) determined that organic material degradation was more efficient in batch mode.

Bioreactors currently used for SSF may be static or moving and may or may not employ forced aeration through the substrate bed. The nature of the substrate, inoculum, and product determine the type of bioreactor selected for a given process. Table 2.6 (Mitchell et al., 2000) provides a guide to the choice of bioreactor, taking into consideration issues such as product type, substrate and organism properties.

The abovementioned bioreactor design requirements are also needed for composting systems where process control is a key element; however conventional composting usually takes place in open environments. Conventional composting is done in windrows or piles where the organic matter is heaped in pyramidal shapes and laid out in parallel rows in the open air. In these traditional systems, aeration is limited because it occurs via diffusion and the substrate needs to be

Table 2.6 Selection criteria for bioreactor design (Mitchell et al., 2000)

Organism Growth Type	Agitation Type	Bioreactor Type
Fast	None	Packed bed
Fast	Gentle	Rotating Drum
Fast	Intermittent – Fast	Stirred drum; stirred bed; gas-solid fluidized bed; rocking drum
Slow	None	Tray fermentation
Slow	Slow-Fast	Stirred bed; rotating or stirring drum

Fast growing indicates an organism that grows within 1-5 days, and slow growing refers to an organism that grows in 1-4 weeks

turned continuously to facilitate even heating and degradation. On the other hand, composting in reactors dictates that the process be carried out in an enclosed space. This facilitates rigorous control over the degradation process by proper management of the environmental conditions through engineering and reactor design.

2.7 Modeling composting systems

Mathematical models and simulations of the composting process play an important role in better understanding the process and the underlying mechanisms that drive observed changes. Models serve as an essential tool for evaluating reactor performance and analysis, optimization and scale up predictability. Due to the complexity of the composting process, a singular model that is broadly applicable does not exist and so several models of composting processes span the literature. Many of these models are specific to the substrates used and the reactor systems in which degradation occurred. It is challenging to obtain kinetic parameters for composting processes and this often differentiates the methods used to model different composting systems. The starting point for many models is to place the system in a thermodynamic framework where an energy balance may be performed on the system: Accumulation = input – output ± reaction.

This energy balance is typically placed in a thermodynamic framework and the resulting equations are solved in a deterministic manner using either a lumped parameter approach or a distributed parameter design. In lumped parameter models (Haug, 1993; Higgins & Walker, 2001; Kaiser, 1996; Petric & Selimbasic, 2008; Sole-Mauri et al., 2007; Vlyssides et al., 2009), kinetic parameters have been estimated for the entire reactor, whereas in distributive models (Fanaei & Vaziri, 2009; Sangsurasak & Mitchell, 1998; VanderGheynst et al., 1997; von Meien & Mitchell, 2002), kinetic parameters are typically estimated for various zones of the reactor. For this reason

lumped parameter models are typically described by ordinary differential equations whereas partial differential equations are used in distributed parameter models. Similarities and differences among models in the literature will be discussed in the following sections based on whether they included micro-scale phenomena such as microbial growth and substrate degradation or the macro-scale phenomena of heat and mass transfer,

2.7.1 Microbial growth kinetics

Microbial activities drive changes in composting processes and thus are a good starting point for modeling the process. There are temporal and spatial shifts in structure and population of microbial communities in response to the cycling of metabolites and heat and is governed by several ecological principles such as symbiosis, commensalism and mutualism. Thus to correctly describe microbial community dynamics, population succession must also be taken into account. The method in which microbial activity has been taken into account has varied from indirect methods to more direct methods in recent years.

One of the most indirect methods for estimating heat generation by microbial growth was proposed by Petric (2008) who estimated that heat was generated through an exothermic reaction that occurred when organic matter was degraded. As a result, he proposed that the heat generated biochemically was directly proportional to changes in the mass of the organic matter present in the substrate with a large reaction enthalpy being the proportionality constant:

$$Q = -\Delta h \frac{dm_{OM}}{dt} \tag{2.1}$$

where h is the reaction enthalpy and m_{OM} is the organic matter. Although the author accounted for the heat produced, he failed to capture the equations describing the underlying microbial community responsible for the generated heat.

A commonly used indirect method to measure microbial activity is the oxygen uptake rate because it gives an indication of how much oxygen is transferred from the incoming air to the microorganisms to support growth. The carbon dioxide evolution rate is also used as an indicator of microbial activity under the assumption that all the emitted carbon dioxide is a result of microbial respiration. VanderGheynst et al. (1997) used the oxygen concentrations to estimate microbial activity from which they developed an empirical relationship to describe heat generation. To do this, the authors first developed a relationship between temperature and oxygen consumption rate (RO_2) by plotting experimental oxygen data versus changes in temperature. From the data scatter, the authors developed an empirical equation with an exponential temperature component :

$$RO_2 = RO_{2,0} + a(1 - e^{-c\bar{T}}) \qquad (2.2)$$

where $RO_{2,0}$ is oxygen depletion rate at time zero and position zero, a and c are constants obtained from temperature data regression and $\bar{T}$ is a given temperature minus the temperature at time zero. Parameter estimations by regression analysis were used to calculate the empirical constant of a and c in equation 2.1. This equation was then used to evaluate the heat generation term in the energy equation.

In a fashion similar to VandergGheynst's approach, Higgins and Walker (2001) used the carbon dioxide evolution rate to estimate microbial activity by relating temperature to the rate of carbon dioxide evolution using the cardinal temperature model with inflection (CTMI):

$$R_{CO_2} = \frac{R_{CO_{2,opt}} (T - T_{max})(T - T_{min})^2}{(T_{opt} - T_{min})[(T_{opt} - T_{min})(T - T_{opt}) - (T_{opt} - T_{max})(T_{opt} + T_{min} - 2T)]} \quad (2.3)$$

where R_{CO2} is the carbon dioxide evolution rate, $R_{CO2,\,opt}$ is the carbon dioxide evolution at the optimum temperature, T_{min} is the minimum temperature for system bioactivity, T_{max} is the maximum temperature for system bioactivity, T_{opt} is the optimum temperature for bioactivity and T is the temperature. The authors then used equation 2.3 to develop a kinetic parameter to describe the fraction of biological volatile solids present. The change in the biological volatile solids fraction was then used to calculate the heat produced in the temperature equation.

Direct methods that have been used to describe microbial growth are in the form of various kinetic equations including the logistic equation (Dalsenter et al., 2005; Fanaei & Vaziri, 2009; Sangsurasak & Mitchell, 1998; Stuart & Mitchell, 2003; von Meien & Mitchell, 2002), the exponential growth equation (Ikasari & Mitchell, 2000; Leon et al., 1991; Sang et al., 2004), Monod kinetics (Haug, 1993; Pommier et al., 2008) and other empirically derived equations (Ikasari & Mitchell, 2000). The linear equation is also used, but it is typically use in combination with other kinetic equations. Other kinetic equations are also used in combination to describe different phases of growth. The logistic equation is the most commonly used because it is able to capture the entire growth process from lag phase to the death phase in one single equation and so does not require a combination of equations (Mitchell et al., 2004). Figure 2.4 shows the profiles of some of the most commonly used kinetic equations while Table 2.7 shows the forms of these equations. In all of the models where microbial growth has been directly incorporated, systems of equations are typically developed and need to be solved simultaneously.

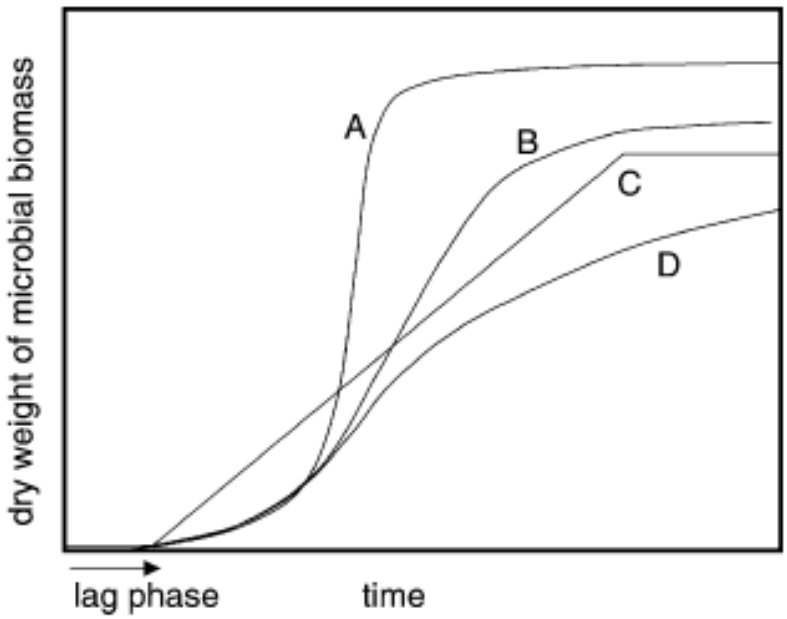

Figure 2.4 Kinetic profiles of commonly used microbial growth equations: (A) exponential, (B) logistic, (C) linear and (D) two phase system with acceleration and deceleration phase. (Mitchell et al., 2004)

Table 2.7 Mathematical forms of commonly used microbial growth kinetic equations

Equation name	Differentiated form	Integrated form
Linear	$\frac{dX}{dt} = C$	$X = Ct + X_0$
Exponential	$\frac{dX}{dt} = \mu X$	$X = X_0 e^{\mu t}$
Logistic	$\frac{dX}{dt} = \mu X\left(1 - \frac{X}{X_m}\right)$	$X = \frac{X_m}{1 + \left(\frac{X_m}{X_0} - 1\right)e^{-\mu t}}$

Kaiser (1996) was the first to separate out microbial biomass into different populations with different rates of growth. For the decomposition of a lignocellulosic substrate, Kaiser divided the microbial community into four different groups based on their ability to degrade various components of the substrate. These microbial groups were bacteria (without actinomycetes), actinomycetes, white rot fungi and brown rot fungi. Kaiser used Monod kinetics to describe the rate of change of growth of these microbial populations on the substrate:

$$\frac{dx_i}{dt} = \mu_{\max,i} f_i^{temp} \frac{S_i}{K_{s,i} + S_i} x_i - \delta x_i \qquad (2.4)$$

where x_i is the microbial population, μ_{max} is the maximum growth rate of organism i, f_i is the coefficient of temperature-dependent growth of organism i, S_i is the total concentration of growth defining substrates for organism i, $K_{s,i}$ is the saturation constant of organism i and δ is the microbial death rate.

Sole-Mauri et al. used a similar approach a few years later in 2007 by separating the microbial populations into three major groups: bacteria, actinomycetes and fungi. These populations were further subdivided into mesophilic and thermophilic populations whose growth was affected by temperature, oxygen concentration, ammonium ion concentration, moisture and substrate availability. The authors in this study also used Monod kinetics, but did not explicitly provide the equations used to calculate microbial growth.

2.7.2 Substrate degradation kinetics

In many composting models, the substrate is regarded as one homogeneous compound that is being acted upon by a microbial community. Although this model

gives a good overall representation of the composting process, it does not account for differences within the substrate itself based on various levels of degradability and structural properties. Kaiser (1996) was the first to recognize the need to partition substrates into different components based on the ability of microbial populations to degrade them, but the difficulty associated with obtaining kinetic parameters for these systems has limited the broad use of such a model in all composting systems.

Kaiser (1996) introduced this concept of separating substrates based on their level of degradability because he recognized that treating the substrate as one compound could not quantitatively represent the performance of composting systems. Kaiser divided lignocellulosic substrates into four components: sugars and starches, hemicelluloses, cellulose and lignin. In his model, bacteria utilize only the sugars and starches, actinomycetes metabolize hemicelluloses and sugars and starches, brown rot fungi utilize sugars and starches, hemicelluloses and cellulose and white rot fungi metabolize lignin in addition to all the components utilized by brown rot fungi. He described this substrate degradation using the following set of equations:

Lignin

$$\frac{ds_4}{dt} = -\frac{1}{Y}\frac{s_4}{s_1 + s_2 + s_3 + s_4}\frac{dx_4}{dt} \tag{2.5}$$

Cellulose

$$\frac{ds_3}{dt} = -\frac{1}{Y}\left(\frac{s_3}{s_1 + s_2 + s_3}\frac{dx_3}{dt} + \frac{s_3}{s_1 + s_2 + s_3 + s_4}\frac{dx_4}{dt}\right) \tag{2.6}$$

Hemicellulose

$$\frac{ds_2}{dt} = -\frac{1}{Y}\left(\frac{s_2}{s_1 + s_2}\frac{dx_2}{dt} + \frac{s_2}{s_1 + s_2 + s_3}\frac{dx_3}{dt} + \frac{s_2}{s_1 + s_2 + s_3 + s_4}\frac{dx_4}{dt}\right) \tag{2.7}$$

Sugars and starches

$$\frac{ds_1}{dt} = -\frac{1}{Y}\left(\frac{dx_1}{dt} + \frac{s_1}{s_1 + s_2}\frac{dx_2}{dt} + \frac{s_1}{s_1 + s_2 + s_3}\frac{dx_3}{dt} + \frac{s_1}{s_1 + s_2 + s_3 + s_4}\frac{dx_4}{dt}\right) \quad (2.8)$$

where Y is the yield coefficient and x_i is the corresponding microbial population for the substrate component. These equations were coupled with the microbial growth equations in order to calculate the heat generated in the overall energy equation.

Sole-Mauri et al. (2007) used a similar approach to Kaiser and broke down the substrate into four components: carbohydrates, proteins and lipids; cellulose, hemicelluloses and lignin. Bacteria, actinomycetes and fungi were selected to grow on carbohydrates, proteins and lipids. In addition, actinomycetes and fungi metabolized hemicelluloses with fungi also being able to utilize cellulose and lignin. The authors also subjected the substrate components to hydrolysis steps before degradation by the microbial populations.

Vlyssides et al. (2009) simplified the substrate partitioning concept introduced by Kaiser by simply separating out the substrate into three categories: that which contained easily biodegradable carbon, difficult biodegradable carbon and inert materials. Under that concept, bacteria were assumed to grow on products resulting from the degradation of easily biodegraded matter, while fungi grew on products resulting from difficult to biodegrade matter:

Easily biodegraded matter

$$\frac{dS_b}{dt} = -\mu_B f_m k_B f_{in} \frac{S_b}{k_{sb} V_L + S_b} X_B \quad (2.9)$$

Difficult biodegraded matter

$$\frac{dS_{db}}{dt} = -\mu_F f_m k_F f_{in} \frac{S_{db}}{k_{sdb} V_L + S_{db}} X_F \quad (2.10)$$

where S is the substrate component, μ_B and μ_F are the maximum uptake rates for bacteria and fungi, respectively, f_m is a moisture content correction factor, k_B and k_F are the growth limiting function of dissolved oxygen for bacteria and fungi, respectively, f_{in} is the inhibition factor, k_{sb} and k_{sdb} are the half saturation constants for bacteria and fungi, respectively, V_L represents the liquid phase and X_B and X_F represent the bacteria and fungi populations. The authors; however did not incorporate equations to describe microbial growth. Instead, they used the substrate degradation equations to calculate carbon dioxide evolution, which was then considered to be directly proportional to the heat produced via biological activity.

2.7.3 Heat balances

The ultimate goal of composting models is to model temperature profiles within composting systems because temperature is one of the most critical variables for evaluating the process. It is for this reason that the method of incorporation of microbial growth kinetics and substrate degradation kinetics differ in the various models. That is, many researchers keep the model as simple as possible as long as the simulated temperature profiles are representative of what was obtained experimentally. As such, there are many composting models that simulate temperature profiles (Fanaei & Vaziri, 2009; Higgins & Walker, 2001; Kaiser, 1996; Petric & Selimbasic, 2008; Sole-Mauri et al., 2007; VanderGheynst et al., 1997; Vlyssides et al., 2009).

Important components of heat balances include heat transport by conduction, convection or radiation, heat production, heat accumulation and latent and sensible heat inputs and outputs. The inclusion on these various components in a model

depend of the reactor system being employed and the simplifications which may be made based on that system. The full general energy equation in cylindrical coordinates is of the form:

$$\rho C_p\left(\frac{\partial T}{\partial t}+v_r\frac{\partial T}{\partial r}+\frac{v_\theta}{r}\frac{\partial T}{\partial \theta}+v_z\frac{\partial T}{\partial z}\right)=k\left[\frac{1}{r}\frac{\partial}{\partial r}\left(r\frac{\partial T}{\partial r}\right)+\frac{1}{r^2}\frac{\partial^2 T}{\partial \theta^2}+\frac{\partial^2 T}{\partial z^2}\right]+\frac{\partial Q}{\partial t} \quad (2.11)$$

which describes temporal changes in temperature in the r, θ and z directions with a heat generation term. The next few paragraphs will give examples of simplifying assumptions used and the resulting heat equation in some composting systems.

VanderGhenyst et al. (1997) developed a temperature model for a cylindrical packed bed reactor with a number of simplifying assumptions. Convective losses to the reactor boundary were considered negligible because the reactors were insulated and diffusion was also considered minimal because of the use of forced aeration. Also, equilibrium was assumed between the gas and solid phase and influent and effluent gases were considered saturated and at constant total pressure. Additionally, based on experimental observations, the transport of energy was considered to be one-dimensional in the direction of air flow and moisture content and mass flux were considered constant during the process. Based on these assumptions, the authors derived the following heat transfer equation:

$$\rho_b\left(c_s+c_w M\right)\frac{\partial \bar{T}}{\partial t}=-G_a\left(c_a+d' e^{m\bar{T}}\right)\frac{\partial \bar{T}}{\partial z}+Q\left(a'-ae^{-cT}\right) \quad (2.12)$$

where ρ_b is the bulk density of dry solids, c_s, c_a and c_w are the heat capacities of the dry solids, air, and waster, respectively, M is the moisture content, t is the time, $\bar{T}$ is

$T - T_0$ where T is the temperature and T_0 is the temperature at time zero, G_a is the mass flux of dry air, d', e, m, a', a and c are from parameter estimations, z is position and Q is the heat generation factor.

The authors produced an analytical solution to this equation by using the method of characteristics and found good agreement between the experimental and predicted values.

Sole-Mauri et al. (2007) rejected the homogeneous assumption made by VanderGheynst et al. (1997) which stated that the gas and solid phases were in equilibrium. Instead Sole-Mauir et al. separated out the two phases into a gas phase and a solid –liquid phase and developed two energy equations based on the separate phases. The two phases are regarded as homogeneous and concentration gradients within particles are considered negligible. The gas phase volume was assumed to be constant and convection was considered to be the main airflow mechanism. Heat is generated in the solid-liquid phase and is transferred to the gas phase by convective heat transfer which is assumed to be proportional to the total mass of compost in the volume. This model was created to simulate a semi-cylindrical composting reactor which utilized insulation and internal mechanical mixers to keep the compost uniform. Based on their assumptions, the authors described temperature in the gas phase (υ):

$$\frac{d\vartheta}{dt} = \frac{q_{Tc} + \vartheta_0 - \vartheta \sum_k \beta_k n_{k0} + T - \vartheta \sum_k \beta_k \max\ 0, Mr_{Tk}}{\sum_k n_k \beta_k} \qquad (2.13)$$

and temperature in the solid-liquid phase (T):

$$\frac{dT}{dt} = \frac{q_{cW} + q_G - q_{Tc} - \sum_k Mr_{Tk} h_k - T - \vartheta_{re} \left(c_{pw} \frac{dw_w}{dt} + \sum_{i=1}^{14} c_{p,i} \frac{dm_i}{dt} \right)}{C_{con} + c_{pw} m_w + \sum_{i=4}^{14} c_{p,i} m_i} \qquad (2.14)$$

where q_{Tc} is convective heat transfer to the gas phase, n_k is the molar flow of the various gases, h_k is the molar enthalpy of the gases, β_k is the dependence of the gases on temperature, Mr_{Tk} is the gas transfer rate, q_G is biological heat generation, q_{cW} is heat transfer through the reactor walls and $m_w c_{pW}$, $m_i c_{p,i}$ and C_{con} represent the thermal capacities of the water, different organic components and the container, respectively. The authors solved this model numerically in MATLAB using the ODE15s routine. It would be interesting to know how much of a difference existed between the gas phase temperature and the solid-liquid phase temperature to determine the validity of the homogeneous assumption used in other models. Given the fact that the experimental set up used by the authors incorporated mechanical mixing to keep the substrate bed uniformly mixed, it is doubtful that major temperature differences existed between the two phases.

Fanaei and Vaziri (2009) also generated a mathematical model to describe temperature profiles in a simple packed bed reactor. The reactor is cylindrical in shape and is supplied with saturated air. The authors assumed that thermal equilibrium exists between the gas and solid phases and that transport in the radial direction is negligible. Based on these assumptions, the authors developed a distributive model with expressions for heat generation, convective and evaporative heat removal:

$$\rho_b C_{pb}\left(\frac{\partial T}{\partial t}\right) = \rho_s (1-\varepsilon)\tilde{Y}_Q \frac{dX}{dt} - \rho_a c_{p,a} V_z \frac{\partial T}{\partial z} - \rho_a f \lambda V_z \frac{\partial T}{\partial z} + k_b \frac{\partial^2 T}{\partial z^2} \qquad (2.15)$$

where ρ_b, ρ_s, ρ_a are the densities of the bed, substrate and moist air, respectively, c_{pb}, c_{pa} are the heat capacities of the substrate bed and moist air, respectively, Y_Q is the metabolic heat yield coefficient, ε is the void fraction, V_Z is the superficial velocity of

the moist air, Z is the bed height, T is the temperature, f is the water carrying capacity of air and λ is the latent heat of evaporation of water.

The authors solved this model numerically using MATLAB by first discretizing their partial differential equations into ordinary differential equations using the method of lines. They then solved their system of equations using the ODE45 routine and found that the distributed heat transfer model compared better with experimental data than the lumped parameter model.

2.7.4 Mass balances

Compared to temperature models, the modeling of mass transfer processes in the literature is limited. This is perhaps due to the implication that the mass transfer of gases and nutrients required for microbial growth must occur in order for heat transfer to take place. Only a few composting models have included explicit equations regarding mass transfer (Higgins & Walker, 2001; Petric & Selimbasic, 2008; Vlyssides et al., 2009).

Higgins and Walker (2001) modeled the transport of oxygen in the composting system designed by VanderGheynst et al. (1997). In the model, the authors assumed that the air exiting the reactor was at the same concentration as the homogeneous bed concentration and that oxygen was only consumed via the biological activity. Also, the oxygen mass fraction within the pore space of the matrix was a good measure of the oxygen within the organic matrix and as such the change in the mass fraction of oxygen in the matrix was described by the equation:

$$\frac{dX_{O_2}}{dt} = \frac{G_a \left(X_{O_{2,a}} - X_{O_{2,exit}} \right) + y_{O2/BVS} \frac{d(BVS)}{dt}}{V_r \varepsilon \rho_a(T)} \tag{2.16}$$

where $X_{O2,a}$ is the concentration of oxygen in ambient air, $X_{O2,exit}$ is the concentration of oxygen in the exit flow, ε is the bed porosity, $y_{O2/BVS}$ is the yield coefficient of oxygen, V_r is the reactor volume, G_a is the mass flow rate of dry air, $\rho_a(T)$ is the temperature dependent air density and BVS is the biological volatile solids. When compared to experimental data, the model frequently over predicted cumulative oxygen concentration, suggesting that drying was influencing the rate of substrate decomposition which had not been accounted for in the model.

Moisture is perhaps the most important mass transfer phenomenon in composting systems because excess drying or too much waster can significantly reduce microbial activities. A moisture transport balance created by Oppenheimer (Oppenheimer, 1997) assumed that water was only generated from metabolic activity and that water loss was reflected in the humidity ratio of the substrate bed at a given temperature, T. Thus, the rate of change of moisture in the system was given by:

$$\frac{dM_d}{dt} = \frac{m_a \left(H_{S(T)} - H_{S(T_{amb})}\right) + \beta_{H_2O} \frac{d(BVS)}{dt}}{\rho_{db} V} \qquad (2.17)$$

where M_d is the moisture content on a dry basis, m_a is the mass flow rate of air, $H_{S(T)}$ is the saturation humidity of exit air at exit reactor temperature, T and $H_{S(Tamb)}$ is the saturation humidity of air at ambient temperature, β_{H2O} is the moisture yield coefficient, BVS is the biological volatile solids, V is the system volume and ρ_{db} is the density of the dry bulk. Oppenheimer found good agreement between experimental data and his model and was able to simulate various moisture profiles based on different water yield coefficients.

Similar to Oppenheimer, Petric and Selimbasic (2008) modeled the transport of water in a composting system with the exception that he separated out the water into

what was present in the gas phase and what was present in the composting material. In addition, the authors accounted for oxygen, carbon dioxide and ammonia gases that had been dissolved in the water. The authors generated the following equation for the mass balance of water in the composting material:

$$\frac{dm_w}{dt} = -Y_w \frac{dm_{OM}}{dt} - k_L a_w \left(P_s - P_v\right) \tag{2.18}$$

where the first expression on the right hand side accounts for the generation of water from organic matter degradation, similar to Oppenheimer's equation and the second term on the right represents the transfer rate of water between the solid-liquid phase and the gas phase. Surprisingly, even though the authors presented equations for moisture content, no mention was made of this mass balance in the results section, so the authors gave no indication of how well their equations simulated experimental findings.

2.7.5 Mathematical solutions

The proper modeling of composting processes often results in systems of nonlinear equations that must be solved simultaneously. As our understanding of the process continues to grow, one can only expect that these systems of equations will become more complex. The modeling of temperature alone may be solved analytically, as was done by VanderGheynst et al. (1997) by using the method of characteristics. With the inclusion of more variables mathematical solutions are trending towards numerical solutions and MATLAB is a powerful software for solving such systems of equations and has been widely used in solving composting models (Fanaei & Vaziri, 2009; Higgins & Walker, 2001; Sole-Mauri et al., 2007; Vlyssides et al., 2009). Most of these systems were solved using the ODE45 routine which uses

a fourth-fifth order Runge Kutta method to solve systems of ordinary differential equations. In distributive methods where partial differential equations are obtained, the system must first be discretized using methods such as finite, central, backward or forward difference before the ODE45 routine may be implemented.

2.8 Summary

Composting may be regarded as the most complex SSF process because of the numerous microbial communities that work together in very intricate relationships to degrade organic matter. Through this microbial activity, waste metabolic heat is produced; thereby, elevating the temperature within the compost pile. The proper management of this generated heat, along with the management of mass transfer aspects is essential for controlling the behavior of SSF processes. In composting, one must first understand how the microbial communities interact to degrade organic material in order to be able to control and eventually predict compost reactor behavior. Molecular biology has evolved to produce numerous high-throughput tools that facilitate the characterization of microbial communities both qualitatively and quantitatively. These tools allow for the tracking of microbial communities over time, the identification of groups present, and the amounts of each group present. Furthermore, these methods can determine which microbial groups are active at a given time and how these groups evolve during the course of the process. In characterizing compost microbial communities, most of the research has focused on the use of qualitative methods to describe process dynamics. In order to turn molecular biology into a predictive science, quantitative data must also be extracted; hence the need for the research presented in this thesis. By quantifying the microbial groups present, one can determine the amounts and types of microbes responsible for a given amount of heat generated. From the quantification of the heat generated, one

can then develop a model that incorporates microbial activity in order to predict reactor behavior.

The ability to predict reactor behavior during composting is also critical because it leads to a better understanding of the process and lays the foundation for better experimental control. Several models have been developed to date to describe composting processes because one overarching general model does not exist. This is due to the complexity of the process and given how different the substrates and reactor systems used, it may not be desirable to have one generalized model. The most important thing may be the ability to correctly link the microbial growth kinetics to the substrate degradation kinetics and incorporate these linkages into traditional heat and mass transfer equations in order to simulate changes in state variables. Accurately grasping these underlying mechanisms will then set the foundation for using these mathematical models as tools for optimizing composting and other solid state bioprocesses.

REFERENCES

Adney, S., van der Lelie, D., Berry, A., M., H. 2008. *Biomass Recalcitrance*. John Wiley and Sons Incorporated.

Alfreider, A., Peters, S., Tebbe, C.C., Rangger, A., Insam, H. 2002. Microbial community dynamics during composting of organic matter as determined by 16S ribosomal DNA analysis. *Compost Science & Utilization*, **10**(4), 303-312.

Alkoaik, F., Ghaly, A.E. 2006. Determination of heat generated by metabolic activities during composting of greenhouse tomato plant residues. *Journal of Environmental Engineering and Science*, **5**(2), 137-150.

Andersson, A.F., Lindberg, M., Jakobsson, H., Backhed, F., Nyren, P., Engstrand, L. 2008. Comparative Analysis of Human Gut Microbiota by Barcoded Pyrosequencing. *Plos One*, **3**(7).

Bachoon, D.S., Otero, E., Hodson, R.E. 2001. Effects of humic substances on fluorometric DNA quantification and DNA hybridization. *Journal of Microbiological Methods*, **47**(1), 73-82.

Bari, Q.H., Koenig, A., Guihe, T. 2000. Kinetic analysis of forced aeration composting - I. Reaction rates and temperature. *Waste Management & Research*, **18**(4), 303-312.

Beck-Friis, B., Smars, S., Jonsson, H., Eklind, Y., Kirchmann, H. 2003. Composting of source-separated household organics at different oxygen levels: Gaining an understanding of the emission dynamics. *Compost Science & Utilization*, **11**(1), 41-50.

Bellon-Maurel, W., Orliac, O., Christen, P. 2003. Sensors and measurements in solid state fermentation: a review. *Process Biochemistry*, **38**(6), 881-896.

Beltz, F. 2000. Acidity in the Early Stages of Composting. in: *Civil and Environmental Engineering*, Vol. Master of Science, Cornell University. Ithaca, pp. 90.

Bibby, K., Viau, E., Peccia, J. 2010. Pyrosequencing of the 16S rRNA gene to reveal bacterial pathogen diversity in biosolids. *Water Research*, **44**(14), 4252-4260.

Blanc, M., Marilley, L., Beffa, T., Aragno, M. 1999. Thermophilic bacterial communities in hot composts as revealed by most probable number counts and molecular (16S rDNA) methods. *Fems Microbiology Ecology*, **28**(2), 141-149.

Cannel, E., Mooyoung, M. 1980. Solid-State Fermentation Systems. *Process Biochemistry*, **15**(5), 2-&.

Cen, P., Xia, L. 1999. Production of Cellulase by Solid-State Fermentation. *Advances in Biochemical Engineering/Biotechnology*, **65**.

Chandra, R.P., Bura, R., Mabee, W.E., Berlin, A., Pan, X., Saddler, J.N. 2007. Substrate pretreatment: The key to effective enzymatic hydrolysis of lignocellulosics? in: *Biofuels*, Vol. 108, Springer-Verlag Berlin. Berlin, pp. 67-93.

Chroni, C., Kyriacou, A., Georgaki, I., Manios, T., Kotsou, M., Lasaridi, K. 2009. Microbial characterization during composting of blowaste. *Waste Management*, **29**(5), 1520-1525.

Cooperband, L. 2002. The Art and Science of Composting - A Resource for Farmers and Compost Producers. University of Wisconsin - Madison.

Dalsenter, F.D.H., Viccini, G., Barga, M.C., Mitchell, D.A., Krieger, N. 2005. A mathematical model describing the effect of temperature variations on the kinetics of microbial growth in solid-state culture. *Process Biochemistry*, **40**(2), 801-807.

Dees, P.M., Ghiorse, W.C. 2001. Microbial diversity in hot synthetic compost as revealed by PCR-amplified rRNA sequences from cultivated isolates and extracted DNA. *Fems Microbiology Ecology*, **35**(2), 207-216.

dos Santos, M.M., da Rosa, A.S., Dal'Boit, S., Mitchell, D.A., Krieger, N. 2004. Thermal denaturation: is solid-state fermentation really a good technology for the production of enzymes? *Bioresource Technology*, **93**(3), 261-268.

Fanaei, M.A., Vaziri, B.M. 2009. Modeling of temperature gradients in packed-bed solid-state bioreactors. *Chemical Engineering And Processing*, **48**(1), 446-451.

Fogarty, A.M., Tuovinen, O.H. 1991. Microbiological Degradation of Pesticides in Yard Waste Composting. *Microbiological Reviews*, **55**(2), 225-233.

Gajalakshmi, S., Abbasi, S.A. 2008. Solid waste management by composting: State of the art. *Critical Reviews in Environmental Science and Technology*, **38**(5), 311-400.

Gervais, P., Molin, P. 2003. The role of water in solid-state fermentation. *Biochemical Engineering Journal*, **13**(2-3), 85-101.

Goldberg, S.M.D., Johnson, J., Busam, D., Feldblyum, T., Ferriera, S., Friedman, R., Halpern, A., Khouri, H., Kravitz, S.A., Lauro, F.M., Li, K., Rogers, Y.H., Strausberg, R., Sutton, G., Tallon, L., Thomas, T., Venter, E., Frazier, M., Venter, J.C. 2006. A Sanger/pyrosequencing hybrid approach tor the generation of high-quality draft assemblies of marine microbial genomes. *Proceedings Of The National Academy Of Sciences Of The United States Of America*, **103**(30), 11240-11245.

Hansgate, A.M., Schloss, P.D., Hay, A.G., Walker, L.P. 2005. Molecular characterization of fungal, community dynamics in the initial stages of composting. *Fems Microbiology Ecology*, **51**(2), 209-214.

Hatsu, M., Ohta, J., Takamizawa, K. 2002. Monitoring of Bacillus thermodenitrificans OHT-1 in compost by whole cell hybridization. *Canadian Journal of Microbiology*, **48**(9), 848-852.

Haug, R.T. 1993. *The Practical Handbook of Compost Engineering*. Lewis Publishers.

Higgins, C.W., Walker, L.P. 2001. Validation of a new model for aerobic organic solids decomposition: simulations with substrate specific kinetics. *Process Biochemistry*, **36**(8-9), 875-884.

Hogan, J.A., Miller, F.C., Finstein, M.S. 1989. Physical Modeling of the Composting Ecosystem. *Applied and Environmental Microbiology*, **55**(5), 1082-1092.

Holker, U., Hofer, M., Lenz, J. 2004. Biotechnological advantages of laboratory-scale solid-state fermentation with fungi. *Applied Microbiology and Biotechnology*, **64**(2), 175-186.

Holker, U., Lenz, J. 2005. Solid-state fermentation - are there any biotechnological advantages? *Current Opinion in Microbiology*, **8**(3), 301-306.

Huang, D.-L., Zeng, G.-M., Feng, C.-L., Hu, S., Lai, C., Zhao, M.-H., Su, F.-F., Tang, L., Liu, H.-L. 2010. Changes of microbial population structure related to lignin degradation during lignocellulosic waste composting. *Bioresource Technology*, **101**(11), 4062.

Ikasari, L., Mitchell, D.A. 2000. Two-phase model of the kinetics of growth of Rhizopus oligosporus in membrane culture. *Biotechnology and Bioengineering*, **68**(6), 619-627.

Ishii, K., Fukui, M., Takii, S. 2000. Microbial succession during a composting process as evaluated by denaturing gradient gel electrophoresis analysis. *Journal of Applied Microbiology*, **89**(5), 768-777.

Kaiser, J. 1996. Modelling composting as a microbial ecosystem: A simulation approach. *Ecological Modelling*, **91**(1-3), 25-37.

Kornillowicz-Kowalska, T., Bohacz, J. 2010. Dynamics of growth and succession of bacterial and fungal communities during composting of feather waste. *Bioresource Technology*, **101**(4), 1268-1276.

Kowalchuk, G.A., Naoumenko, Z.S., Derikx, P.J.L., Felske, A., Stephen, J.R., Arkhipchenko, I.A. 1999. Molecular analysis of ammonia-oxidizing bacteria of the beta subdivision of the class Proteobacteria in compost and composted materials. *Applied and Environmental Microbiology*, **65**(2), 396-403.

Lenz, J., Hofer, M., Krasenbrink, J.B., Holker, U. 2004. A survey of computational and physical methods applied to solid-state fermentation. *Applied Microbiology and Biotechnology*, **65**(1), 9-17.

Leon, R., Torres, A., Echevarria, J., Saura, G. 1991. Energy-Balance in Solid-State Fermentation Processes. *Acta Biotechnologica*, **11**(1), 9-14.

Lu, W.J., Wang, H.T., Nie, Y.F., Wang, Z.C., Huang, D.Y., Qiu, X.Y., Chen, J.C. 2004. Effect of inoculating flower stalks and vegetable waste with ligno-cellulolytic microorganisms on the composting process. *Journal of Environmental Science and Health Part B-Pesticides Food Contaminants and Agricultural Wastes*, **39**(5-6), 871-887.

Madigan, M., Martinko, J., Parker, J. 2002. *Brock Biology of Microorganisms*. *10 ed*. Prentice Hall, Upper Saddle River.

Malinen, E., Kassinen, A., Rinttila, T., Palva, A. 2003. Comparison of real-time PCR with SYBR Green I or 5 '-nuclease assays and dot-blot hybridization with rDNA-targeted oligonucleotide probes in quantification of selected faecal bacteria. *Microbiology-Sgm*, **149**, 269-277.

Margulies, M., Egholm, M., Altman, W.E., Attiya, S., Bader, J.S., Bemben, L.A., Berka, J., Braverman, M.S., Chen, Y.J., Chen, Z.T., Dewell, S.B., Du, L., Fierro, J.M., Gomes, X.V., Godwin, B.C., He, W., Helgesen, S., Ho, C.H.,

Irzyk, G.P., Jando, S.C., Alenquer, M.L.I., Jarvie, T.P., Jirage, K.B., Kim, J.B., Knight, J.R., Lanza, J.R., Leamon, J.H., Lefkowitz, S.M., Lei, M., Li, J., Lohman, K.L., Lu, H., Makhijani, V.B., McDade, K.E., McKenna, M.P., Myers, E.W., Nickerson, E., Nobile, J.R., Plant, R., Puc, B.P., Ronan, M.T., Roth, G.T., Sarkis, G.J., Simons, J.F., Simpson, J.W., Srinivasan, M., Tartaro, K.R., Tomasz, A., Vogt, K.A., Volkmer, G.A., Wang, S.H., Wang, Y., Weiner, M.P., Yu, P.G., Begley, R.F., Rothberg, J.M. 2005. Genome sequencing in microfabricated high-density picolitre reactors. *Nature*, **437**(7057), 376-380.

Mitchell, D., Berovic, M., Kriegerm, N. 2000. Biochemical Engineering Aspects of Solid State Bioprocessing. *Advances in Biochemical Engineering/Biotechnology*, **68**.

Mitchell, D.A., von Meien, O.F., Krieger, N., Dalsenter, F.D.H. 2004. A review of recent developments in modeling of microbial growth kinetics and intraparticle phenomena in solid-state fermentation. *Biochemical Engineering Journal*, **17**(1), 15-26.

Montiel-Gonzalez, A.M., Viniegra-Gonzalez, G., Fernandez, F.J., Loera, O. 2004. Effect of water activity on invertase production in solid state fermentation by improved diploid strains of Aspergillus niger. *Process Biochemistry*, **39**(12), 2085-2090.

Muyzer, G. 1999. Genetic Fingerprinting of Microbial Communities - Present Status and Future Perspectives. *International Symposium on Microbial Ecology*, Halifax, Canada. Atlantic Canada Society for Microbial Ecology.

Nakasaki, K., Akakura, N., Atsumi, K., Takemoto, M. 1998. Degradation patterns of organic material in batch and fed-batch composting operations. *Waste Management & Research*, **16**(5), 484-489.

Nakasaki, K., Akakura, N., Takemoto, M. 2000. Predicting the Degradation Pattern of Organic Materials in the Composting of a Fed-batch Operation as Inferred from the Results of a Batch Operation. *J Mater Cylcles Waste Management*, **2**, 31-37.

Oppenheimer, J.R. 1997. Compost Process Model Development, Validation, and Simulation to Assess Moisture and Energy Management. in: *Biological and Environmental Engineering*, Vol. M.S., Cornell University. Ithaca, pp. 148.

Oppenheimer, J.R., Martin, A.G., Walker, L.P. 1997. Measurements of air-filled porosity in unsaturated organic matrices using a pycnometer. *Bioresource Technology*, **59**(2-3), 241-247.

Oriol, E., Raimbault, M., Roussos, S., Viniegragonzales, G. 1988. Water and Water Activity in the Solid-State Fermentation of Cassava Starch by Aspergillus-Niger. *Applied Microbiology and Biotechnology*, **27**(5-6), 498-503.

Pandey, A. 2003. Solid-state fermentation. *Biochemical Engineering Journal*, **13**(2-3), 81-84.

Pandey, A., Soccol, C.R., Mitchell, D. 2000. New developments in solid state fermentation: I-bioprocesses and products. *Process Biochemistry*, **35**(10), 1153-1169.

Pedro, M.S., Haruta, S., Hazaka, M., Shimada, R., Yoshida, C., Hiura, K., Ishii, M., Igarashi, Y. 2001. Denaturing gradient gel electrophoresis analyses of microbial community from field-scale composter. *Journal of Bioscience and Bioengineering*, **91**(2), 159-165.

Pedro, M.S., Haruta, S., Nakamura, K., Hazaka, M., Ishii, M., Igarashi, Y. 2003. Isolation and characterization of predominant microorganisms during decomposition of waste materials in a field-scale composter. *Journal of Bioscience and Bioengineering*, **95**(4), 368-373.

Perez-Guerra, N., A., T.-A., C., L.-M., Pastrana, L. 2003. Main Characteristics and Applications of Solid Substrate Fermentation. *Electronic Journal of Environmental, Agricultural and Food Chemistry*, **2**(3), 343-350.

Peters, S., Koschinsky, S., Schwieger, F., Tebbe, C.C. 2000. Succession of microbial communities during hot composting as detected by PCR-single-strand-conformation polymorphism-based genetic profiles of small-subunit rRNA genes. *Applied and Environmental Microbiology*, **66**(3), 930-936.

Petric, I., Selimbasic, V. 2008. Development and validation of mathematical model for aerobic composting process. *Chemical Engineering Journal*, **139**(2), 304-317.

Pfaffl, M.W. 2001. A new mathematical model for relative quantification in real-time RT-PCR. *Nucleic Acids Research*, **29**(9).

Pommier, S., Chenu, D., Quintard, M., Lefebvre, X. 2008. Modelling of moisture-dependent aerobic degradation of solid waste. *Waste Management*, **28**(7), 1188-1200.

Prakasham, R.S., Rao, C.S., Rao, R.S., Sarma, P.N. 2005. Alkaline protease production by an isolated Bacillus circulans under solid-state fermentation using agroindustrial waste: Process parameters optimization. *Biotechnology Progress*, **21**(5), 1380-1388.

Pryor, S.W. 2005. Optimization of the Solid State Fermentation of Bacillus Subtilis: Production of Antifungal Lipopeptides and use as a Biological Control Agent. in: *Biological and Environmental Engineering*, Vol. Doctor of Philosophy, Cornell University. Ithaca, pp. 203.

Qiagen. 2010. Critical Factors for Successful Real Time PCR.

Raghavarao, K.S.M.S., Ranganathan, T.V., Karanth, N.G. 2003. Some engineering aspects of solid-state fermentation. *Biochemical Engineering Journal*, **13**(2-3), 127-135.

Raimbault, M. 1998. General and Microbiological Aspects of Solid Substrate Fermentation. *Electronic Journal of Biotechnology*, **1**(3).

Ranjard, L., Poly, F., Lata, J.C., Mougel, C., Thioulouse, J., Nazaret, S. 2001. Characterization of bacterial and fungal soil communities by automated ribosomal intergenic spacer analysis fingerprints: Biological and methodological variability. *Applied and Environmental Microbiology*, **67**(10), 4479-4487.

Sang, B.I., Hori, K., Unno, H. 2004. A mathematical description for the fungal degradation process of biodegradable plastics. *Mathematics And Computers In Simulation*, **65**(1-2), 147-155.

Sangsurasak, P., Mitchell, D.A. 1998. Validation of a model describing two-dimensional heat transfer during solid-state fermentation in packed bed bioreactors. *Biotechnology and Bioengineering*, **60**(6), 739-749.

Saucedocastaneda, G., Gutierrezrojas, M., Bacquet, G., Raimbault, M., Viniegragonzalez, G. 1990. Heat-Transfer Simulation in Solid Substrate Fermentation. *Biotechnology and Bioengineering*, **35**(8), 802-808.

Schloss, P.D. 2002. Quantitative Molecular Analysis of Microbial Succession in Compost and its Ramifications on Process Reproducibility. in: *Biological and Environmental Engineering*, Vol. Doctor of Philosophy, Cornell University. Ithaca, pp. 170.

Schloss, P.D., Hay, A.G., Wilson, D.B., Gossett, J.M., Walker, L.P. 2005. Quantifying bacterial population dynamics in compost using 16S rRNA gene probes. *Applied Microbiology and Biotechnology*, **66**(4), 457-463.

Schloss, P.D., Hay, A.G., Wilson, D.B., Walker, L.P. 2003. Tracking temporal changes of bacterial community fingerprints during the initial stages of composting. *Fems Microbiology Ecology*, **46**(1), 1-9.

Shuler, M., Kargi, F. 2002. *Bioprocess Engineering Basic Concepts*. *Second ed*. Prentice Hall, Upper Saddle River.

Smit, E., Leeflang, P., Glandorf, B., van Elsas, J.D., Wernars, K. 1999. Analysis of fungal diversity in the wheat rhizosphere by sequencing of cloned PCR-amplified genes encoding 18S rRNA and temperature gradient gel electrophoresis. *Applied and Environmental Microbiology*, **65**(6), 2614-2621.

Sole-Mauri, F., Illa, J., Magri, A., Prenafeta-Boldu, F.X., Flotats, X. 2007. An integrated biochemical and physical model for the composting process. *Bioresource Technology*, **98**(17), 3278-3293.

Spiegelman, D., Whissell, G., Greer, C.W. 2005. A survey of the methods for the characterization of microbial consortia and communities. *Canadian Journal of Microbiology*, **51**(5), 355-386.

Steger, K., Eklind, Y., Olsson, J., Sundh, I. 2005. Microbial community growth and utilization of carbon constituents during thermophilic composting at different oxygen levels. *Microbial Ecology*, **50**(2), 163-171.

Strom, P.F. 1985a. Effect of Temperature on Bacterial Species-Diversity in Thermophilic Solid-Waste Composting. *Applied and Environmental Microbiology*, **50**(4), 899-905.

Strom, P.F. 1985b. Identification of Thermophilic Bacteria in Solid-Waste Composting. *Applied and Environmental Microbiology*, **50**(4), 906-913.

Stuart, D.M., Mitchell, D.A. 2003. Mathematical model of heat transfer during solid-state fermentation in well-mixed rotating drum bioreactors. *Journal of Chemical Technology and Biotechnology*, **78**(11), 1180-1192.

Sundberg, C., Jonsson, H. 2008. Higher pH and faster decomposition in biowaste composting by increased aeration. *Waste Management*, **28**(3), 518-526.

Sundberg, C., Smars, S., Jonsson, H. 2004. Low pH as an inhibiting factor in the transition from mesophilic to thermophilic phase in composting. *Bioresource Technology*, **95**(2), 145-150.

Tang, J.C., Kanamori, T., Inoue, Y., Yasuta, T., Yoshida, S., Katayama, A. 2004. Changes in the microbial community structure during thermophilic composting of manure as detected by the quinone profile method. *Process Biochemistry*, **39**(12), 1999-2006.

Tengerdy, R.P., Szakacs, G. 2003. Bioconversion of lignocellulose in solid substrate fermentation. *Biochemical Engineering Journal*, **13**(2-3), 169-179.

Trautmann, N., Olynciw, E. 2002. Compost Microorganisms. in: *Cornell Composting Science & Engineering*, Vol. 2007. Ithaca.

Tuomela, M., Vikman, M., Hatakka, A., Itavaara, M. 2000. Biodegradation of lignin in a compost environment: a review. *Bioresource Technology*, **72**(2), 169-183.

VanderGheynst, J.S., Walker, L.P., Parlange, J.Y. 1997. Energy transport in a high-solids aerobic degradation process: Mathematical modeling and analysis. *Biotechnology Progress*, **13**(3), 238-248.

Viniegra-Gonzalez, G., Favela-Torres, E., Aguilar, C.N., Romero-Gomez, S.D., Diaz-Godinez, G., Augur, C. 2003. Advantages of fungal enzyme production in solid state over liquid fermentation systems. *Biochemical Engineering Journal*, **13**(2-3), 157-167.

Vlyssides, A., Mai, S., Barampouti, E.M. 2009. An integrated mathematical model for co-composting of agricultural solid wastes with industrial wastewater. *Bioresource Technology*, **100**(20), 4797-4806.

von Meien, O.F., Mitchell, D.A. 2002. A two-phase model for water and heat transfer within an intermittently-mixed solid-state fermentation bioreactor with forced aeration. *Biotechnology and Bioengineering*, **79**(4), 416-428.

Walker, L.P., Nock, T.D., Gossett, J.M., VanderGheynst, J.S. 1999. The role of periodic agitation and water addition in managing moisture limitations during high-solids aerobic decomposition. *Process Biochemistry*, **34**(6-7), 601-612.

Wyman, C.E., Dale, B.E., Elander, R.T., Holtzapple, M., Ladisch, M.R., Lee, Y.Y. 2005. Coordinated development of leading biomass pretreatment technologies. *Bioresource Technology*, **96**(18), 1959-1966.

Xu, W.P., Reuter, T., Xu, Y.P., Alexander, T.W., Gilroyed, B., Jin, L.J., Stanford, K., Larney, F.J., McAllister, T.A. 2009. Use of Quantitative and Conventional PCR to Assess Biodegradation of Bovine and Plant DNA during Cattle Mortality Composting. *Environmental Science & Technology*, **43**(16), 6248-6255.

Yu, H., Zeng, G.M., Huang, H.L., Xi, X.M., Wang, R.Y., Huang, D.L., Huang, G.H., Li, J.B. 2007. Microbial community succession and lignocellulose degradation during agricultural waste composting. *Biodegradation*, **18**(6), 793-802.

CHAPTER 3

ABIOTIC AND BIOTIC DYNAMICS DURING THE INITIAL STAGES OF HIGH-SOLIDS SWITCHGRASS DEGRADATION[†]

Abstract

Understanding the underlying dynamics of how biotic variables drive changes in abiotic parameters in the early stages of biomass biodegradation is essential for better control of the process. Probe hybridization was used to quantitatively study the growth of bacteria, yeast and fungi for three initial moisture content (MC): 60%, 65% and 75% over a period of 64h. Changes in abiotic parameters were also documented. By 64h, samples were significantly differentiated both in the temporal and spatial dimension, proving that considerable changes had occurred in these initial stages. Maximum carbon (C) conversion occurred in the 75% MC reactor at a peak value of 49%, with 40% and 37% in the 65 and 60% MC reactors, respectively. Higher T, higher pH, higher rates of O_2 consumption and CO_2 evolution were also observed in the highest moisture reactor; suggesting that of the 3 MCs studied, 75% MC was the best MC for the process. MC during the process also proved to be important because it greatly influenced variation in the spatial dimension, further underscoring the importance of characterizing changes with bed height. Most importantly, we were able to positively correlate the rate of substrate degradation with the bacterial biomass levels and highlight the critical role of bacteria in biological decomposition.

[†] This work has been accepted for publication in Environmental Technology as Fontenelle, L.T., Corgie, SC., Walker LP.2010. Abiotic and biotic dynamics during the initial stages of high solids switchgrass degradation.

3.1 Introduction

Microbial degradation is an effective way of liberating the chemical components and energy content of lignocellulosic biomass. In natural systems, this occurs via a complex ecology of heterotrophic bacterial and fungal microorganisms that generate heat and other gaseous products in an intricate feedback loop that produces dramatic changes in abiotic state variables such as temperature (T), pH and substrate composition. The underlying mechanism of microbial degradation processes is poorly characterized and remains challenging because of the complexity of the biotic and abiotic interactions which vary in spatial and temporal dimensions to maximize nutrient cycling and the biochemical rate of carbon cycling (Adney et al., 2008). Thus, better understanding of the coupled biotic and abiotic mechanisms and feedback loops is essential for deploying high-solids microbial processes for bioenergy and bioproducts process applications.

A key variable in biodegradation processes that may be manipulated to control the process is moisture. The amount of moisture in the substrate is critical because decomposition occurs at the thin liquid films on the surfaces of particles and involves enzymatic action, biomass growth, and nutrient and gas transport (Bellon-Maurel et al., 2003; Gervais & Molin, 2003) and major losses in moisture dramatically decrease rates of organic decomposition (Haug, 1993). Variations in moisture content (MC) occur as a result of water evaporation through mass transfer and from water production via metabolism. Also, in systems employing forced aeration, high aeration rates can lead to significant drying of the organic matrix and a reduction in microbial activity; thus, to minimize drying, high-solids reactors are often aerated with saturated air (Hogan et al., 1989; Oriol et al., 1988; VanderGheynst et al., 1997) or water is periodically added (Nakasaki et al., 1998; Walker et al., 1999) to the substrate bed. Therefore, maintaining sufficient amounts of moisture to sustain microbial growth and

activity is essential for the proper functioning of the underlying microbial community that drives the process.

Heterotrophic microbial activity drive biodegradation processes through a series of phases that are most easily differentiated based on T values. The initial phase is characterized by rapid increases in T and decreases in pH. This stage, known as the mesophilic phase, is characterized by T in the range of 10 to 40^{o}C (Gajalakshmi & Abbasi, 2008) and the presence yeasts, lactic acid bacteria, fungi and Gram-negative bacteria (Steger et al., 2005). During the next phase, termed the thermophilic phase, basic pH conditions and high T in the range of 45 to 60^{o}C (Gajalakshmi & Abbasi, 2008) are sustained through the metabolism of many Bacillus spp. and Thermus thermophilus (Steger et al., 2005). In the final phase, which is the cooling phase, T decrease and complex substrates, such as lignin, are degraded by a new mesophilic community (Steger et al., 2005). Many studies have described changes in physico-chemical parameters throughout these phases (see (Gajalakshmi & Abbasi, 2008) for summary) and more recently, advancements in molecular biology have provided culture-independent tools for recent investigations into the composition of microbial communities (Chroni et al., 2009; Dees & Ghiorse, 2001; Franke-Whittle et al., 2005; Lei & VanderGheynst, 2000; Pedro et al., 2003; Peters et al., 2000; Schloss et al., 2005). Much less work has been done; however on linking changes in physico-chemical variables to quantitative changes in biotic parameters and investigating how these changes vary in the spatial dimension.

The main goal of this study was to provide greater insight into the temporal and spatial dynamics and interactions of abiotic and biotic parameters in the initial stages of high-solids switchgrass degradation, where the most rapid changes in physico-chemical variables occur. Experiments were conducted over a period of 64 hr where major changes in abiotic and biotic state variables were observed, and temporal

changes in moisture content (MC) and bed compaction was kept to a minimum. The dimensions of this study were further increased by studying the effect of the initial MC on the degradation process because moisture is a key variable that may be manipulated to better control the process.

3.2 Materials and Methods

3.2.1 Reactor design and construction

Bench-scale reactors with a working volume of 50L each were constructed from a high density polyethylene (HDPE) pipe with an inner diameter of 0.3m. In each reactor, sampling ports of diameter 3.2cm were placed 10cm apart along the length of the reactor to facilitate spatial sampling. The sampling ports were placed at four different positions along the circumference of the reactor to minimize bed disturbance during sampling. A perforated plate was placed at 0.2m from the bottom of the reactor on top of a polyvinylchloride (PVC) ring to support the substrate bed and to evenly distribute the incoming air throughout the substrate bed. Approximately 95% of the perforated plate was made up of 10mm holes. The sampling ports were placed at 0.1m, 0.2m, 0.3m, 0.4m, 0.5m, 0.6m and 0.7m above the perforated plate and were named accordingly. Stainless steel racks were custom made to fit inside of the reactors to provide an immobile support for the thermocouples. PVC fittings were mounted at the base of the reactors to allow for the inlet of air and the collection of leachate. The reactors were insulated with a foil and fiberglass duct insulation (Thermwell Products Co. Inc., Mahwa, NJ). The reactor set-up is illustrated in Figure 3.1.

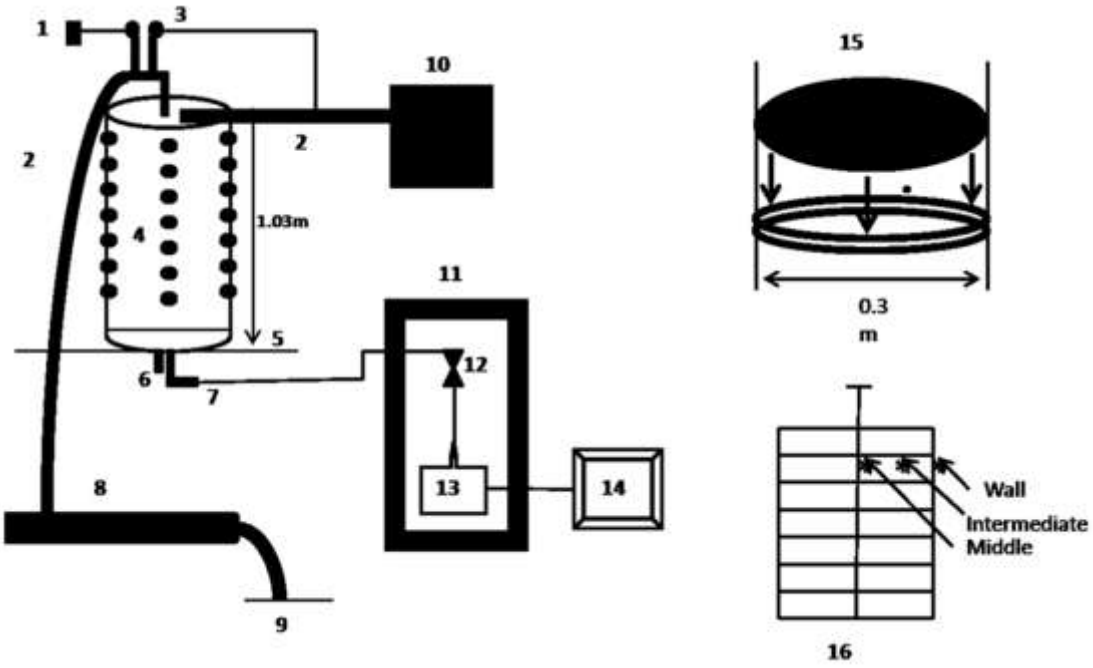

Figure 3.1 Schematic of reactor setup where 1= carbon dioxide sensor and monitor; 2 = exhaust line; 3= oxygen sensor; 4= reactor; 5 = wooden frame; 6 = leachate drain; 7 = air inlet; 8 = PVC pipe; 9 = underground building exhaust line; 10 = data acquisition system; 11= incubator; 12= flow meter; 13 = humidifier; 14 = air compressor; 15 = perforated plate setup for reactor interior; 16 = stainless steel rack for reactor interior

Table 3.1 Physico-chemical properties of substrates

Property	Switchgrass	Dog food
Carbon (%)	44.0	25.0
Nitrogen (%)	0.5	5.3
Volatile solids (%)	80.1	89.5
Moisture (%)	9.0	7.0
pH	6.79	4.5

3.2.2 Substrate Preparation

Switchgrass (Stickle Farm, Ligonier, PA) was used as the lignocellulosic source for this study because it has been identified as one of the most suitable energy crops. The switchgrass (*shelter*) was size-reduced using a Buffalo Hammer Mill (Schutte-Buffalo, Hammer Mill, Buffalo, NY) and was mixed with dog food (Big Red Puppy Food, Pro Pet Inc., Syracuse) – a reproducible source of soluble nutrients for high rate degradation – in a mass ratio of 1:1 resulting in a carbon to nitrogen ratio of 15 to 1, with a total combined dry mass of 7kg. Physico-chemical properties of switchgrass and dog food are given in Table 1. Given that for most substrates, MC in the range of 60-70% results in rapid increases in microbial activity (Gajalakshmi & Abbasi, 2008; Liang et al., 2003), water was added to the substrate mixtures to bring them to initial MC of 60%, 65% and 75% (wet basis). Initial MC was verified by oven drying the wet samples for 24h at 100^{o}C.

3.2.3 Reactor Operating Conditions

Compressed air entering the reactor was humidified by bubbling it through a water column to minimize drying of the substrate bed. Based on previous work done in our research group (VanderGheynst, 1994), the air flow rate was regulated to 20 L/min before it entered the reactors. Copper-constantan thermocouple wire (PP-T-24, Omega Engineering, Stamford, CT) was used to measure T at three radial points per bed height: one at the wall of the reactor and the other one was placed halfway between the other two thermocouples. Oxygen (O_2) and carbon dioxide (CO_2) concentrations were monitored continuously at the exit of the reactor using O_2 sensors (NeuwGhent Technology, LaGrangeville, NY) and hand-held CO_2 meters (Vaisala, Woburn, MA). A LabVIEW (National Instruments, Austin, TX) program was

designed to record and display the data being acquired from three CIO-EXP 32 data acquisition boards (Measurement Computing, Middleboro, MA).

3.2.4 Sample Collection

Between 3 – 5 g of sample were removed from the sampling ports at all heights of each reactor at 6 or 8h intervals up to 64h. Sampling ports at each reactor height were labeled A, B, C, D and samples at the first time point were all taken from column A, then those at the next time point were all taken from column B, etcetera. This was to minimize bed disturbance at the same point in the substrate bed, with the underlying assumption being that samples from ports A, B, C, and D at a given height were similar to each other. The study was limited to 64h because this time frame captures the dynamics of the initial stages of aerobic high-solids switchgrass degradation where the most dramatic changes in state variables occur. pH was determined by adding 10ml of water to 1g of each sample and then read with a standard electrode pH meter (Thermo Orion, Beverly, MA) (Council, 2007). Thirty milligrams of each sample were stored at -20^{o}C for subsequent DNA extraction. The remaining solids for each reactor sample were weighed and dried for 24h at 100^{o}C for moisture content measurements.

3.2.5 DNA Extraction

Procedures were performed at 4^{o}C using DNAse-free plasticware and reagents. Glass beads and 800µL of extraction buffer were added to each sample and then agitated using a bead beater (Scientific Industries, Bohemia, NY) for 4 min. The extraction buffer consisted of 100mM EDTA, 100mM NaCl, 100mM Tris, 5% w/v PVPP, 2% w/v SDS and 2% CTAB. Samples were then centrifuged for 2 min at 14,000 x g followed by the addition of 800µL of phenol:chloroform:isoamyl solution,

25:24:1, v:v:v with subsequent agitation for 1 min and centrifugation for 2 min at 14,000 x g. The aqueous layer was then transferred to 2ml phase lock gel tubes (5 Prime, Gaithersburg, MD) that contained 800 µL of chloroform:isoamyl alcohol, 24:1, v:v solution and homogenized by inverting the tubes several times, then centrifuged for 5 min at 14, 000 x g. Chloroform purification was subsequently repeated and the aqueous layer was gently homogenized with 800 µL of isopropanol and placed on ice for 15 min. After centrifugation for 20 min at 4^{o}C and 14,000 x g, the supernatant was discarded and the pellet was washed twice with 100 µL of 70% ethanol. Any remaining ethanol was discarded and 100 µL of nuclease-free water was added to each tube to re-suspend the pellets. Absorbance readings at 230nmand 280nm were collected to assess DNA purity. To quantify the amount of DNA present, absorbance readings at 260nm were taken and used in the following equation (Held, 2001):

DNA quantity = A_{260} * 50µg/mL * dilution factor (3.1)

For reference and quantitative standards during the hybridization, DNA was also extracted from samples of yeast, bacteria and fungi using a MasterPure DNA purification kit (Epicentre Biotechnologies, Madison, WI) according to the manufacturer's instructions. All extracted samples were stored at -20^{o}C until the hybridization procedure.

3.2.6 Dot blots, probe hybridization and detection

Samples were diluted in 2X SSC buffer and denatured by boiling for 5 min at 100^{o}C and immediately placed on ice. Samples were then blotted onto positively charged nylon membranes (Ambion, Austin, TX) and DNA was cross linked to the membrane by baking for 15 min at 80^{o}C. The membranes were hybridized with the probes overnight using Northern Max hybridization buffer **(**Ambion, Austin, TX).

Table 3.2 Hybridization probe data for bacteria, fungi and yeast probes.

Probe Name	Sequence 5 to 3	Target Group	Melting Temperature ^{o}C	Hybridization Temperature ^{o}C	Reference
S-D-Bact-0338-a-A-18	GCTGCCTCCCGTAGGAGT	Universal Bacteria	55	45.5	(Schloss et al., 2005)
NS8	TCCGCAGGTTCACCTACGGA	Universal fungal	56	43	(Peters et al., 2000)
PF2	CTCTGGCTTCACCCTATTC	Yeast	51	35.8	(Loy et al., 2007)

Table 2 lists the properties of the probes used and the probe hybridization temperatures. The non-isotopic chemilumiscent detection of the probes was accomplished using a BrightStar BioDetect kit (Ambion, Austin, TX) according to the manufacturer's instructions. a G:Box HR Imager (Syngene, Frederick, MD) with a one hour exposure time.Light emissions from the membrane were captured using a G:Box HR Imager (Syngene, Frederick, MD) with a one hour exposure time. Using Imager software (Syngene, Frederick, MD), the intensities of the bands from the reactor samples were compared to the intensities of the known mass standards in order to assign a mass to the unknown samples. The mass of microbial DNA in each sample was then standardized to the mass of the sample used for the DNA extraction and the amount of DNA that was extracted from the sample.

3.2.7 Statistical Analysis

Results were subjected to Pearson correlation analyses to determine variable correlations in JMP 7 (SAS Institute, Cary, NC), using $p < 0.05$ as the criterion for significance. Principal component analysis (PCA) was also completed in JMP 7 to highlight patterns of variation between the microbial community data and other physical variables.

3.3 Results

3.3.1 Abiotic Phenomena

3.3.1.1 Temperature

Axial T gradients were evident along the reactor bed with lower T at the bottom of the bed and higher T at the top for all three initial MC (Figure 3.2). For the most part, the lower half of the reactors remained at mesophilic T whereas the top half

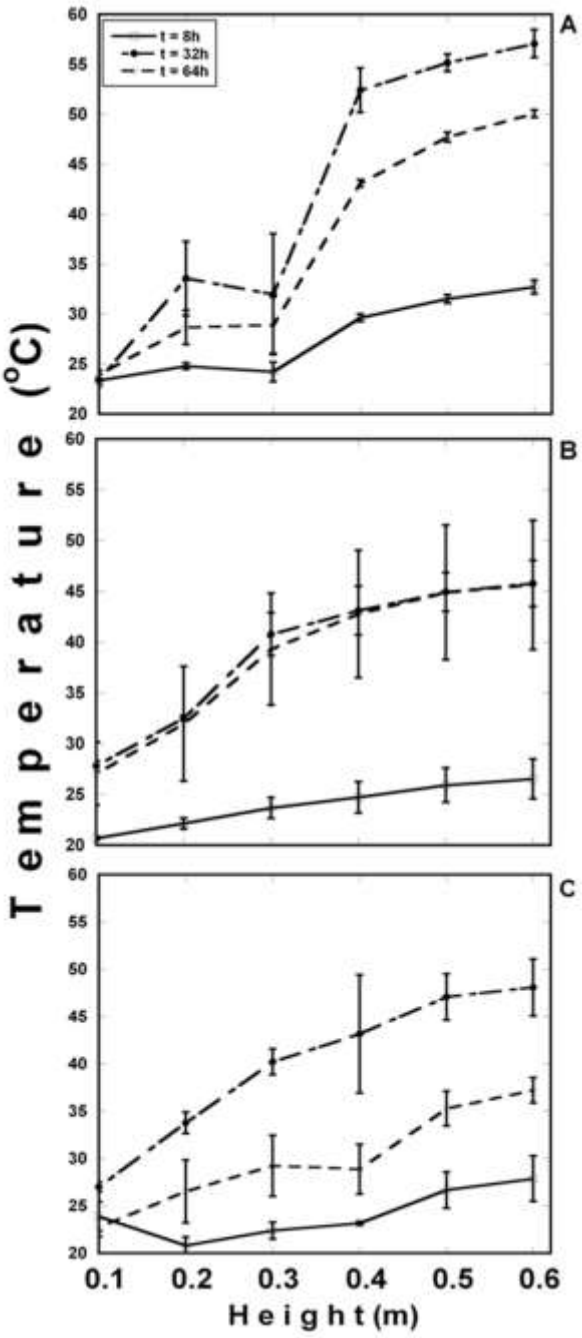

Figure 3.2 Temperature profiles of switchgrass and dog food reactors with initial moisture contents (wet basis) of (A) 75%, (B) 65% and (C) 60% at 8, 32 and 64h into the process

Table 3.3 Physico-chemical properties of samples at various reactor heights at 8, 32 and 64h for reactors of initial MC of 60, 65 and 75%

Variable	Height (m)	75% MC			65% MC			60% MC		
		8h	32h	64h	8h	32h	64h	8h	32h	64h
pH	0.1	4.86	7.46	8.72	4.86	5.46	7.50	4.91	5.79	7.82
	0.2	4.77	7.17	8.71	4.77	5.50	7.67	4.88	5.70	7.31
	0.3	4.74	7.91	8.71	4.74	5.55	8.34	4.84	5.99	7.27
	0.4	4.76	7.32	8.61	4.76	5.58	7.88	4.77	5.48	7.35
	0.5	4.68	6.88	8.76	4.68	5.57	7.30	4.79	5.97	7.21
	0.6	4.74	7.23	8.17	4.74	5.39	7.26	4.76	5.87	7.64
MC (%)	0.1	73.8	71.9	67.4	65.9	66.4	47.8	61.0	59.5	44.7
	0.2	72.3	70.9	64.8	66.3	62.6	52.9	60.1	62.0	47.3
	0.3	73.0	73.5	66.4	65.7	67.3	60.8	61.5	59.4	51.9
	0.4	72.5	70.6	75.1	67.4	66.0	68.2	62.3	59.3	59.0
	0.5	71.4	70.9	74.0	66.8	66.8	68.4	60.5	60.2	62.5
	0.6	72.6	71.9	78.2	73.5	67.4	75.1	61.5	63.9	64.9
OCR(mol/min)	n/a	0.0226	0.0414	0.039	0.0186	0.0358	0.0346	0.0199	0.0376	0.0263

of the reactors rose to thermophilic T. The largest gradient along the reactor bed occurred at 32h in the 75% MC reactor, with a variation of 0.87^{o}C/cm at 32h between the peak T location and the bottom of the reactor. Average peak reactor T values of 57, 49 and 47^{o}C were observed for the 75%, 60% and 65% MC reactors, respectively at the top of the reactors.

Radial T gradients for the three reactors were less than 1˚C/cm (data not shown) indicating that dynamics of energy transport in all three MC reactors occurred mainly in one direction

3.3.1.2 pH

Initial pH of the mixed substrate was moderately acidic, which was not surprising, given that both switchgrass and dog food had an acidic pH. The mixture became increasingly more acidic within the first 12hr, after which point began a steep increase to basic conditions. Across the three initial MCs, pH continually increased with time, but appeared to be almost constant along the reactor bed height (Table 3.3). Temporal pH increases appear to follow increases in reactor T. This is most readily seen in the 75% MC reactor which had the highest T, and transitioned from acidic to alkaline conditions within 24h. The 60 and 65% MC reactors, on the other hand, were still under acidic conditions at 40h into the process and produced lower T. This was confirmed by the Pearson correlations which showed that for all three reactors, there was a positive correlation between pH and T with the strongest correlation occurring in the 65% MC reactor.

3.3.1.3 MC

In the first 32h, MC in the three reactors remained relatively constant, after which point, some spatial gradients developed (Table 3.3). There was an increase in

MC at the top half of all three reactors by the end of this study, which corresponds with peak T locations in the reactors; whereas decreases in MC were observed at the bottom half of the reactors. The MC at the top of the reactors had average increases of 3.26% in the 75% moisture reactor, 7.79% in the 65% moisture reactor and 4.21% in the 60% moisture reactor. This increase in MC at the top of the reactors is most likely due to the combined effect of increased microbial activity in the middle of the reactors which resulted in greater axial moisture transport and some condensation of the effluent water vapour at the top of the reactors. At the middle and bottom of the reactors, the rate of decrease of MC ranged from 0.03 to 0.28 kg water /kg compost h. Indeed, the correlation matrix revealed significant positive correlations between MC and height for all three reactors.

3.3.1.4 Effluent Gas

Effluent O_2 and CO_2 concentrations mirrored each other and had strong negative correlations for all three reactors (Figure 3.3). The O_2 concentrations were also positively correlated to pH and T. Using the O_2 concentration data, the O_2 consumption rate (OCR) was calculated (Table 3.33) because this parameter is a better indication of microbial activity since it indicates how much O_2 is transferred from the gas phase to the solid substrate as a function of time. The oxygen consumption rate (OCR) was calculated using the following equation:

$$OCR = O_i - O_e \qquad 3.2$$

where O_i is the oxygen concentration rate in influent gas (moles/min) and O_e is the O_2 concentration rate in the effluent gas (moles/min). The resulting OCR showed that the highest activity was found in the reactor with the highest initial MC. At peak OCR values, the rate of oxygen consumption was 2.69 times greater than its initial value in the 75% MC reactor; 2.6 times higher in the 65% MC reactor and 2.4 times higher in

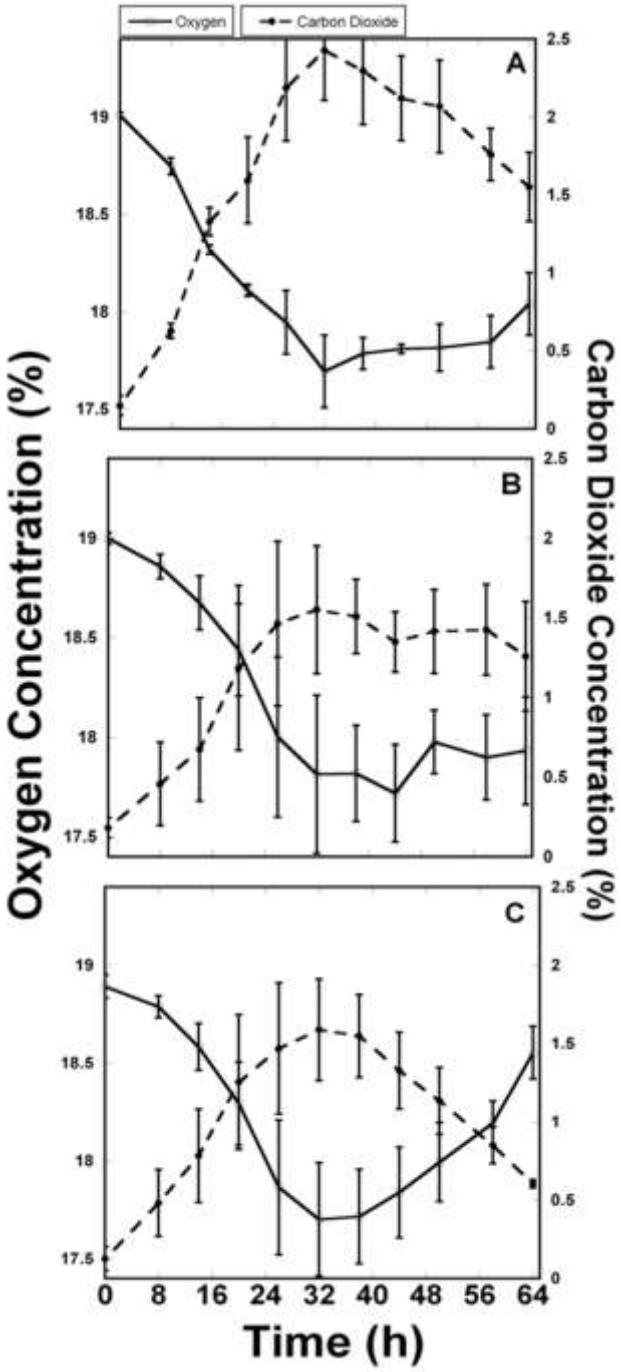

Figure 3.3 Effluent gas concentration profiles of switchgrass and dog food reactors with initial moisture contents (wet basis) of (A) 75%, (B) 65% and (C) 60% at 8, 32 and 64h into the process

the 60% MC reactor. Overall trends observed in the OCR profiles are consistent with those found in the temperature profiles at the top of the reactors. Using the effluent CO_2 concentrations, the rate of carbon (C) conversion was calculated as follows:

$$\% \text{ Conversion} = (c * M * G_a * t) / x \quad (3.3)$$

where c is the concentration of CO_2 in the exhaust gas (g CO_2/ L_{air}), M is the atomic weight of C, G_a is the mass flow rate of air (L_{air}/min), t is time (min) and x is the molar fraction of C in dog food (due to catabolite repression, it was assumed that the microbial community would preferentially degrade the dog food first and then metabolize the C sources in the switchgrass). The resulting rates of C conversion indicate that the greatest extent of degradation occurred in the 75% MC reactor (Figure 3.4) with 49% C conversion. For the first 32h, the rate of C conversion increased with increasing MC except for the period of 32-50h where the 60% MC reactor displayed higher rates of degradation than the 65% MC reactor. By 64h, there was a 73% difference between the rate of C conversion in the 75% MC reactor compared to the 60% MC reactor and a 55% difference between the 65% MC and 60% MC reactors. Not surprisingly, the correlation matrix revealed positive correlations between the amount of C converted and T, pH and CO_2 concentration and thus a negative correlation with O_2 concentration.

3.3.2 Biotic Phenomena

Presented in Figure 3.5, 3.6 and 3.7 are the results from the hybridization probing for bacteria, fungi and yeast, respectively, for the three MC reactors. As a measure of the reproducibility of the process, the error bars presented in the figure represent the deviations over three replicate reactor runs. These error bars are relatively large because the reactors were non-sterile and contained minimal inoculation. Despite this process variability, two key observations from these results

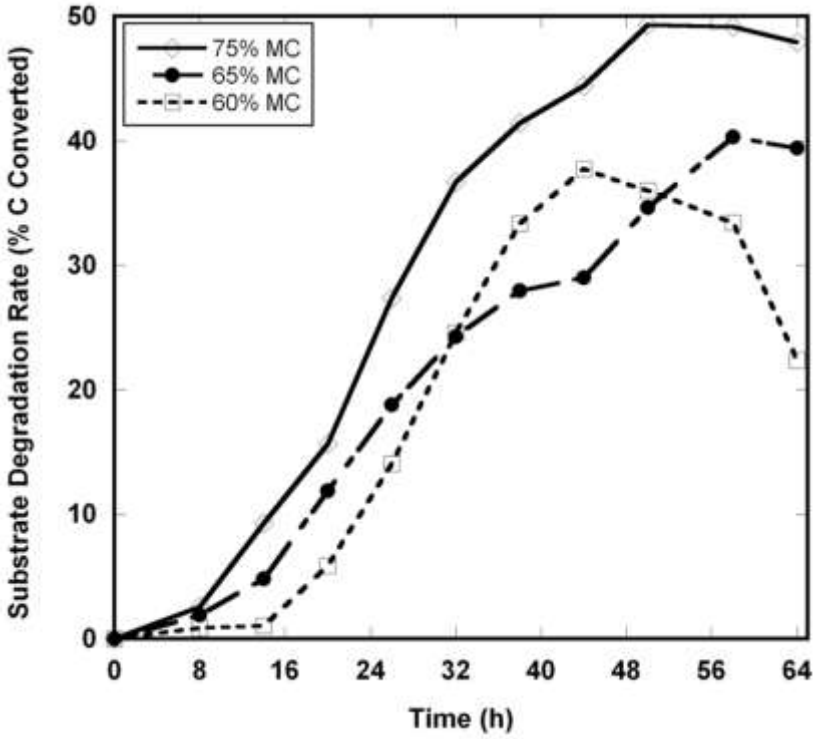

Figure 3.4 Rate of substrate degradation during initial stages of degradation

are that the highest MC reactor was dominated by the bacterial biomass population whereas the 60% and 65% MC reactors were dominated by the yeast population and that the extent of substrate degradation was directly linked to the bacterial biomass levels.

3.3.2.1Bacteria

By far, bacteria biomass levels were highest in the 75% MC with the highest production occurring at 32hr where reactor bed T were at their maximum (Figure 3.5). The maximum OCR was also observed at 32 hr (see Table 3.3). Both the 60 and 65% MC reactors had significantly lower bacterial biomass levels with maximum levels in the 75% MC reactor being four times higher than the maximum observed in the 65% MC reactor and 7 times higher for that observed in the 60% MC reactor. Across all three reactors, bacterial biomass levels were higher in the top half of the reactor than the bottom half. These spatial bacterial gradients were particularly pronounced for the 75% MC reactor, and reflected in the T data, but interestingly, these spatial gradients are not observed in pH data (see Table 3.3). This may be explained by the observation that pH was positively correlated with the fungal biomass levels (which had no correlation with height) in the 75% MC reactor, whereas, pH in the 60 and 65% MC reactors correlated positively with the bacterial biomass population. The most interesting correlation; however, was a positive one between the bacterial biomass levels and the amounts of C converted for all three reactors (R^2 = 0.43, 0.23 and 0.23 for 60, 65 and 75% MC reactors, respectively). The significant correlation between these two variables suggests that bacteria were the dominant microorganisms in the degradation of our mixed substrate. Thus, the greater extent of degradation in the 75% MC reactor was attributed to the higher bacterial biomass population in that reactor.

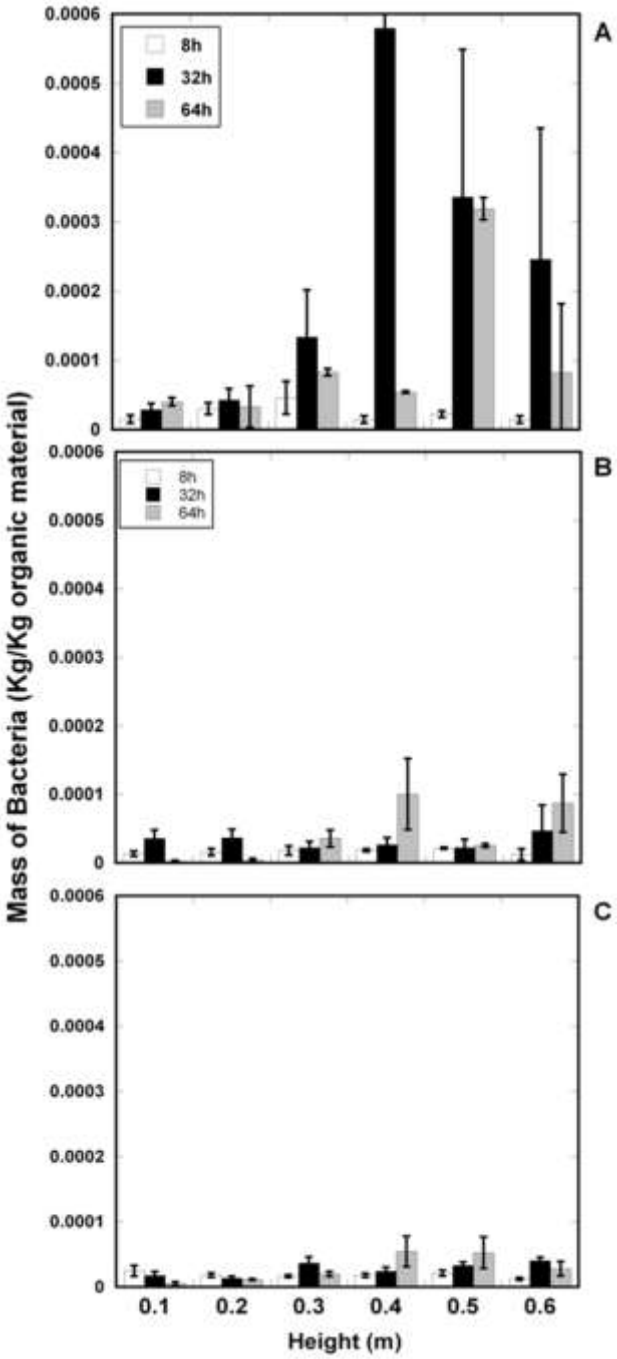

Figure 3.5 Profiles of mass of bacterial biomass versus height in vertical, static-bed reactors during the degradation of high-solids switchgrass mixtures with initial moisture contents (wet basis) of (A) 75%, (B) 65% and (C) 60% at 8, 32 and 50h into the process

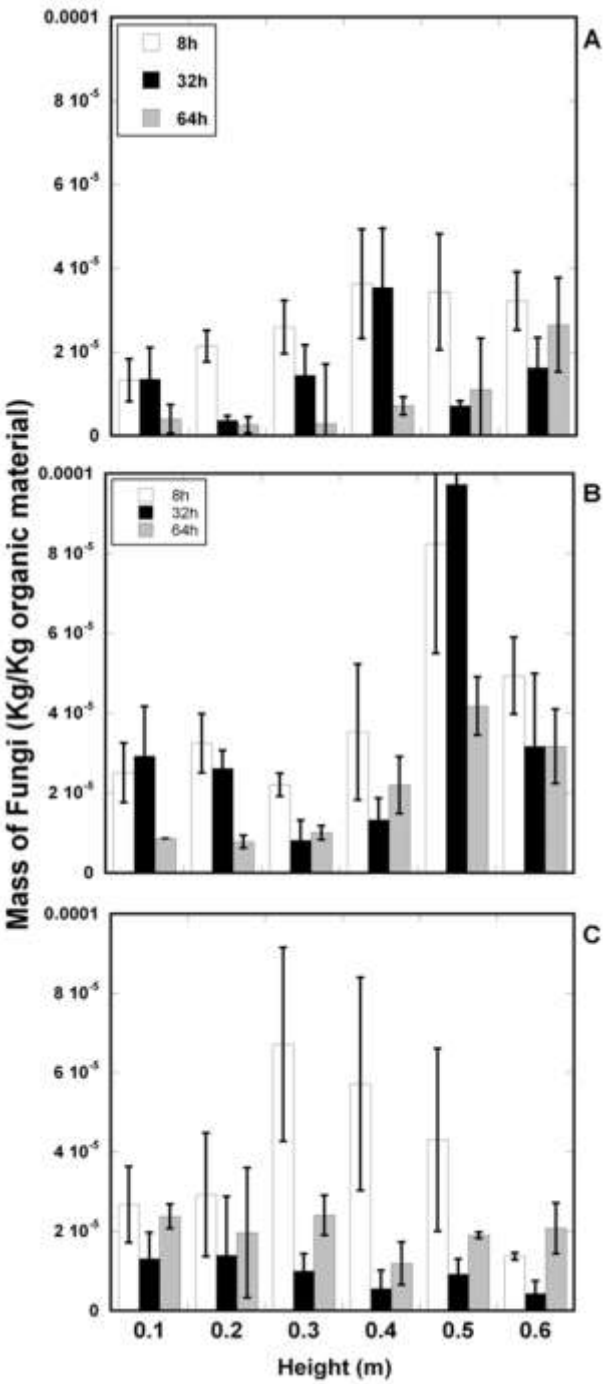

Figure 3.6 Profiles of mass of fungal biomass versus height in vertical, static-bed reactors during the degradation of high-solids switchgrass mixtures with initial moisture contents (wet basis) of (A) 75%, (B) 65% and (C) 60% at 8, 32 and 50h into the process

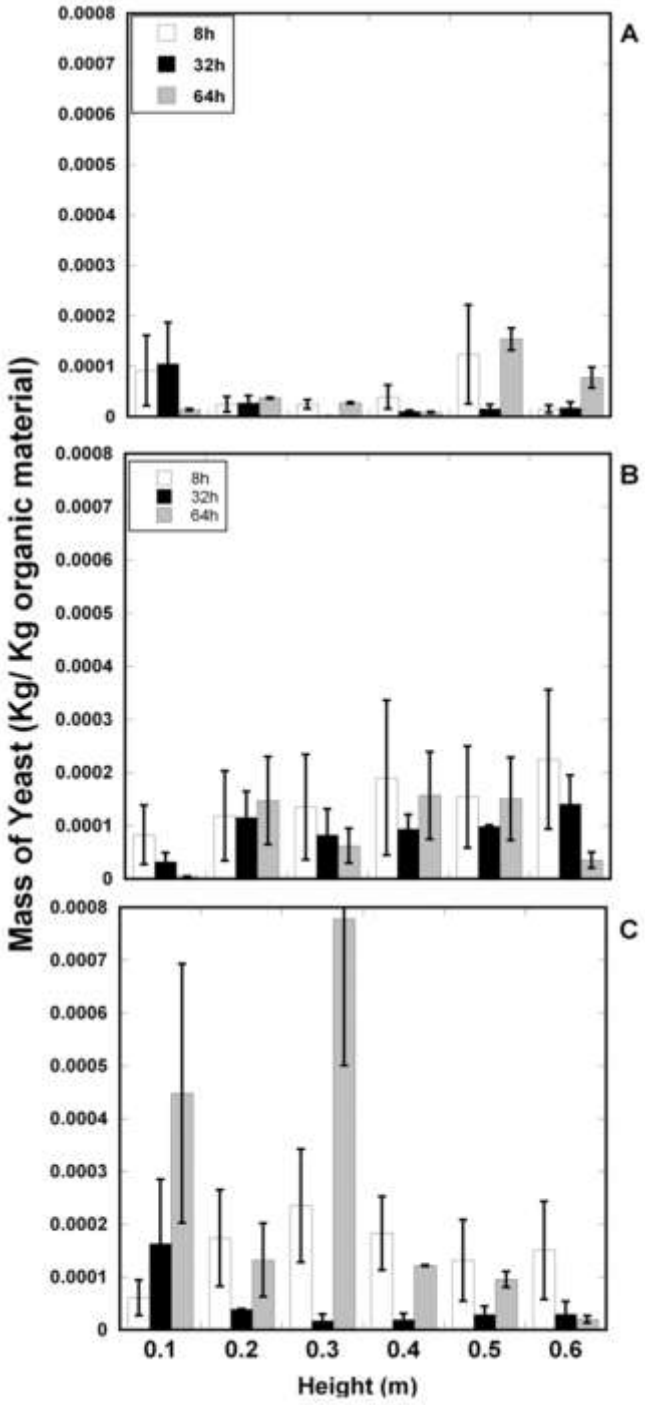

Figure 3.7 Profiles of mass of yeast biomass versus height in vertical, static-bed reactors during the degradation of high-solids switchgrass mixtures with initial moisture contents (wet basis) of (A) 75%, (B) 65% and (C) 60% at 8, 32 and 50h into the process

3.3.2.2 Fungi

Of the three groups probed, fungi were present in the lowest quantities (Figure 6). The maximum fungal biomass level was as much as 90% lower than the maximum observed for bacterial biomass population, with the highest population of fungal biomass being found in the 65% MC reactor. For the most part, the fungal biomass population was highest near the beginning of the process and decreased with time. Spatially, no noticeable gradients were observed across any of the three reactors, except at 32h, when some spatial gradients were apparent in the three reactors.

3.3.2.3 Yeasts

Profiles of the yeast biomass population show that yeasts completely dominated the 60% MC reactor and were the most abundant population on the 65% MC reactor (Figure 3.7). The single highest quantity of yeast biomass was detected in the 60% MC reactor at 64h and was 15% higher than the maximum observed bacterial biomass level. No spatial or temporal variation was observed in the 75% MC reactor, with minimal variation occurring in the 60% and 65% MC reactors.

3.3.3 Interactions between biotic and abiotic variables

Due to the high dimensionality of the data, PCA was used to visualize any patterns that would provide insight into the major factors the drove process changes (Figure 3.8). The first important observation from the PCA is that the amount of variability explained by the principal components increases with increasing MC. This suggests that increasing the initial MC increases the descriptive power of the major components. The other key observation from the PCA is that all the samples in all

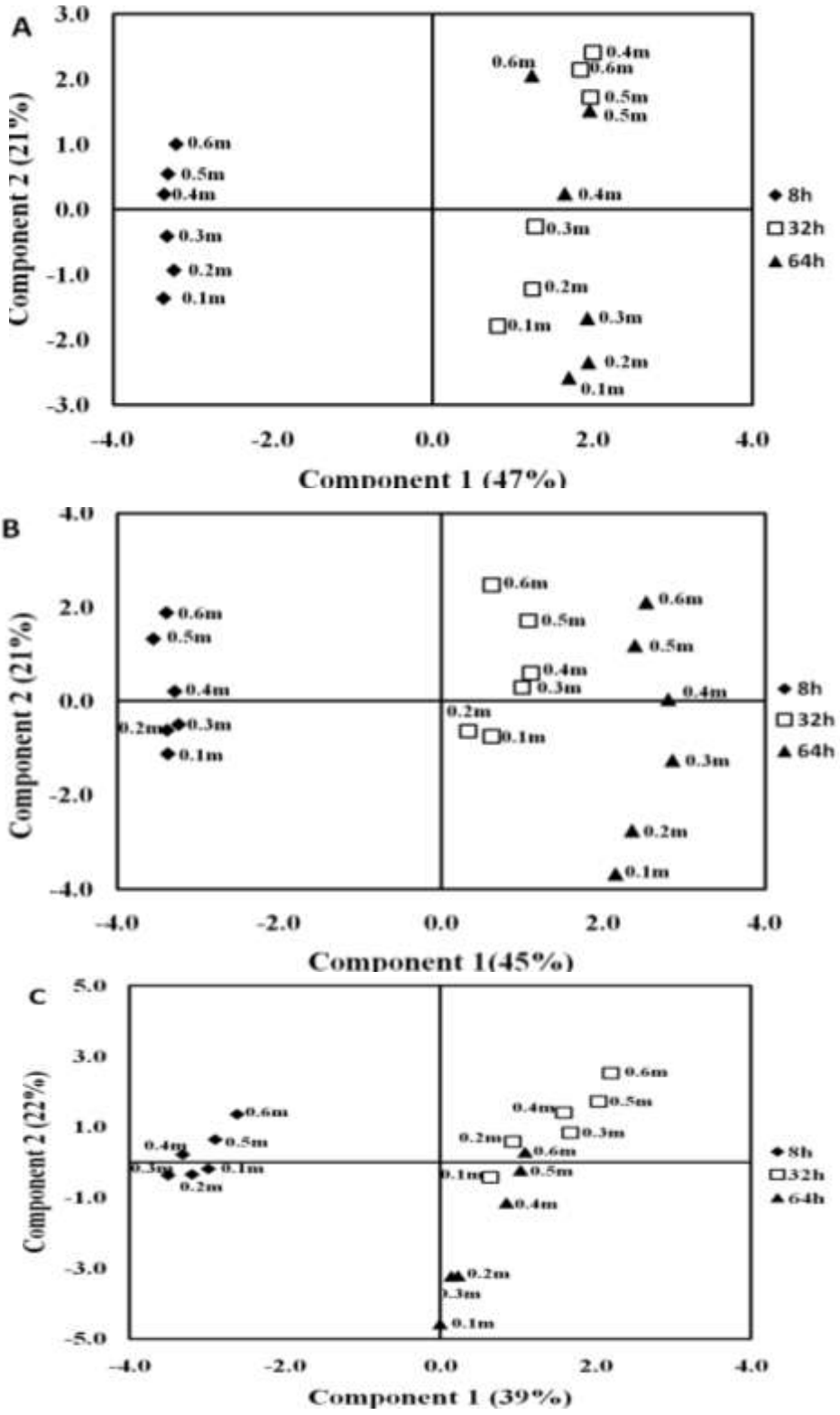

Figure 3.8 Score plot of PCA of abiotic and biotic data from initial degradation of high-solids switchgrass mixtures with initial moisture contents (wet basis) of (A) 75%, (B) 65% and (C) 60% at 8, 32 and 50h into the process

three reactors are significantly differentiated over time, confirming that we have captured major changes in the process variables, including microbial succession within 64h. This also suggests that the most significant component (horizontal axis) in explaining the variability seen in the data is time. The major contributors to these temporal changes were pH, temperature and effluent gas concentrations as revealed by the squared cosines of the variables to the horizontal factor. Along the vertical axis, samples clustered according to their height in the reactor, implying that height was the second major component, and again confirming the importance of spatial variation in such systems. The major contributor to spatial changes was the MC, with bacteria being a major contributor for the 75%MC reactor only. Most importantly, the fact that these interactions are almost the same for all three different initial MC reactors further validates the importance of these major factors towards driving process changes in our system.

3.4 Discussion

The rate of organic C conversion is often used as a conventional indicator of the extent of substrate degradation because it provides a measure of the bio-oxidation of C to CO_2 (Hao et al., 2004; Larney et al., 2006; Tiquia et al., 2002). Indeed, the rate of C conversion allowed us to document that at 58h, we had as much as 49%, 40% and 33% substrate degradation in our 75%, 65% and 60% MC reactors, respectively. This again highlights that dramatic changes are occurring in the initial stages of biodegradation and suggests that we can manipulate these initial stages to increase the rate of biological decomposition. Furthermore, the ability to correlate the rate of degradation to abiotic and biotic parameters provides an avenue for process control.

A significant positive correlation between the rate of degradation and bacterial biomass levels is not surprising because bacteria have been shown to play a dominant

role in biodegradation processes (Blanc et al., 1999; Dees & Ghiorse, 2001; Ishii et al., 2000; Pedro et al., 2003; Schloss et al., 2005; Schloss et al., 2003). It is surprising that a negative correlation between yeast biomass levels and the extent of degradation was only significant for the 75% MC reactor, because the activity of yeasts favors biodegradation by metabolizing organic acids to reduce the initial acidity of the system and pave the way for the growth of thermophilic bacteria (Choi & Park, 1998; Sundberg et al., 2004). Although no correlation was found between the rate of degradation and the fungal biomass quantities, fungi are known to withstand a broad range of growth conditions and have been shown to play an important role in the biological decomposition of organic material (Dees & Ghiorse, 2001; Gusse et al., 2006; Hansgate et al., 2005; Huang et al., 2008; Peters et al., 2000; Trautmann & Olynciw, 2002). It is possible that we were not able to extract the total fungal biomass present because their mode of growth through highly-branched hyphae limits the amount of DNA found in a small sample (Tengerdy & Szakacs, 2003). It should also be noted that all the DNA samples were limited by the efficiency of the extraction procedure. In this study, absorbance readings were obtained at 230nm, 260nm, and 280nm to estimate the efficiency of the extraction and purification procedures. The ratio of absorbance at 260nm to 280nm was used to estimate the extraction efficiency, whereas the purification efficiency was determined by comparing the absorbance at 260nm to that at 230nm (phenolic compounds). A ratio value of 1.5 is generally accepted as good extraction and purification efficiency (Held, 2001) and for this study, this value ranged from 1.2 to 1.7 for the compost DNA samples and from 1.7 to 2 for the pure culture DNA samples, which shows that we had a good handle on both the extraction and purification efficiency.

For the abiotic parameters of temperature, pH, moisture content, OCR and CO_2 evolution rate, our results show that we have captured the bulk dynamics of heat and

mass transfer in the system for varying initial MC. Managing MC is essential for rapid microbial degradation of switchgrass and other plant materials. If the MC is too low (< 30%), microbial activity will be severely diminished (Gervais & Molin, 2003). In addition, substrate swelling, which is necessary for microbial activity on the substrate, will not occur. On the other hand, if the MC is too high (> 75%), the void spaces within the solid matrix will be filled with water that will inhibit the transfer of oxygen to the substrate particles and the transfer of metabolic products such as carbon dioxide away from the substrate particle (Tiquia et al., 2002). Based on these MC limits, the vast majority of decomposition processes have utilized initial MCs of 60-70% (see (Gajalakshmi & Abbasi, 2008) for an extensive list). Given the increased activity at 75% MC in this study, it is postulated that this represents an ideal starting MC for our substrates; however further tests at higher MCs are required to determine if this is the optimum initial MC. Better reactor performance at 75% MC is not surprising because this is near the water holding capacity of switchgrass which ranges from 70 – 75%. These results are consistent with other degradation studies of grass substrates that use high starting MCs and produce higher decomposition rates (Dresboll & Thorup-Kristensen, 2005; Petric et al., 2009). Despite the increased activity of the 75% moisture reactor, dynamic changes were also seen in the 65% and 60% moisture reactors, indicating that there was enough moisture for relatively high microbial activity.

The other factors which affected the rate of substrate degradation and thus, had positive correlations with the rate of C conversion were the T and pH for all three initial MC. T is a critical factor for biodegradation because it influences microbial activity as well as energy transfer in the reactors and temporal profiles, similar to those generated in this study, have been well documented (Dalsenter et al., 2005; Fanaei & Vaziri, 2009; Ryckeboer et al., 2003; Schloss & Walker, 2000; Tengerdy & Szakacs,

2003; VanderGheynst et al., 1997; von Meien & Mitchell, 2002; Walker et al., 1999; Weber et al., 2002; Wong et al., 2009); however, only a few of these studies have looked at variations in the spatial dimension (Fanaei & Vaziri, 2009; VanderGheynst et al., 1997). Compared to these studies, our spatial T profiles followed the same profile of reaching peak T at the top of the reactors, and we have shown further, that higher T produce higher extents of substrate degradation. These results highlight the existence of different temperature zones in vertical static bed degradation bioreactors (Luo et al., 2008; VanderGheynst, 1997). In fact, multivariate analyses in this study revealed 3 zones of activity that were very different from each other; separating the reactor into a top, bottom and middle zone based on temperature and MC data across all 3 reactors. The presence of these zones in the early stages of degradation has important consequences for the entire process as it suggests that the conversion of organic matter will be non-uniform and may be significantly less in some zones. This transition into zones has further consequences for degradation process where the objective is to kill off pathogenic microorganisms because this goal may not be reached in all zones of the reactor. Additionally, as substrate degradation occurs, and matter is converted, the mechanical strength of the substrate bed changes, making the bed more susceptible to compaction and the transfer of material from one zone to another. This in turn affects air flow and permeability through the system, but it remains uncertain whether there is a direct correlation between compaction and MC (Richard et al., 2004). As expected, for the time period studied, there was not much decrease (less than 10%) in bed height and this suggests that compaction was low.

Similar to T, pH is an important indicator of microbial community dynamics because optimal pH growth conditions vary according to population (Gajalakshmi & Abbasi, 2008) and this helps explain why the fungal population controlled the pH in the 75% MC reactor, which had higher pH values, whereas the bacterial population

controlled pH in the 60 and 65% MC reactors, where lower pH values were observed. Our temporal pH profiles are very comparable to previous studies (Cen & Xia, 1999; Schloss & Walker, 2000) and indicate changes in community structure over time (Chroni et al., 2009; Lei & VanderGheynst, 2000). Again these findings highlight that it is worthwhile to use highly-instrumented reactors as designed in this study to capture both temporal and spatial dynamics of biotic and abiotic phenomena because this design facilitates critical insights for reactor scale-up, such as the variable dynamics of microbial populations with height and the minimization of radial T gradients.

The most challenging part of biodegradation studies remains linking the interactions between the abiotic and biotic phenomena for better process control and reproducibility. We have successfully shown that time, as influenced by changes in T, pH and effluent gas concentrations, was the main driving factor for differentiating the data. These abiotic parameters then drive changes in microbial community structure and succession that select for more efficient microbes for lignocellulosic degradation (Yu et al., 2009). Other studies have also been able to show a link between microbial community structure and degradation over time (Steger et al., 2005; Yu et al., 2007). Again, none of these studies investigated the variation with bed height, but our study has shown that for reactors above 0.3m tall, height also plays a leading role in the transfer of nutrients and energy in the system. Of particular importance is the result that MC had the largest influence on the spatial separation because drying of the substrate bed can lead to slowed microbial growth which in turn hinders the rate of degradation (Gervais & Molin, 2003). More importantly, we have shown that greater spatial differentiation occurred when the initial MC of the reactor increased and that this also led to higher rates of degradation.

3.5 Conclusions

It remains challenging to build a fully integrated framework containing biotic and abiotic parameters to describe biological decomposition systems because this process is extremely complex and highly non-linear with myriad variables. For such systems, statistical tools, such as principal component analysis, are needed to gain insight into how to control the intricate feedback loops and make the process more reproducible. In this study, we have produced a highly-instrumented reactor system that allowed us to investigate both the spatial and temporal dynamics of biotic and abiotic phenomena. We have shown that a 10% increase in the initial MC dramatically increases the biotic and abiotic activities and results in a greater extent of substrate degradation. We have also shown that higher bacterial populations lead to higher rates of substrate bioconversion and have highlighted the role of yeasts as acidity reducers. Most importantly, we have documented how these changes occur over both space and time. Thus, the findings of this study allow us to begin to build a bioengineering framework to make biological decomposition of a high-solids switchgrass mixture more predictable on a larger scale, by providing key insights into some of the variables which should be manipulated in the initial stages for future studies, such as pH, MC and yeast population.

REFERENCES

Adney, S., van der Lelie, D., Berry, A., M., H. 2008. *Biomass Recalcitrance*. John Wiley and Sons Incorporated.

Bellon-Maurel, W., Orliac, O., Christen, P. 2003. Sensors and measurements in solid state fermentation: a review. *Process Biochemistry*, 38(6), 881-896.

Blanc, M., Marilley, L., Beffa, T., Aragno, M. 1999. Thermophilic bacterial communities in hot composts as revealed by most probable number counts and molecular (16S rDNA) methods. *Fems Microbiology Ecology*, 28(2), 141-149.

Cen, P., Xia, L. 1999. Production of Cellulase by Solid-State Fermentation. *Advances in Biochemical Engineering/Biotechnology*, 65.

Choi, M.H., Park, Y.H. 1998. The influence of yeast on thermophilic composting of food waste. *Letters in Applied Microbiology*, 26(3), 175-178.

Chroni, C., Kyriacou, A., Manios, T., Lasaridi, K.E. 2009. Investigation of the microbial community structure and activity as indicators of compost stability and composting process evolution. *Bioresource Technology*, 100(15), 3745-3750.

Council, U.S.C. 2007. Test Methods for Evaluation of Compost and Composting.

Dalsenter, F.D.H., Viccini, G., Barga, M.C., Mitchell, D.A., Krieger, N. 2005. A mathematical model describing the effect of temperature variations on the kinetics of microbial growth in solid-state culture. *Process Biochemistry*, 40(2), 801-807.

Dees, P.M., Ghiorse, W.C. 2001. Microbial diversity in hot synthetic compost as revealed by PCR-amplified rRNA sequences from cultivated isolates and extracted DNA. *Fems Microbiology Ecology*, 35(2), 207-216.

Dresboll, D.B., Thorup-Kristensen, K. 2005. Delayed nutrient application affects mineralisation rate during composting of plant residues. *Bioresource Technology*, 96(10), 1093-1101.

Fanaei, M.A., Vaziri, B.M. 2009. Modeling of temperature gradients in packed-bed solid-state bioreactors. *Chemical Engineering And Processing*, 48(1), 446-451.

Franke-Whittle, I.H., Klammer, S.H., Insam, H. 2005. Design and application of an oligonucleotide microarray for the investigation of compost microbial communities. *Journal of Microbiological Methods*, 62(1), 37-56.

Gajalakshmi, S., Abbasi, S.A. 2008. Solid waste management by composting: State of the art. *Critical Reviews in Environmental Science and Technology*, 38(5), 311-400.

Gervais, P., Molin, P. 2003. The role of water in solid-state fermentation. *Biochemical Engineering Journal*, 13(2-3), 85-101.

Gusse, A.C., Miller, P.D., Volk, T.J. 2006. White-rot fungi demonstrate first biodegradation of phenolic resin. *Environmental Science & Technology*, 40(13), 4196-4199.

Hansgate, A.M., Schloss, P.D., Hay, A.G., Walker, L.P. 2005. Molecular characterization of fungal, community dynamics in the initial stages of composting. *Fems Microbiology Ecology*, 51(2), 209-214.

Hao, X.Y., Chang, C., Larney, F.J. 2004. Carbon, nitrogen balances and greenhouse gas emission during cattle feedlot manure composting. *Journal Of Environmental Quality*, 33(1), 37-44.

Haug, R.T. 1993. *The Practical Handbook of Compost Engineering*. Lewis Publishers.

Held, P. 2001. BioTek PowerWave HT Microplate Spectrophotometer: Quantitation of Nucleic Acids. in: *Application Note*. Winooski, VT.

Hogan, J.A., Miller, F.C., Finstein, M.S. 1989. Physical Modeling of the Composting Ecosystem. *Applied and Environmental Microbiology*, 55(5), 1082-1092.

Huang, D.L., Zeng, G.M., Feng, C.L., Hu, S., Jiang, X.Y., Tang, L., Su, F.F., Zhang, Y., Zeng, W., Liu, H.L. 2008. Degradation of lead-contaminated lignocellulosic waste by Phanerochaete chrysosporium and the reduction of lead toxicity. *Environmental Science & Technology*, 42(13), 4946-4951.

Ishii, K., Fukui, M., Takii, S. 2000. Microbial succession during a composting process as evaluated by denaturing gradient gel electrophoresis analysis. *Journal of Applied Microbiology*, 89(5), 768-777.

Larney, F.J., Buckley, K.E., Hao, X.Y., McCaughey, W.P. 2006. Fresh, stockpiled, and composted beef cattle feedlot manure: Nutrient levels and mass balance estimates in Alberta and Manitoba. *Journal Of Environmental Quality*, 35(5), 1844-1854.

Lei, F., VanderGheynst, J.S. 2000. The effect of microbial inoculation and pH on microbial community structure changes during composting. *Process Biochemistry*, 35(9), 923-929.

Liang, C., Das, K.C., McClendon, R.W. 2003. The influence of temperature and moisture contents regimes on the aerobic microbial activity of a biosolids composting blend. *Bioresource Technology*, 86(2), 131-137.

Loy, A., Maixner, F., Wagner, M., Horn, M. 2007. probeBase - an online resource for rRNA-targeted oligonucleotide probes: new features 2007. *Nucleic Acids Research*, 35, D800-D804.

Luo, W., Chen, T.B., Zheng, G.D., Gao, D., Zhang, Y.A., Gao, W. 2008. Effect of moisture adjustments on vertical temperature distribution during forced-aeration static-pile composting of sewage sludge. *Resources Conservation And Recycling*, 52(4), 635-642.

Nakasaki, K., Akakura, N., Atsumi, K., Takemoto, M. 1998. Degradation patterns of organic material in batch and fed-batch composting operations. *Waste Management & Research*, 16(5), 484-489.

Oriol, E., Raimbault, M., Roussos, S., Viniegragonzales, G. 1988. Water and Water Activity in the Solid-State Fermentation of Cassava Starch by Aspergillus-Niger. *Applied Microbiology and Biotechnology*, 27(5-6), 498-503.

Pedro, M.S., Haruta, S., Nakamura, K., Hazaka, M., Ishii, M., Igarashi, Y. 2003. Isolation and characterization of predominant microorganisms during decomposition of waste materials in a field-scale composter. *Journal of Bioscience and Bioengineering*, 95(4), 368-373.

Peters, S., Koschinsky, S., Schwieger, F., Tebbe, C.C. 2000. Succession of microbial communities during hot composting as detected by PCR-single-strand-conformation polymorphism-based genetic profiles of small-subunit rRNA genes. *Applied and Environmental Microbiology*, 66(3), 930-936.

Petric, I., Sestan, A., Sestan, I. 2009. Influence of initial moisture content on the composting of poultry manure with wheat straw. *Biosystems Engineering*, 104(1), 125-134.

Richard, T.L., Veeken, A.H.M., de Wilde, V., Hamelers, H.V.M. 2004. Air-filled porosity and permeability relationships during solid-state fermentation. *Biotechnology Progress*, 20(5), 1372-1381.

Ryckeboer, J., Mergaert, J., Coosemans, J., Deprins, K., Swings, J. 2003. Microbiological aspects of biowaste during composting in a monitored compost bin. *Journal of Applied Microbiology*, 94(1), 127-137.

Schloss, P.D., Hay, A.G., Wilson, D.B., Gossett, J.M., Walker, L.P. 2005. Quantifying bacterial population dynamics in compost using 16S rRNA gene probes. *Applied Microbiology and Biotechnology*, 66(4), 457-463.

Schloss, P.D., Hay, A.G., Wilson, D.B., Walker, L.P. 2003. Tracking temporal changes of bacterial community fingerprints during the initial stages of composting. *Fems Microbiology Ecology*, 46(1), 1-9.

Schloss, P.D., Walker, L.P. 2000. Measurement of process performance and variability in inoculated composting reactors using ANOVA and power analysis. *Process Biochemistry*, 35(9), 931-942.

Steger, K., Eklind, Y., Olsson, J., Sundh, I. 2005. Microbial community growth and utilization of carbon constituents during thermophilic composting at different oxygen levels. *Microbial Ecology*, 50(2), 163-171.

Sundberg, C., Smars, S., Jonsson, H. 2004. Low pH as an inhibiting factor in the transition from mesophilic to thermophilic phase in composting. *Bioresource Technology*, 95(2), 145-150.

Tengerdy, R.P., Szakacs, G. 2003. Bioconversion of lignocellulose in solid substrate fermentation. *Biochemical Engineering Journal*, 13(2-3), 169-179.

Tiquia, S.M., Richard, T.L., Honeyman, M.S. 2002. Carbon, nutrient, and mass loss during composting. *Nutrient Cycling in Agroecosystems*, 62(1), 15-24.

Trautmann, N., Olynciw, E. 2002. Compost Microorganisms. in: *Cornell Composting Science & Engineering*, Vol. 2007. Ithaca.

VanderGheynst, J.S. 1994. Design and Process Ananlysis of a High-Solids Aerated Static Bed. in: *Biological and Environmental Engineering*, Vol. Masters of Science, Cornell University. Ithaca, pp. 167.

VanderGheynst, J.S. 1997. Experimentation, Modeling and Analysis of a High-Solids Aerobic Decomposition Process. in: *Biological and Environmental Engineering*, Vol. Doctor of Philosophy, Cornell University. Ithaca, pp. 135.

VanderGheynst, J.S., Walker, L.P., Parlange, J.Y. 1997. Energy transport in a high-solids aerobic degradation process: Mathematical modeling and analysis. *Biotechnology Progress*, 13(3), 238-248.

von Meien, O.F., Mitchell, D.A. 2002. A two-phase model for water and heat transfer within an intermittently-mixed solid-state fermentation bioreactor with forced aeration. *Biotechnology and Bioengineering*, 79(4), 416-428.

Walker, L.P., Nock, T.D., Gossett, J.M., VanderGheynst, J.S. 1999. The role of periodic agitation and water addition in managing moisture limitations during high-solids aerobic decomposition. *Process Biochemistry*, 34(6-7), 601-612.

Weber, F.J., Oostra, J., Tramper, J., Rinzema, A. 2002. Validation of a model for process development and scale-up of packed-bed solid-state Bioreactors. *Biotechnology and Bioengineering*, 77(4), 381-393.

Wong, J.W.C., Fung, S.O., Selvam, A. 2009. Coal fly ash and lime addition enhances the rate and efficiency of decomposition of food waste during composting. *Bioresource Technology*, 100(13), 3324-3331.

Yu, H., Zeng, G.M., Huang, H.L., Xi, X.M., Wang, R.Y., Huang, D.L., Huang, G.H., Li, J.B. 2007. Microbial community succession and lignocellulose degradation during agricultural waste composting. *Biodegradation*, 18(6), 793-802.

Yu, M., Zeng, G.M., Chen, Y.N., Yu, H.Y., Huang, D.L., Tang, L. 2009. Influence of Phanerochaete chrysosporium on microbial communities and lignocellulose degradation during solid-state fermentation of rice straw. *Process Biochemistry*, 44(1), 17-22.

CHAPTER 4

INTEGRATING MIXED MICROBIAL POPULATION DYNAMICS INTO MODELING ENERGY TRANSPORT DURING THE INITIAL STAGES OF THE AEROBIC COMPOSTING OF A SWITCHGRASS MIXTURE

Abstract

A mathematical model which integrates empirically derived microbial growth kinetics with heat and mass transfer phenomena and substrate degradation kinetics has been developed to capture the dynamics of the aerobic composting of a switchgrass and dog food mixture over a period of 64h. The model incorporated three microbial populations of yeasts, bacteria and fungi that metabolized composting material consisting of sugars and starches, cellulose and hemicelluloses to produce heat and utilize oxygen in a static, cylindrical reactor employing forced aeration. Model predictions captured well the dynamics obtained experimentally between physical and microbial variables and the model has the potential to become a predictive tool for substrate degradation during aerobic composting processes.

4.1 Introduction

Composting may be defined as the degradation of organic material through microbial growth and activity. From an engineering point of view, this process has to be aerobic and may be better controlled by using forced aeration. Aerobic decomposition processes are driven by complex microbial communities that yield metabolic products such as CO_2 and heat and drive energy and mass transfer processes that define the key environmental variables such as temperature, pH, moisture content

and O_2 concentration. In turn, dynamic changes in the environmental state variables drive microbial successions and adaptations as part of an intricate feedback loop. Given the complexities of these biotic and abiotic interactions, it is challenging to control or simulate such processes. However, molecular biology tools are providing unique opportunities to measure dynamic microbial community changes and for correlating these changes with dynamic changes in the environmental state variables; thus, creating a framework to better control, design and model composting processes.

A key component to modeling composting processes is the correct description of microbial activity and coupling this activity to the mass and heat transport processes. The structure and population of microbial communities can change spatially and temporally in response to the cycling of metabolites and heat and is governed by several ecological principles such as symbiosis, commensalism and mutualism (Adney et al., 2008). A typical composting cycle goes through three stages, the first of which is characterized by the presence yeasts, lactic acid bacteria, fungi and Gram-negative bacteria; followed by a period where high temperatures are sustained by the metabolism of many *Bacillus* spp. and *Thermus thermophilus* and finally a cooling phase where more complex substrates, such as lignin, are degraded by a new microbial community (Steger et al., 2005). Thus, simulating this environment is a difficult challenge and a varying number of simplifying assumptions are often made to capture the activity of aerobic degradation microorganisms. Earlier models incorporated microbial activity indirectly by using variables such as oxygen uptake rate (VanderGheynst et al., 1997), carbon dioxide evolution rate (Richard & Walker, 2006; Richard et al., 2006) and biological volatile solids (Haug, 1993; Higgins & Walker, 2001) as surrogates for microbial growth kinetics. Other modeling efforts have sought to incorporate microbial growth kinetics explicitly into the model by treating the microbial community as a single population that can described by the

logistic equation (Dalsenter et al., 2005; Sangsurasak & Mitchell, 1998; Stuart & Mitchell, 2003; von Meien & Mitchell, 2002), the exponential growth equation (Leon et al., 1991; Sang et al., 2004), Monod kinetics (Haug, 1993; Pommier et al., 2008) and other empirically derived growth equations (Ikasari & Mitchell, 2000). However, because these models do not explicitly incorporate microbial population and community dynamics equations they are unsuccessful in simulating the broad range of process behavior that is observed in aerobic degradation processes. To circumvent this limitation, researchers have divided microbial populations according to their specificity for a given substrate (Kaiser, 1996; Sole-Mauri et al., 2007) and used Monod-type kinetics to describe the microbial community (Kaiser, 1996; Sole-Mauri et al., 2007); but the use of Monod kinetics is problematic because of the emergence of mixed and variable microbial populations during substrate decomposition.

The goal of this study is to integrate empirically derived microbial growth kinetics into traditional mass and energy transfer equations and substrate degradation kinetics to model energy transfer in a composting reactor. The composting material is divided into 3 characteristic substrates: sugars and starches, hemicelluloses and cellulose and incorporates microbial dynamics for three different microbial populations: bacteria, yeasts and fungi. Microbial kinetic parameters were obtained by performing a non-linear regression on microbial quantification data that were acquired via probe hybridization. The 64 h time frame for the model is the time period under which experiments were conducted because this period captures the dynamics of the initial stages of aerobic switchgrass degradation where the most dramatic changes in state variables occur. Also, the composting material is divided into labile and recalcitrant components as this will affect the biodegradability of the substrate and the ability of different populations to attack the given component. This is especially important when using plant biomass as a substrate, as is done in this study, because of

the chemical heterogeneity in the plant cell wall composition. This biological information was integrated into a mathematical model that used heat and mass transfer equations to describe both the temporal and spatial rate of change of temperature and oxygen utilization. The model was validated against experimental data.

4.2 Materials and Methods

4.2.1 Experimental Design

Reactor design and operation, substrate preparation, DNA extraction and probe hybridization are described in detail elsewhere (Fontenelle et al., 2010, In Press). Briefly, switchgrass (Stickle Farm, Ligonier, PA) and dog food (Big Red Puppy Food, Pro-Pet Inc., Syracuse) were size reduced and mixed together in a carbon to nitrogen ratio of 15 to 1. The dog food was chosen because its chemical composition provides readily soluble nutrients for microbial growth. Tap water was added to the substrate mixture to make an initial moisture content of 60% (wet basis). The substrate mixture was loaded into 50L bench-scale reactors and aerated at 20L/min with humidified air. Copper-constantan thermocouple wire (PP-T-24, Omega Engineering, Stamford, CT) was used to measure temperature along the height of the reactor bed with 3 thermocouples at each height: one in the middle of the reactor, one at the wall of the reactor and the other one was placed halfway between the other two thermocouples. Oxygen (O_2) concentration and carbon dioxide (CO_2) concentration were measured at the reactor effluent.

Samples were collected from the reactors at pre-defined times for the duration of the reactor run (64hr). The pH, moisture content and amounts of bacteria, fungi and yeast DNA were measured for each sample. The DNA was extracted from the samples using a bead beating method with a phenol/chloroform/isoamyl precipitation (Fontenelle et al., 2010, In Press). DNA was also extracted from samples of yeast,

bacteria and fungi to serve as reference and quantitative standards during the hybridization, using a MasterPure DNA purification kit (Epicentre Biotechnologies, Madison, WI) according to the manufacturer's instructions. DNA samples were hybridized to bacteria, fungi and yeast probes according to manufacturer's instructions. The chemiluminiscent emissions of the probes were captured using a G:Box HR Imager (Syngene, Frederick, MD) with a 1 hr exposure time. Using Imager software (Syngene, Frederick, MD), the intensities of the bands from the reactor samples were compared to the intensities of the known mass standards in order to assign a mass to the unknown samples. The mass of probes microbial DNA in each sample was then standardized to the mass of the sample used for the DNA extraction.

4.2.2 Model Development

The model simulates temporal microbial degradation in an insulated cylindrical packed bed reactor that is forcefully aerated from the bottom using humidified air. A mixed substrate containing 60% moisture (wet basis) is supported on a perforated plate and remains static for the duration of the 64hr study. The model considers the generation of metabolic heat from aerobic reactions of 3 major microbial populations, each with a distinct specificity for various components of the substrate. The equations for the state variables and the microbial kinetics are described in the following subsections.

4.2.2.1 Substrate Utilization Kinetics

The model of substrate degradation corresponding to the microbial growth kinetics assumes that fungi and bacteria utilize all of the substrates present and yeasts grow from the degradation of sugars and starches. The equations describing substrate degradation were adapted from Kaiser (1996):

sugars and starches = s_1

$$\frac{ds_1}{dt} = -Y_1\left(s_1\frac{dx_1}{dt} + \frac{s_1}{s_1+s_2+s_3}\frac{dx_2}{dt} + \frac{s_1}{s_1+s_2+s_3}\frac{dx_3}{dt}\right) \quad 4.1$$

hemicellulose = s_2

$$\frac{ds_2}{dt} = -Y_2\left(\frac{s_2}{s_1+s_2+s_3}\frac{dx_2}{dt} + \frac{s_2}{s_1+s_2+s_3}\frac{dx_3}{dt}\right) \quad 4.2$$

cellulose = s_3

$$\frac{ds_3}{dt} = -Y_3\left(\frac{s_3}{s_1+s_2+s_3}\frac{dx_2}{dt} + \frac{s_3}{s_1+s_2+s_3}\frac{dx_3}{dt}\right) \quad 4.3$$

where s_i (kg component/kg organic material) is the concentration of substrate i (i=1=sugars and starches, i=2=hemicelluloses and i=3=cellulose), Y_i is the growth yield coefficient (kg substrate/kg organisms) and x_i (kg microbial population/kg organic material) is the microbial population (i=1 = yeast, i=2 = bacteria and i=3=fungi).

4.2.2.2 Microbial growth kinetics

Metabolic activities were considered to be driven by three main populations – yeasts, bacteria and fungi on specific components of the substrate. Temporal profiles of the biomass levels revealed two separate periods, which have been termed the growth phase and the deceleration phase. An exponential model provided the best fit for both of these phases when compared to logistic and linear growth models. Accordingly, parameters for both of these phases were approximated using the following exponential equation:

$$\frac{dx}{dt} = \beta x \tag{4.4}$$

where x is the microbial population (kg/kg organic material) and β is an overall growth or deceleration rate (hr^{-1}) that represents the difference between the growth rate and the death rate because these parameters cannot be uniquely approximated from our system. Values for β were estimated using a non-linear Gauss-Newton iterative regression technique in MATLAB 7.7 (The Mathworks Inc., Natick, MA) based on quantified microbial masses during the decomposition process at each bed height of the reactor. Assuming that the overall growth rates were dependent on the substrate concentrations, the substrate-dependent integrated model of microbial growth was described by the following equations:

$$\frac{dx_1}{dt} = \beta_1 x_1 \left(\frac{s_1}{Ks_1 + s_1}\right) \tag{4.5}$$

$$\frac{dx_2}{dt} = \beta_2 x_2 \left(\frac{s_1 + s_2 + s_3}{Ks_2 + s_1 + s_2 + s_3}\right) \tag{4.6}$$

$$\frac{dx_3}{dt} = \beta_3 x_3 \left(\frac{s_1 + s_2 + s_3}{Ks_3 + s_1 + s_2 + s_3}\right) \tag{4.7}$$

4.2.2.3 Energy Balance

An energy balance must account for convective, conductive and evaporative heat production and removal, heat generation by microbial activity, heat and mass diffusion and energy accumulation in the axial, radial and angular directions. The significance of each of these transport mechanisms in the energy balance for a microbial degradation system is highly dependent on the system design. In this study, the system design has allowed for several simplifying assumptions in performing the

energy balance. As a result of insulating the reactors, it is assumed that transport in the radial and angular directions is negligible. Conduction and diffusion in the substrate bed in any direction is considered to be minimal because of the use of forced aeration. The substrate bed is also treated as a homogeneous mixture, implying that at any particular location within the reactor, the gas and solid phases are in thermal equilibrium. Assuming that all of the heat produced was a result of microbial activity, the amount of heat released per unit time from the reactor was modeled using the equation:

$$\frac{dQ_{bio}}{dt} = q\sum_{i=1}^{3}\frac{dx_i}{dt} \qquad 4.8$$

where q is the metabolic heat yield coefficient (kJ/kg biomass). Therefore we model the temporal rate of energy transfer within the reactor using the following distributed dynamic heat transfer model:

$$\frac{\partial T}{\partial t} = \frac{\frac{dQ_{bio}}{dt} - V\rho_a(T)(c_{p,a} + de^{mT})V_z\frac{\partial T}{\partial z}}{V[\varepsilon\rho_a(T)(c_{p,a} + de^{mT}c_{p,v}) + (1-\varepsilon)\rho_s(c_{p,s} + c_{p,w}M_d)}} \qquad 4.9$$

subject to the following conditions:

Initial condition: at t=0, T = 296K

Boundary condition: at z = H, $\frac{\partial T}{\partial z} = 0$

where T is the temperature (K), V is the system volume (m^3), ρ_a (temperature dependent) and ρ_s are the densities of air and the dry bulk, respectively, ε is the porosity of the substrate bed, $c_{p,a}$, $c_{p,s}$, $c_{p,w}$, $c_{p,v}$ are the specific heats at constant pressure (KJ/Kg K) of air, dry bulk, water and water vapor, respectively, V_z is the

superficial air velocity and M_d is the moisture content on a dry basis. The expression de^{mT} was derived from steam tables (Elliot & Lira, 1999) to estimate the phase change energy associated with water transport. Table 4.1 lists the parameters used in Equation 4.9 with their associated values.

4.2.2.4 Oxygen mass balance

The change in oxygen concentration of the reactor provides a good indication of the level of microbial activity within the system. A mass balance on oxygen flow for this model assumes that the only oxygen reaction occurring is the consumption of oxygen by growing microbes. The model also assumes that the only mechanism by which oxygen enters the reactor is via forced aeration and that the effluent oxygen concentration has equilibrated with the oxygen concentration at the very top of the reactor before exiting. The time rate of change of oxygen mass concentration (o_2) is modeled as follows:

$$\frac{do_2}{dt} = \frac{\dot{m}_a(o_{2,a} - o_2) - m\sum_{i=1}^{3}\beta_{o2,i}\frac{dx_i}{dt}}{\rho_a(T)V\varepsilon} \qquad 4.10$$

where $\dot{m}_a$ is the mass flow rate of air (kg dry air/hr), $o_{2,a}$ is the ambient oxygen mass concentration in air (kg O_2/kg dry air), o_2 is the oxygen concentration of the substrate bed (kg O_2/kg dry air), m is the mass of the substrate bed (kg organic material), $\beta_{o2,i}$ is the specific oxygen uptake rate for population i, $\rho_a(T)$ is the temperature-dependent density of air (kg/m^3), V is the system volume (m^3) and ε is the porosity of the substrate bed.

Table 4.1 Parameters and coefficients used in the energy transfer model

Parameter	Description	Value	Source
V (m^3)	Reactor volume	0.05	Experiment
ρ_a (kg/m^3)	Density of air (temperature dependent)	P_{atm}/R_dT	(ASAE, 1983)
P_{atm} (Pa)	Atmospheric pressure	101325	(ASAE, 1983)
$C_{p,a}$ (kJ/kg K)	Specific heat of dry air at constant pressure	1.0132	(Higgins & Walker, 2001)
d	Latent heat coefficient	$1.21 * 10^{-7}$	Parameter estimation
m (1/K)	Latent heat coefficient	0.0568	Parameter estimation
V_z (m/h)	Superficial air velocity	16.4	Experiment
ε	Void fraction	0.4	(Lam et al., 2007)
$C_{p,v}$ (kJ/kg K)	Specific heat of water vapor at constant pressure	1.8673	(Higgins & Walker, 2001)
ρ_{db} (kg/m^3)	Dry bulk density	160	Experiment
$C_{p,s}$ (kJ/kg K)	Specific heat of dry solids	2.0	(Higgins & Walker, 2001), (Lam et al., 2007)
$C_{p,w}$ (kJ/kg K)	Specific heat of water	4.1868	(Higgins & Walker, 2001)
Y_1(kg/kg)	Yield coefficient of carbohydrates	4.4	(Sole-Mauri et al., 2007)
Y_2 (kg/kg)	Yield coefficient of cellulose	3.0	(Sole-Mauri et al., 2007)
Y_3 (kg/kg)	Yield coefficient of hemicellulose	3.8	(Sole-Mauri et al., 2007)

Table 4.1 Continued

Ks_1 (kg/kg)	Saturation constant of yeast	0.06	Optimized for model validation
Ks_2 (kg/kg)	Saturation constant of bacteria	0.08	Optimized for model validation
Ks_3 (kg/kg)	Saturation constant of fungi	0.08	Optimized for model validation
$s_{1,0}$ (kg/kg)	Initial quantity of sugars and starches	1.728	(VanderGheynst, 1997)
$s_{2,0}$ (kg/kg)	Initial quantity of hemicellulose	1.4442	(Qin et al., 2006)
$s_{3,0}$ (kg/kg)	Initial quantity of cellulose	1.6689	(Qin et al., 2006)
$\beta_{o2,1}$	Yeast oxygen yield	1.5	(Haug, 1993)
$\beta_{o2,2}$	Bacteria oxygen yield	3.0	(Haug, 1993)
$\beta_{o2,3}$	Fungi oxygen yield	1.5	(Haug, 1993)
M_d	Moisture content (dry basis)	1.5	Experiment

4.2.2.5 Numerical Method

To solve the distributed heat transport model, the method of lines was used, where discretization of the spatial component was accomplished using the central difference approximation for the partial derivatives. The spatial component of Equation 4.9 was divided into n equal space grids and the following non-linear ordinary differential equation was obtained for each space grid:

$$\frac{dT_i}{dt} = \left(\frac{1}{A}\right)\left(\frac{dQ_{bio}}{dt} - V\rho_a(T_i)(c_{p,a} + de^{mT})V_z \left(T_{i+1} - T_{i-1}\right)\frac{1}{2h}\right) \qquad 4.11$$

for i = 2,3,….,n and where A = $V[\varepsilon\rho_a(T)(c_{p,a} + de^{mT}c_{p,v}) + (1-\varepsilon)\rho_s(c_{p,s} + c_{p,w}M_d)$ and h is the height step size; subject to the boundary conditions that at z = 0 and z = n, $\frac{\partial T}{\partial z} = 0$. Microbial growth rates for intermediate space points were obtained by interpolating between preceding and subsequent heights at which the values were known.

Numerical integration of the resulting set of 9 non-linear ordinary differential equations (Eq. 4.1 – 4.3, 4.5 – 4.7 and 4.10 – 4.11) was performed at each space point using the calculated overall microbial growth rates at that reactor height. The integration was carried out using the ODE45 routine in MATLAB, which uses a fourth and fifth order Runge-Kutta approximation with an adaptive time step to minimize errors while simultaneously solving the equations.

4.3 Results & Discussion

4.3.1 Verification of Assumptions

One of the key assumptions used in the development of this model was negligible radial gradients and this was observed in our experimental runs. Figure 4.1 shows the radial temperature profile at a height of 0.6m above the perforated plate and the results obtained for the other reactor bed heights are consistent with this plot. The calculated radial gradients (not shown) between the center and the wall of the reactors were less than 1^{o}C/cm for the vast majority of bed heights along the reactor. These results confirm that the bulk flow of energy may be modeled as a one dimensional heat transfer problem, as has been done before (VanderGheynst et al., 1997).

Another assumption used in the model was that of constant moisture content. Given that saturated air was continuously fed into the reactor, it is not surprising that no significant moisture losses were observed and this is reflected in Figure 4.2, which confirms the assumption that the moisture content of the substrate matrix remained relatively constant at all bed heights for the duration of this study. In fact, the experimental data show a maximum moisture loss of 8% at a height of 0.2m in the bed.

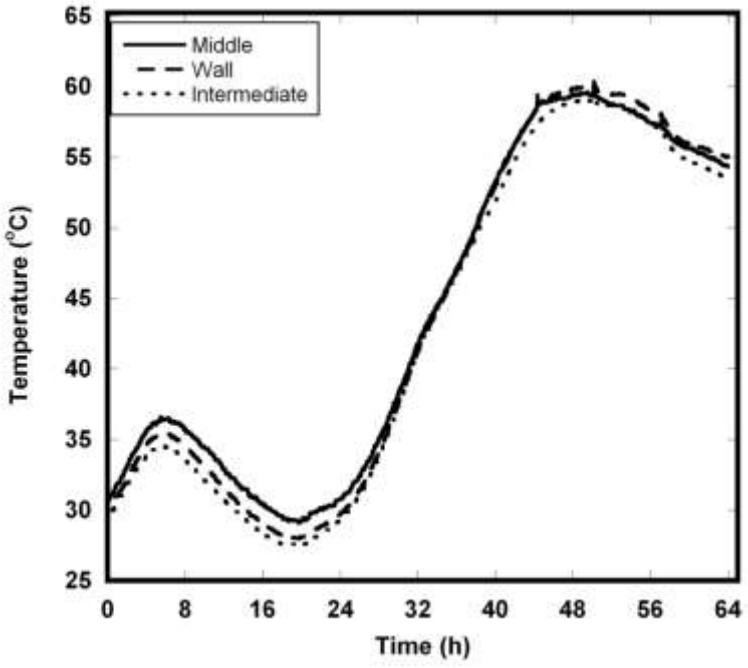

Figure 4.1 Radial temperature profile of experimental data at a bed height of 0.6m

4.3.2 Parameter estimations

Microbial growth parameters were obtained by plotting the mass of the various microbial populations versus time. The distinction between the two growth phases was determined by the point at which microbial mass ceased to increase and began to decrease. For the bacteria, yeast and fungi populations, this transition from growth to deceleration occurred between 38 to 50h for all reactor heights. The estimated values of the microbial growth parameters and the goodness of fit of the exponential equation to the experimental data are presented in Table 4.2. Estimates of the initial microbial population mass were in most cases almost identical to the experimentally-determined mass and are not presented in Table 4.2. The results show that for the growth phase, bacteria provided the best fits to the exponential growth model, followed by yeasts and fungi. This is not surprising considering that bacteria were the dominant microbial population. During the deceleration phase, yeasts had the most rapid decrease in population and thus experienced the best fits to the exponential decay model, followed by bacteria and then fungi. Overall, the use of a two-phase growth model was necessary in order to fully capture the dynamics of the biomass profiles over time and resulted in parameters that enabled the model to better predict the experimental data.

Table 4.2 Parameter estimations for the exponential equation describing the growth and deceleration phases for bacteria, yeast and fungi populations

Height	Growth Phase					
(m)	Yeast		Bacteria		Fungi	
	$\beta(h^{-1})$	R^2	$\beta(h^{-1})$	R^2	$\beta(h^{-1})$	R^2
0.1	0.11	0.91	0.08	0.81	0.05	0.60
0.2	0.07	0.99	0.06	0.96	0.03	0.67
0.3	0.10	0.93	0.06	0.93	0.01	0.61
0.4	0.14	0.98	0.08	0.99	0.04	0.97
0.5	0.11	0.85	0.06	0.92	0.03	0.68
0.6	0.10	0.82	0.07	0.88	0.03	0.85

Height	Deceleration Phase					
(m)	Yeast		Bacteria		Fungi	
	$\beta(h^{-1})$	R^2	$\beta(h^{-1})$	R^2	$\beta(h^{-1})$	R^2
0.1	-0.20	0.99	-0.44	0.99	-0.04	0.70
0.2	-0.16	0.97	-0.50	0.99	-0.12	0.81
0.3	-0.13	0.98	-0.50	0.99	-0.07	0.98
0.4	-0.12	0.98	-0.57	0.99	-0.04	0.80
0.5	-0.21	0.99	-0.09	0.77	-0.03	0.92
0.6	-0.06	0.87	-0.06	0.73	0.05	0.72

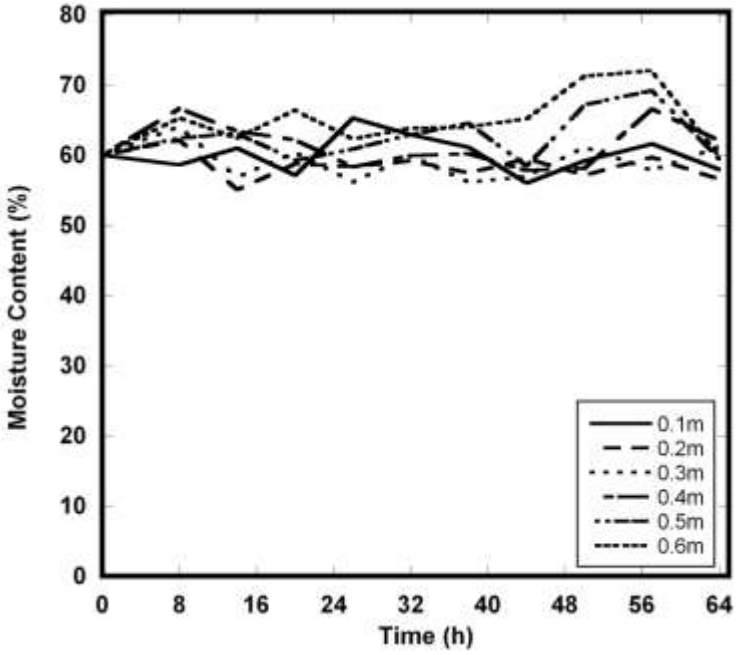

Figure 4.2. Moisture content (wet basis) profile of experimental data

4.3.3 Model Validation

Growth of the bacterial, fungal and yeast populations, as predicted by the model is reasonably consistent with the observed experimental data (Figure 4.3). The yeast and bacterial profiles predicted by the model are in better agreement with the experimental data than the fungal profile. This is most likely due to having weaker correlations for the fungal data during the parameter estimations. Such reasonable agreement between the observed and predicted microbial profiles lends credence to the use of a two-phase model for describing microbial growth in decomposition processes. Previous studies, which have only looked at the temporal aspect of composting processes, have also found the use of a two- phase microbial growth model to be a better predictor of energy transfer as opposed to single phase growth (Ikasari & Mitchell, 2000; Sole-Mauri et al., 2007). Obtaining both spatial and temporal agreement between models and experiments, as shown in Figure 3 is challenging and this study is one of the first to model spatial variation in the underlying microbial growth and to place it in an energy transfer framework. In composting processes, it is typically desirable to assess growth dynamics using empirically derived kinetics because microbial growth occurs in undefined mixed cultures whose dynamics vary from pure culture in controlled environments. However, in several cases of modeling composting processes, pure-culture kinetic parameters were not adjusted for mixed and variable populations (Dalsenter et al., 2005; Fanaei & Vaziri, 2009; Sangsurasak & Mitchell, 1998; Saucedocastaneda et al., 1990; Sole-Mauri et al., 2007; Stuart & Mitchell, 2003; von Meien & Mitchell, 2002; Weber et al., 2002). In this study, we were able to overcome this limitation by monitoring microbial population growth during the study period and extracting the data required to estimate parameters for the microbial growth equations.

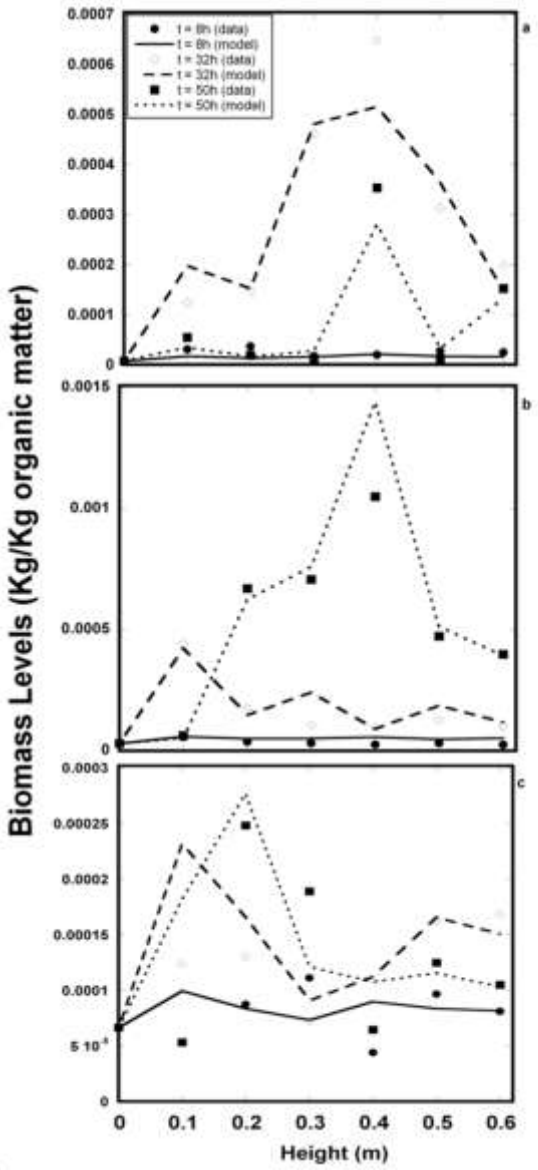

Figure 4.3. Comparison of the (a) yeast population (b) bacterial population and (c) fungal population profiles of experimental data with the model prediction

Integrating substrate degradation kinetics into the sub routine describing microbial growth kinetics is another factor which sets this model apart from many other models. Figure 4.4(a) shows the degradation profiles of the substrate components as predicted by the model where initial substrate concentrations were obtained from (VanderGheynst, 1994) and (Qin et al., 2006). A notable decrease in the cellulose, hemicelluloses and sugars/starches content is evident, even in the initial stages monitored in this study. Although lignin is a major component of the switchgrass plant cell wall, it was not included in this analysis because studies of microbial succession in composting processes have revealed that lignin degradation, which occurs from the activity of actinobacteria and white rot fungi, takes place in later stages of the process (Chroni et al., 2009; Danon et al., 2008; Huang et al.; Ishii et al., 2000; Ryckeboer et al., 2003; Sanchez, 2009; Vargas-Garcia et al., 2006). Substrate degradation kinetics were first incorporated into composting mathematical models by (Kaiser, 1996) and more recently by (Sole-Mauri et al., 2007) and (Vlyssides et al., 2009). These studies used Monod kinetics to integrate microbial growth into substrate degradation but are usually limited because Monod kinetics are not well suited for mixed, undefined microbial composting populations (Petric & Selimbasic, 2008). This limitation was overcome in this study by incorporating individual substrate components into empirically-determined microbial growth using a two-phase growth model that uses first order kinetics. This study would also greatly benefit from characterization of substrate conversion to obtain the experimental data for comparison with the predicted substrate degradation profiles presented in Figure 4.4(a).

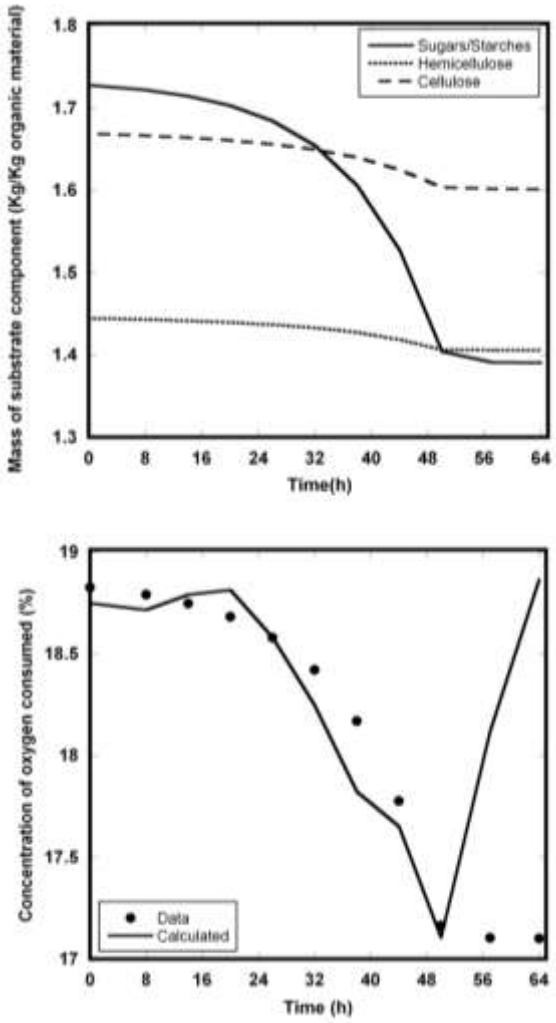

Figure 4.4. (a) Predicted substrate degradation profile at a bed height of 0.6m and (b) Comparison of experimental oxygen utilization values to those calculated based on the predicted substrate composition by using the stoichiometric oxygen requirements for glucose oxidation

To lend credence to the predicted substrate degradation profiles, the total quantity of substrate at each time point, as predicted by the model, was used to calculate the amount of oxygen required for substrate decomposition based on the stoichiometry of glucose oxidation (Haug, 1993):

$$C_6H_{12}O_6 + 6\ O_2 \longrightarrow 6\ CO_2 + 6\ H_2O$$

Comparing these calculated values for oxygen utilization based on the predicted substrate compositions to experimental oxygen utilization quantities showed good agreement between these two sets of values for the majority of the time period (Figure 4.4(b)); thus, demonstrating that the model accurately depicted the substrate degradation profiles. Towards the end of the study period, the calculated and experimental oxygen utilization values appear to diverge; suggesting that estimating substrate decomposition based solely on glucose oxidation is no longer valid because more complex substrates are being broken down in this region (Cooperband, 2002). These more complex substrates are most likely proteins, urea and other nitrogenous compounds which are typical in composting systems where the starting C/N ratio is less than 25/1 and is an effect of mineralization where several biochemical reactions lead to the transformation of the excess nitrogenous materials (Gajalakshmi & Abbasi, 2008).

Similar to the microbial growth, good agreement was found between the experimental and model temperatures (Figure 4.5). The spatial temperature profile captured well the gradual increase in temperature as a function of increasing height. A 4% difference existed between the maximum temperature predicted by the model and the experimentally observed maximum temperature, which occurred at a bed height of

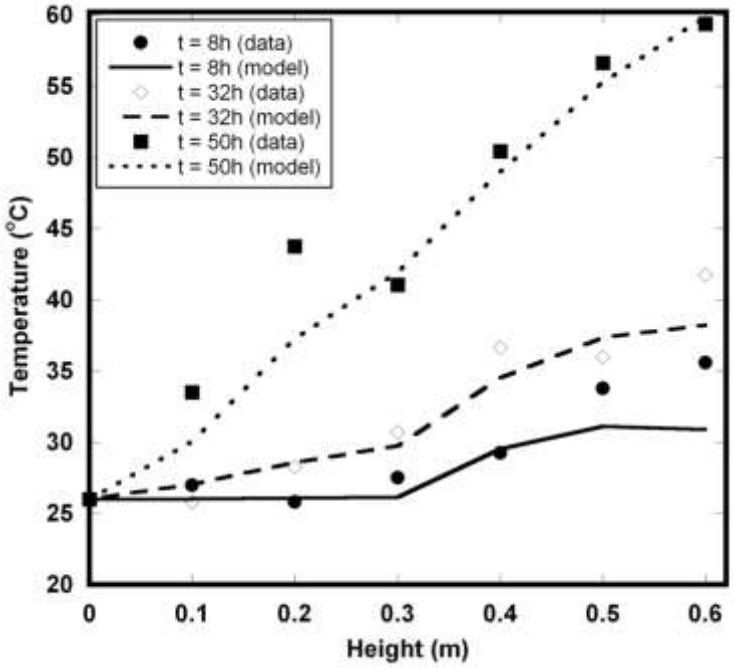

Figure 4.5. Comparison of experimental spatial temperature profiles to profiles predicted by the heat transfer model

0.6m. The favorable agreement between the model and experimental data shows that incorporating a sub routine of empirically described microbial growth kinetics may be effectively used in traditional heat and mass transfer equations to accurately capture energy dynamics in the system. This is in keeping with a review of mathematical models of composting processes which found that for the most part, models which integrated empirical kinetic expressions produced more accurate predictions of temperature and other state variables (Mason, 2006). Furthermore, the simplicity of the microbial growth model presented here is desirable because very comprehensive models that attempt to simulate all the intricate interactions in microbial metabolism rapidly become overly complicated and cumbersome to implement. Sole-Mauri et al. (2007) introduced a fully detailed model, but the large number of parameters included in the model produced some results that were difficult to interpret. The use of static packed bed reactors is also important because such systems are easier to engineer and control, making them predominant in degradation processes (Sangsurasak & Mitchell, 1998).

Another state variable that was reasonably predicted by this model was the oxygen concentration. Using the oxygen concentration predictions, the oxygen consumption rate (OCR) was calculated and compared to experimental data because the OCR gives a better indication of microbial activity (Figure 4.6). The profiles shown in Figure 4.6 show that the OCR predicted by the model was in good agreement with the experimental data, with only a 0.4% difference between the maximum value obtained experimentally and that predicted by the model. Very few models have actually predicted either the OCR or oxygen concentration (Higgins & Walker, 2001; Petric & Selimbasic, 2008; Weber et al., 2002) despite the importance of this variable in aerobic composting systems.

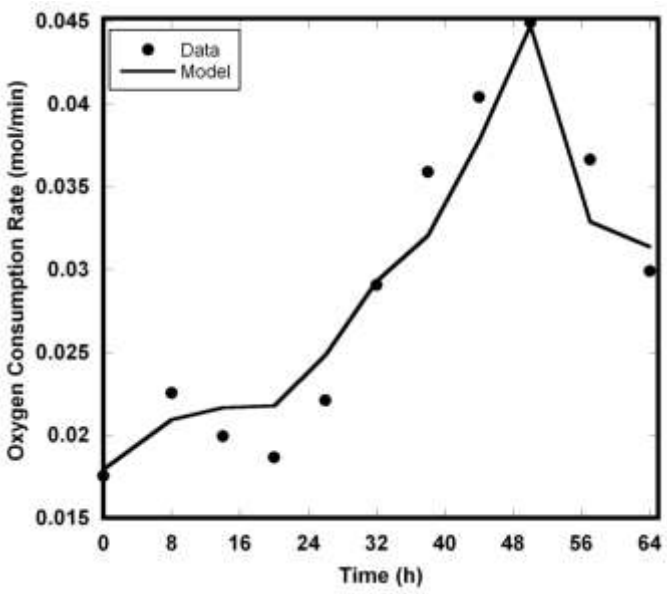

Figure 4.6. Comparison of effluent oxygen consumption rate (OCR) profiles of experimental data with model predictions

4.3.3 Sensitivity Analysis

A sensitivity analysis was performed to assess the significance of key parameters of the empirical microbial growth kinetics sub routine on the output model temperature because temperature encompasses all of the pertinent biological, chemical and physical interactive phenomena in the system. By analyzing the temperature output, more direct comparisons may be made about the effect of parameter modifications on the model. The effect of these key parameters on temperature were evaluated by increasing and decreasing the growth rate and initial mass of biomass of the 3 microbial populations by 50% of its original value and the output peak temperatures are recorded in Table 4.3. Of the three populations assessed, the maximum temperature produced by the model was most drastically affected by the bacterial population, as shown in Table 4.3. This result is not surprising, given that bacteria played a dominant role in the microbial community for the duration of the experimental study. This predominance of bacteria is typical in composting processes. In contrast to the dramatic effects of bacterial population, the model was least sensitive to changes in the fungal population parameters. This is a direct reflection of the experimentally observed profiles. For all the population parameters, with the exception of the initial fungal biomass population, decreasing the value of that parameter led to a decrease in the maximum predicted temperature with the converse occurring when the parameters were increased by 50%.

Table 4.3. Sensitivity of peak temperatures predicted by the model to deviations in parameters describing microbial population growth kinetics at a bed height of 0.6m

Parameter	Description	Peak Temperature (^oC)
$0.5\beta_1$		58.3
β_1	Yeast growth	59.9
$1.5\ \beta_1$		70.7
$0.5\ X_{0,1}$	Yeast initial mass	58.9
$X_{0,1}$		59.9
$1.5\ X_{0,1}$		60.7
$0.5\beta_2$	Bacteria Growth	35.5
β_2		59.9
$1.5\ \beta_2$		79.8
$0.5\ X_{0,2}$	Bacteria initial mass	44.3
$X_{0,2}$		59.9
$1.5\ X_{0,2}$		75.2
$0.5\beta_3$	Fungi Growth	59.4
β_3		59.9
$1.5\ \beta_3$		60.6
$0.5\ X_{0,3}$	Fungi initial mass	59.9
$X_{0,3}$		59.9
$1.5\ X_{0,3}$		60.2

4.4 Conclusions

Advancements in molecular biology have provided tools for characterizing microbial communities and have allowed us to estimate microbial growth kinetic parameters and incorporate these parameters into a system of energy transfer equations to simulate the biodegradation of a mixed substrate. Three microbial populations were considered each with a different specificity for the three components of the substrate, resulting in model predictions that were in good agreement with experimental data, thereby validating the assumed kinetics of microbial growth on the substrates. Such characterization of switchgrass biodegradation is of importance for bioenergy and bioproducts applications where switchgrass is often used as the main lignocellulosic substrate.

REFERENCES

Adney, S., van der Lelie, D., Berry, A., M., H. 2008. *Biomass Recalcitrance*. John Wiley and Sons Incorporated.

ASAE. 1983. Psychrometric Data. in: *1982-1983 Agricultural Engineers Yearbook*, pp. 331-333.

Chroni, C., Kyriacou, A., Manios, T., Lasaridi, K.E. 2009. Investigation of the microbial community structure and activity as indicators of compost stability and composting process evolution. *Bioresource Technology*, **100**(15), 3745-3750.

Cooperband, L. 2002. The Art and Science of Composting - A Resource for Farmers and Compost Producers. University of Wisconsin - Madison.

Dalsenter, F.D.H., Viccini, G., Barga, M.C., Mitchell, D.A., Krieger, N. 2005. A mathematical model describing the effect of temperature variations on the kinetics of microbial growth in solid-state culture. *Process Biochemistry*, **40**(2), 801-807.

Danon, M., Franke-Whittle, I.H., Insam, H., Chen, Y., Hadar, Y. 2008. Molecular analysis of bacterial community succession during prolonged compost curing. *Fems Microbiology Ecology*, **65**(1), 133-144.

Elliot, J.R., Lira, C.T. 1999. *Introductory Chemical Engineering Thermodynamics*. Prentice Hall.

Fanaei, M.A., Vaziri, B.M. 2009. Modeling of temperature gradients in packed-bed solid-state bioreactors. *Chemical Engineering And Processing*, **48**(1), 446-451.

Haug, R.T. 1993. *The Practical Handbook of Compost Engineering*. Lewis Publishers.

Higgins, C.W., Walker, L.P. 2001. Validation of a new model for aerobic organic solids decomposition: simulations with substrate specific kinetics. *Process Biochemistry*, **36**(8-9), 875-884.

Huang, D.-L., Zeng, G.-M., Feng, C.-L., Hu, S., Lai, C., Zhao, M.-H., Su, F.-F., Tang, L., Liu, H.-L. 2010. Changes of microbial population structure related to lignin degradation during lignocellulosic waste composting. *Bioresource Technology*, **101**(11), 4062.

Ikasari, L., Mitchell, D.A. 2000. Two-phase model of the kinetics of growth of Rhizopus oligosporus in membrane culture. *Biotechnology and Bioengineering*, **68**(6), 619-627.

Ishii, K., Fukui, M., Takii, S. 2000. Microbial succession during a composting process as evaluated by denaturing gradient gel electrophoresis analysis. *Journal of Applied Microbiology*, **89**(5), 768-777.

Kaiser, J. 1996. Modelling composting as a microbial ecosystem: A simulation approach. *Ecological Modelling*, **91**(1-3), 25-37.

Lam, P.S., Sokhansanj, S., Bi, X., Mani, S., Lim, C.J., Womac, A.R., Hoque, M., Peng, J., JayaShankar, T., Naimi, L.J., Nayaran, S. 2007. Physical Characterization of wet and dry wheat straw and switchgrass - bulk and specific density. *ASABE*.

Leon, R., Torres, A., Echevarria, J., Saura, G. 1991. Energy-Balance in Solid-State Fermentation Processes. *Acta Biotechnologica*, **11**(1), 9-14.

Mason, I.G. 2006. Mathematical modelling of the composting process: A review. *Waste Management*, **26**(1), 3-21.

Petric, I., Selimbasic, V. 2008. Development and validation of mathematical model for aerobic composting process. *Chemical Engineering Journal*, **139**(2), 304-317.

Pommier, S., Chenu, D., Quintard, M., Lefebvre, X. 2008. Modelling of moisture-dependent aerobic degradation of solid waste. *Waste Management,* **28**(7), 1188-1200.

Qin, X., Mohan, T., El-Halwagi, M., Cornforth, G., McCarl, B. 2006. Switchgrass as an alternate feedstock for power generation; an integrated, environmental, energy and economic life-cycle assessment. *Clean Technologies and Environmental Policy*, **8**(4), 233-249.

Richard, T.L., Walker, L.P. 2006. Modeling the temperature kinetics of aerobic solid-state biodegradation. *Biotechnology Progress,* **22**(1), 70-77.

Richard, T.L., Walker, L.P., Gossett, J.M. 2006. Effects of oxygen on aerobic solid-state biodegradation kinetics. *Biotechnology Progress,* **22**(1), 60-69.

Ryckeboer, J., Mergaert, J., Coosemans, J., Deprins, K., Swings, J. 2003. Microbiological aspects of biowaste during composting in a monitored compost bin. *Journal of Applied Microbiology,* **94**(1), 127-137.

Sanchez, C. 2009. Lignocellulosic residues: Biodegradation and bioconversion by fungi. *Biotechnology Advances,* **27**(2), 185-194.

Sang, B.I., Hori, K., Unno, H. 2004. A mathematical description for the fungal degradation process of biodegradable plastics. *Mathematics And Computers In Simulation,* **65**(1-2), 147-155.

Sangsurasak, P., Mitchell, D.A. 1998. Validation of a model describing two-dimensional heat transfer during solid-state fermentation in packed bed bioreactors. *Biotechnology and Bioengineering*, **60**(6), 739-749.

Saucedocastaneda, G., Gutierrezrojas, M., Bacquet, G., Raimbault, M., Viniegragonzalez, G. 1990. Heat-Transfer Simulation in Solid Substrate Fermentation. *Biotechnology and Bioengineering*, **35**(8), 802-808.

Sole-Mauri, F., Illa, J., Magri, A., Prenafeta-Boldu, F.X., Flotats, X. 2007. An integrated biochemical and physical model for the composting process. *Bioresource Technology*, **98**(17), 3278-3293.

Steger, K., Eklind, Y., Olsson, J., Sundh, I. 2005. Microbial community growth and utilization of carbon constituents during thermophilic composting at different oxygen levels. *Microbial Ecology*, **50**(2), 163-171.

Stuart, D.M., Mitchell, D.A. 2003. Mathematical model of heat transfer during solid-state fermentation in well-mixed rotating drum bioreactors. *Journal of Chemical Technology and Biotechnology*, **78**(11), 1180-1192.

VanderGheynst, J.S. 1994. Design and Process Ananlysis of a High-Solids Aerated Static Bed. in: *Biological and Environmental Engineering*, Vol. Masters of Science, Cornell University. Ithaca, pp. 167.

VanderGheynst, J.S., Walker, L.P., Parlange, J.Y. 1997. Energy transport in a high-solids aerobic degradation process: Mathematical modeling and analysis. *Biotechnology Progress*, **13**(3), 238-248.

Vargas-Garcia, M.D., Suarez-Estrella, F.F., Lopez, M.J., Moreno, J. 2006. Influence of microbial inoculation and co-composting material on the evolution of humic-like substances during composting of horticultural wastes. *Process Biochemistry*, **41**(6), 1438-1443.

Vlyssides, A., Mai, S., Barampouti, E.M. 2009. An integrated mathematical model for co-composting of agricultural solid wastes with industrial wastewater. *Bioresource Technology*, **100**(20), 4797-4806.

von Meien, O.F., Mitchell, D.A. 2002. A two-phase model for water and heat transfer within an intermittently-mixed solid-state fermentation bioreactor with forced aeration. *Biotechnology and Bioengineering*, **79**(4), 416-428.

Weber, F.J., Oostra, J., Tramper, J., Rinzema, A. 2002. Validation of a model for process development and scale-up of packed-bed solid-state Bioreactors. *Biotechnology and Bioengineering*, **77**(4), 381-393.

CHAPTER 5

LIGNOCELLULOSIC DEGRADATION AND BIOCHEMICAL DYNAMICS OF THE INITIAL STAGES OF SWITCHGRASS DECOMPOSITION

Abstract

Physical, chemical and microbial dynamics of the initial stages of the biodegradation of switchgrass (*Panicum virgatum*) amended with nitrogen fertilizer were studied in a composting environment. Both temporal and spatial dynamics were monitored in highly-instrumented reactors. Temperatures increased rapidly by 38^{o}C within the first 8h while pH also rapidly increased to alkaline conditions. Changes in pH were highly correlated to changes in temperature and acetic acid concentration, with acetic acid being the dominant organic acid in most samples. At the end of the study, 19%, 24% and 26% degradation was recorded in the lignin, cellulose and hemicellulose contents, respectively of the substrate, with changes in these components being commensurate with each other and variations in pH, effluent gas concentration and total organic acid concentration. Real time PCR was successfully used to track changes in the microbial populations of general bacteria and fungi, *Aspergillus spp.* and lactic acid bacteria which indicated a shift from a predominance of lactic acid bacteria to other bacteria and a noticeable increase in *Aspergillus spp.* after temperatures had peaked.

5.1 Introduction

Switchgrass (*Panicum virgatum*) has been identified as a lignocellulosic crop which holds great promise as a substrate for the sustainable production of cellulosic ethanol (Tilman et al., 2009). Although great efforts and breakthroughs are being made to biologically convert this substrate into liquid fuels, there is still a need to understand how switchgrass decomposes biologically to liberate the energy content

and the chemical components of its biomass. Microbial degradation via composting represents a cheap and practical option for studying this complex environment. During composting, intricate networks of heterotrophic microorganisms grow and metabolize organic substrates to yield heat, carbon dioxide and a humic substance that is often used as a soil amendment. Although composting has been studied for many decades, the underlying driving force for the process is poorly understood and characterization is dependent on the substrate used.

The sturdy plant cell wall of switchgrass, made up of intertwined polymer networks of cellulose, hemicelluloses and lignin makes it particularly recalcitrant and difficult to degrade microbially (Adney et al., 2008). In nature this process may take decades, so to expedite the process switchgrass needs to be amended with a nitrogen source to decrease the carbon to nitrogen ratio to favor microbial cell growth. Available literature on the microbial degradation of switchgrass is limited to a very small number of studies where switchgrass was amended with dog food for natural microbial growth (Fontenelle et al., 2010) and with green waste compost for the growth of glycoside hydrolases (Allgaier et al.). These studies have begun to shed some light into the dynamics of the process, but more work is needed in order to develop the most efficient system for switchgrass composting.

In this study, switchgrass, the main carbon source, was amended with nitrogen fertilizer to increase its rate of biodegradation. This study was limited to the initial stages of biodegradation because this period captures dramatic changes in biotic and abiotic state variables and because we believe that this is a key transition period where we can manipulate variables in order to increase the overall rate of biodegradation once we understand the couplings of various parameters. A further goal of this study was to obtain key kinetic parameters because these parameters facilitate the comparison of processes where different substrates are used and because these

parameters may be used to develop models to describe the microbial degradation process.

5.2 Materials and Methods

5.2.1 Reactor operation and sampling

Reactor design and operation are described in detail elsewhere (Fontenelle et al., 2010). Briefly, 50L bench-scale reactors were built and aerated at 20L/min with humidified air. Copper-constantan thermocouple wire (PP-T-24, Omega Engineering, Stamford, CT) was used to measure temperature at the 0.1m, 0.3m and 0.6m heights of the reactor bed. Oxygen (O_2) concentration and carbon dioxide (CO_2) concentration were measured at the reactor effluent.

Switchgrass (Stickle Farm, Ligonier, PA) was used as the carbon source for this study because of its suitability as a high energy crop. The switchgrass (*shelter* variety) was size-reduced using a Buffalo Hammer Mill (Schutte-Buffalo, Hammer Mill, Buffalo, NY) and was mixed with organic nitrogen fertilizer (Milorganite, Milwaukee, WI) in a carbon to nitrogen ratio of 16 to 1 at an initial moisture content of 63% because preliminary tests between 60 and 75% moisture revealed that this moisture content resulted in the most reproducible reactor performance. Three reactors were run in parallel to assess performance reproducibility.

At 8h intervals, up to 96h, samples were collected from sampling ports at reactor bed heights of 0.1m, 0.3m and 0.6m because the results of Chapter 3 showed that the differences in height along the reactor were only significant between the bottom, middle and top of the reactors. The study was limited to 96h because this time frame captures the biodegradation period where the most dynamic changes in state variables occur. Triplicate pH measurements were determined by adding 10ml of water to 1g of each sample and then read with a standard electrode pH meter

(Thermo Orion, Beverly, MA) (Council, 2007). The slurries used for pH measurements were filtered through 0.2μmWhatman filter paper and organic acid content was analyzed using a gas chromatograph (GC) (Hewlett-Packard 5980 Series II) equipped with a flame ionization detector (FID). The GC column was Supelco Nukol phase of 15m by 0.53μm i.d. with helium (10ml/min) as the column carrier gas. The temperatures for the injector and detector were both set at 230^{o}C. The oven was set to 100^{o}C for 2min, followed by a temperature gradient of 100 to 220^{o}C at a rate of 12^{0}C/min, with a final step at 220^{o}C for 2min. Samples were injected once at a volume of 1ml. C1 t0 C7 organic acids were identified by their retention time, corresponding to their standards. Measurements were done in triplicate. Between 30 to 100mg of each sample were stored at -20^{o}C for subsequent DNA extraction. The remaining solids for each reactor sample were divided into three for triplicate measurements, weighed and dried for 24h at 100^{o}C for moisture content measurements. The dried samples were sent to the Dairy One Forage testing Laboratory (Ithaca, NY) where the AOAC method was used to measure acid detergent fiber (ADF), neutral detergent fiber (NDF) and lignin (acid detergent method) content. From this data, the cellulose content was calculated as ADF minus lignin content and hemicellulose was calculated as NDF minus ADF content.

5.2.2 DNA extraction, quantification and real-time PCR

DNA was extracted from samples using a bead beating method with a phenol/chloroform/isoamyl precipitation (Fontenelle et al., 2010). Absorbance readings at 230nm, 260nm and 280nm were collected to assess extracted DNA purity and quantity. Real-time PCR was performed using a CFX96 system (Biorad,Hercules, CA) using SYBR Green detection to estimate bacterial, fungal, *Aspergillus spp.* and lactic acid bacteria biomass. Amplification of bacterial 16S rRNA genes was

estimated using the forward primer 338f (5'-ACT CCT ACG GGA GGC AGC AG-3') and the reverse primer 518r (5'-ATT ACC GCG GCT GCT GG -3') (Einen et al., 2008). Each PCR mixture contained 1X iQ SYBR Green super mix, 0.5μM of each primer, 5μL of compost DNA and PCR-grade water. A negative control without template DNA was included in each PCR run. The thermal cycling program consisted of 3min at 95^{o}C, then 45 cycles of denaturation at 94^{o}C for 15s, annealing at 60^{o}C for 30s, extension at 72^{o}C for 30s, plate read at 72^{o}C, followed by a final extension at 72^{o}C for 7min and a melting curve analysis from 65-95^{o}C with a plate read in increments of 0.5^{o}C. Samples were run in triplicate and a tenfold dilution series of genomic *E. coli* DNA was used to generate a standard curve.

Concentrations of fungal 18S rRNA genes were estimated using the forward primer ITS1F (5'-CTT GGT CAT TTA GAG GAA GTA A-3') and the reverse primer ITS4 (5'-TCC TCC GCT TAT TGA TAT GC -3') (Lee et al., 2010). Each PCR mixture contained 1X iQ SYBR Green super mix, 0.5μM of each primer, 5μL of compost DNA and PCR-grade water. A negative control without template DNA was included in each PCR run. The thermal cycling program consisted of 3min at 95^{o}C, then 45 cycles of denaturation at 94^{o}C for 25s, annealing at 50^{o}C for 25s, extension at 72^{o}C for 25s, plate read at 72^{o}C, followed by a final extension at 72^{o}C for 7min and a melting curve analysis from 65-95^{o}C with a plate read in increments of 0.5^{o}C. Samples were run in triplicate and a tenfold dilution series of genomic *Pluerotus Ostreatus* DNA was used to generate a standard curve.

The amplification of *Aspergillus* 18S rRNA genes were estimated using the forward primer 5'-ATT GGA GGG CAA GTC TGG TG -3' and the reverse primer 5'-CCG ATC CCT AGT CGG CAT AG -3' (Ramirez et al., 2009). Each PCR mixture contained 1X iQ SYBR Green super mix, 0.3μM of each primer, 5μL of compost DNA and PCR-grade water. A negative control without template DNA was

included in each PCR run. The thermal cycling program consisted of 3min at 95^{o}C, then 45 cycles of denaturation at 95^{o}C for 15s, annealing at 58^{o}C for 30s, extension at 72^{o}C for 30s, plate read at 72^{o}C, followed by a final extension at 72^{o}C for 7min and a melting curve analysis from 65-95^{o}C with a plate read in increments of 0.5^{o}C. Samples were run in triplicate and a tenfold dilution series of genomic *Aspergillus fumigatis* DNA was used to generate a standard curve.

Concentrations of lactic acid bacteria 16S rRNA genes were estimated using the forward primer Lac1 (5'-AGC AGT AGG GAA TCT TCC A -3') and the reverse primer Lac2 (5'-ATT YCA CCG CTA CAC ATG -3') (Hemmi et al., 2004). Each PCR mixture contained 1X iQ SYBR Green super mix, 0.3µM of each primer, 5µL of compost DNA and PCR-grade water. A negative control without template DNA was included in each PCR run. The thermal cycling program consisted of 3min at 95^{o}C, then 45 cycles of denaturation at 95^{o}C for 15s, annealing at 51.5^{o}C for 30s, extension at 72^{o}C for 30s, plate read at 72^{o}C, followed by a final extension at 72^{o}C for 7min and a melting curve analysis from 65-95^{o}C with a plate read in increments of 0.5^{o}C. Samples were run in triplicate and a tenfold dilution series of genomic *Lactobacillus acidophillus* DNA was used to generate a standard curve.

To calculate the number of gene copies in each sample, the following equation was used: Number of gene copies/g dry wt = (DNA concentration (ng/g dry wt) * Avogradro's Number) / (genome size * 660 Da * $1*10^{9}$ g). The genome sizes used were 4.64 x 10^{6}bp for E. coli (Einen et al., 2008), 3.51 x 10^{7}bp for *Pleurotus Ostreatus* (Larraya et al., 2000) 3 x 10^{7}bp for *Aspergillus fumigatis* (Denning et al., 2002), and 1.99 x 10^{6}bp for *Lactobacillus acidophilus* (Peterson et al., 2001).

5.2.3 Statistical Analysis

Results were subjected to Pearson correlation analyses to determine variable correlations in JMP 7 (SAS Institute, Cary, NC), using $p < 0.05$ as the criterion for significance. Principal component analysis (PCA) was also completed in JMP 7 to highlight patterns of variation between the microbial community data and other physical variables. Best fit parameter estimations were completed in Kaleidagraph (Synergy Software, Reading, PA).

5.3. Results and Discussion

5.3.1 Reactor dynamics and performance

The temperature profile of the reactor shows a rapid increase to thermophilic temperatures followed by a decrease back to mesophilic conditions (Figure 5.1). Such behavior is consistent with other temperature profiles in biodegradation studies (Chroni et al., 2009; Fanaei & Vaziri, 2009; Tengerdy & Szakacs, 2003; Wong et al., 2009), although the rate of increase to a maximum temperature was steeper than in most other studies. The data presented in Figure 5.1 represents the average temperature values from three different reactors in order to test for reactor reproducibility, which is an important factor in biodegradation processes (Holker & Lenz, 2005). The small error bars prove that reproducibility was established for this system and that process variability was minimized. Within the first 8h in this study, the temperature had increased by as much as 38^{o}C at the top of the reactor. This immediate rapid increase in temperature shows that initial conditions were perfect for microbial growth. A peak temperature of 63^{o}C was observed at the top of the reactor and thermophilic temperatures were sustained for about 24h during which time readily soluble parts of the substrate were being degraded. Temperatures subsequently decreased to environmental conditions which favored the growth of fungi for the

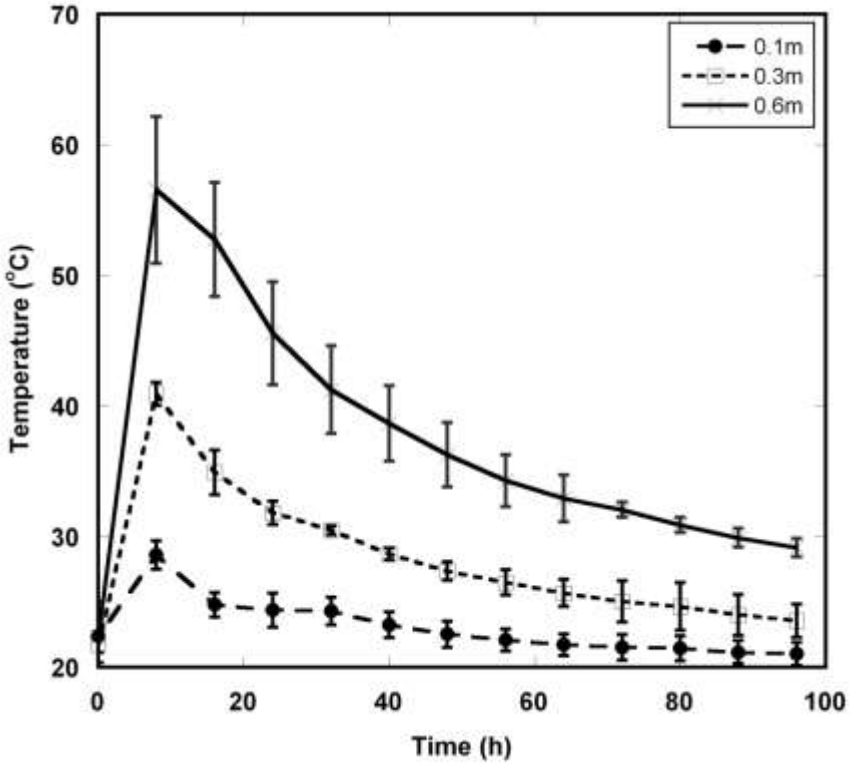

Figure 5.1. Temperature profiles at different reactor heights during the biodegradation of switchgrass amended with nitrogen fertilizer averaged over three reactors. Error bars represent standard deviations of three reactors.

decomposition of more complex substrates. Indeed, at the end of the study period, visual inspection of the substrate revealed the presence of a tremendous amount of white rot fungi.

Figure 5.1 also shows a distinct spatial pattern in temperature with the bottom on the reactor experiencing the lowest temperatures while the top of the reactor had the highest temperatures. This is not surprising given that this static, packed bed reactor was forcefully aerated from the bottom. Statistical analyses confirmed a strong positive correlation between temperature and reactor height ($p < 0.0001$).

Similar to the temperature profile, the O_2 consumption rate (OCR) and CO_2 evolution rate (CER), as calculated from the O_2 and CO_2 concentrations, respectively, rapidly peaked within the first 8h of the process and then steadily decreased (Figure 5.2). As expected, changes in the O_2 concentration were mirror images of changes in the CO_2 concentration (data not shown), demonstrating that the respiration quotient was close to one and that microbial metabolism was consistently active. This relationship between the O_2 and CO_2 concentrations was highly significant and had a strong negative correlation ($p < 0.0001$).

5.3.2 pH and organic acids dynamics

Unlike the associations observed between height and temperature, height did not play a major role in the pH profiles observed for the reactors ($p = 0.49$), resulting in pH profiles that were not significantly different from each other along the height of the reactor bed (Figure 5.3). For all the reactor heights, the pH increased from slightly acidic conditions to basic conditions within the first 8h and continued to increase in alkalinity with some stabilization around pH 9 being observed. This pH profile is typical in composting environments where cellulosic substrates are used. Initially, pH is in the range of 4.5-6.5 due to the formation of carbon dioxide and volatile fatty

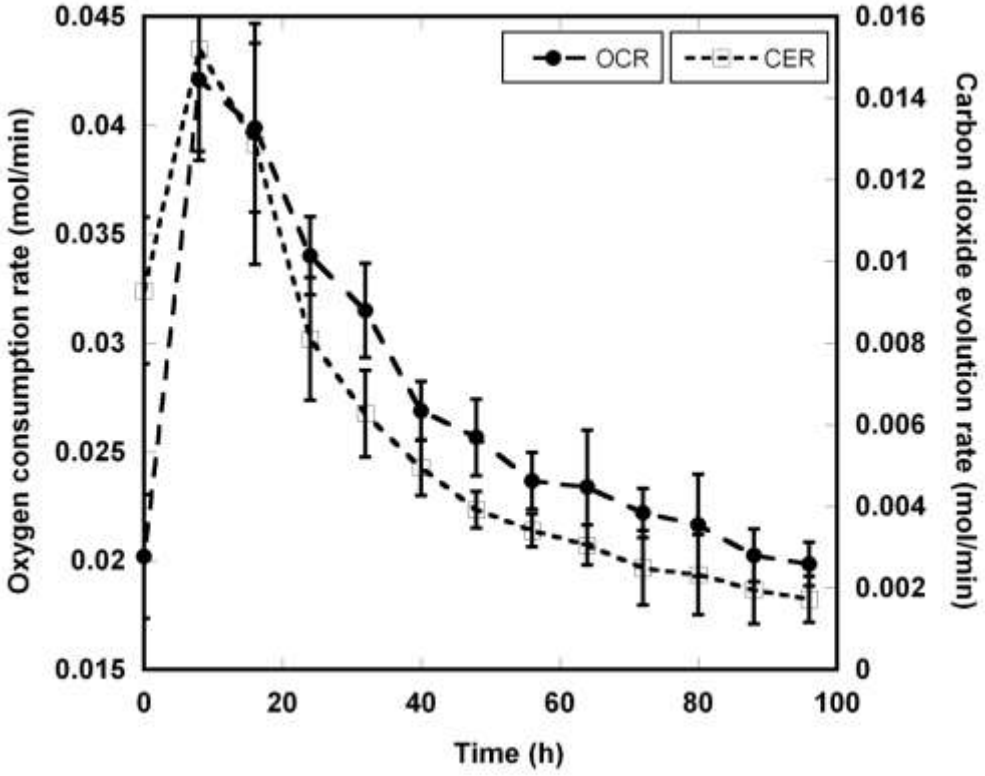

Figure 5.2 Profiles of oxygen consumption rate (OCR) and carbon dioxide evolution rate (CER) averaged over three reactors during the biodegradation of switchgrass amended with nitrogen fertilizer. Error bars represent standard deviations of three reactors.

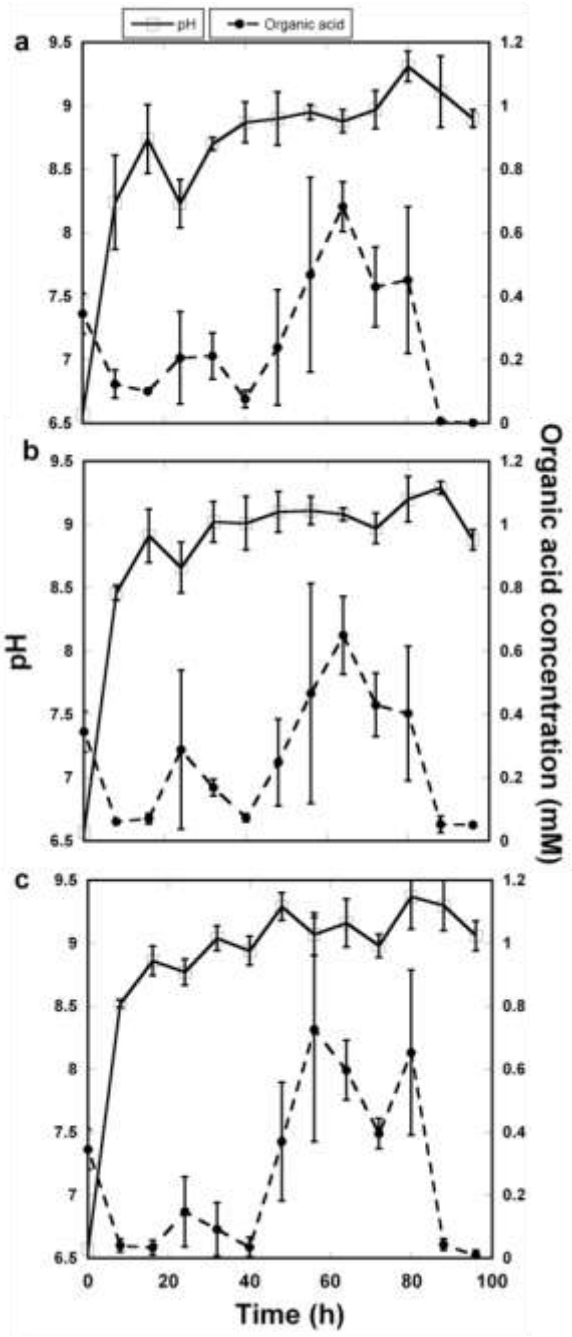

Figure 5.3 pH profiles at reactor heights of (a) 0.1m, (b) 0.3m, and (0.6m) compared to the total organic acids detected at that height averaged over three reactors. Error bars represent standard deviations of three reactors.

acids (Cen & Xia, 1999), and then as the process progresses, may increase to values that often exceed pH 8 (Gajalakshmi & Abbasi, 2008).

In a number of studies, changes in pH in composting environments have been attributed to the presence of organic acids (Choi & Park, 1998; Simandi et al., 2005; Sundberg et al., 2004), but as can be seen in Figure 5.3, variations in total organic acid concentration were not commensurate with changes in pH, except for the first 8h where an increase in pH coincides with a drop in organic acid concentration. While no significant association was found between the overall total organic acids and pH, a strong negative correlation was found between pH and acetic acid concentration ($p = 0.0001$). Acetic acid represented the major fraction of the total organic acid concentration for most of the samples tested and was present in all samples (Figure 5.4). This is not surprising given that acetic acid is an intermediate product in the degradation of sugars to carbon dioxide. The immediate and continuous increase in pH may also be explained by the production of ammonia from the nitrogen fertilizer since ammonia volatilization in composting systems employing substrates of high nitrogen content has been well documented (Bueno et al., 2008; Koenig et al., 2005; Liang et al., 2006). As with the pH, there were no significant differences between the total organic acid concentrations and reactor height.

In addition to showing the dominance of acetic acid in the C1-C7 organic acids detected, the distribution of these organic acids also shows an increase in all the acids from around 48h. This increase in organic acid concentration is not reflected in the pH may be due to changes in the underlying microbial community; however, the only overall correlation found between the C1-C7 acids and microbial community was a positive correlation between fungi and heptanoic acid ($p = 0.0001$). Other correlations were also found at the individual reactor heights. At 0.3m, bacteria and fungi copy numbers were positively correlated isobutyric concentration ($p = 0.008$ and

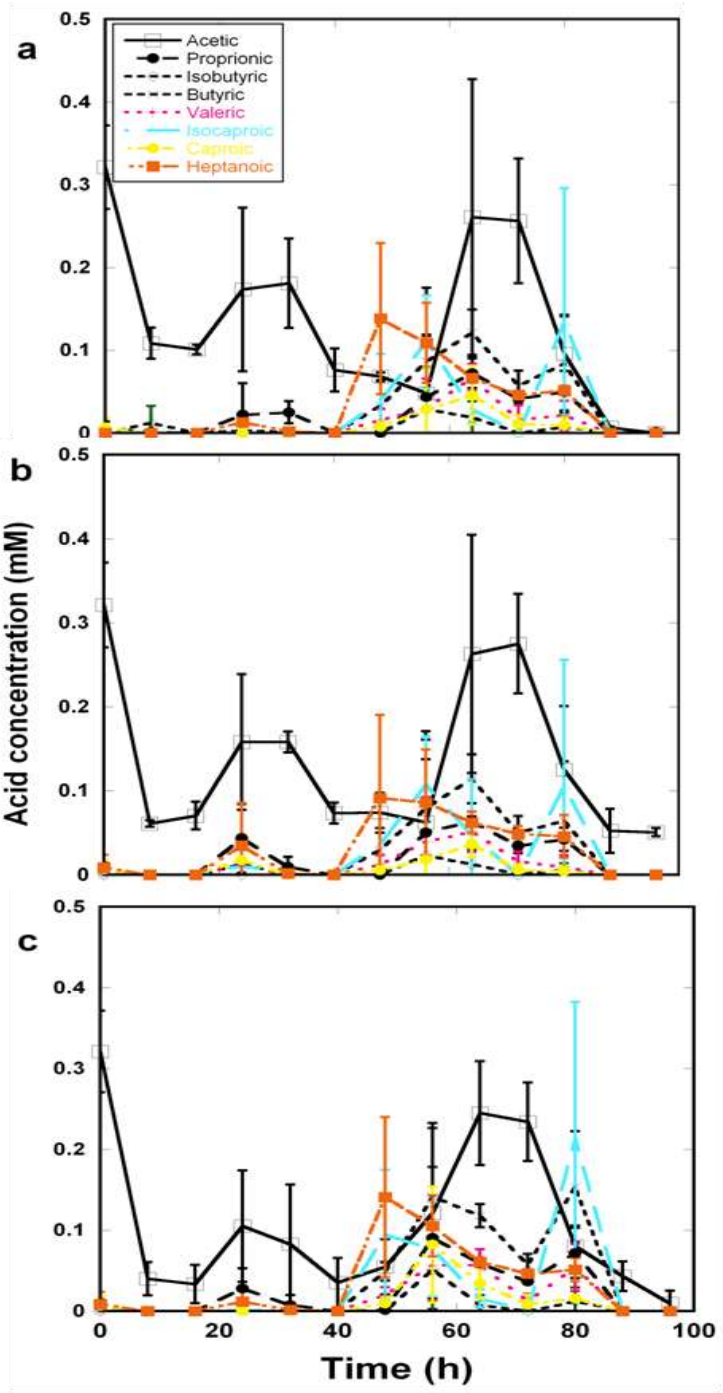

Figure 5.4 Profiles of C1-C7 organic acids at reactor heights of (a) 0.1m, (b) 0.3m, and (0.6m) averaged over three reactors. Error bars represent standard deviations of three reactors.

< 0.0001, respectively) and isocaproic acid concentration was positively correlated with fungi and lactic acid bacteria copy numbers (p = 0.008 and 0.024, respectively). At 0.6m, the positive correlation between bacteria and valeric acid was significant (p = 0.019), as was the positive relationship between fungi and heptanoic acid (p = 0.007) and *Aspergillus spp* and butyric and isocaproic acids (p = 0.036 and 0, respectively). Isovaleric acid was the only C1-C7 acid not detected in any of the samples.

5.3.3 Lignocellulose degradation dynamics and kinetics

Similar to the rapid increases seen in the temperature and pH profiles, the lignocellulosic substrate components of cellulose, hemicellulose and lignin experienced a quick increase in degradation, followed by an almost steady rate in decomposition (Figure 5.5). At 8h, an average of 9% of the lignin, 21% of the hemicellulose and 33% of the cellulose initially present in the switchgrass had been degraded across the three reactor heights. At the end of the 96h study, there was an average of 19% degradation in lignin content, 26% degradation in hemicellulose content and 24% degradation in the cellulose content of the reactor samples across the three reactor heights. Surprisingly, the variations in degradation on the basis of reactor height were not significant (p = 0.43 to 0.46). This suggests that although the microbial communities may have been different due to the large spatial distribution of temperature, there was sufficient microbial activity at all heights to facilitate biodegradation. In a study investigating the composting of rice straw amended with vegetables and bran, 20% lignin degradation, 25% hemicellulose degradation and 30% cellulose degradation was observed after 28 days (Yu et al., 2007). In another study, ryegrass was found to have lost 6 and 44% of its lignin and cellulose contents under incubation at 25^{o}C and 14 and 64% of its lignin content at 50^{o}C for a 30 day incubation period (Horwath & Elliott, 1996). In one of the few studies on switchgrass

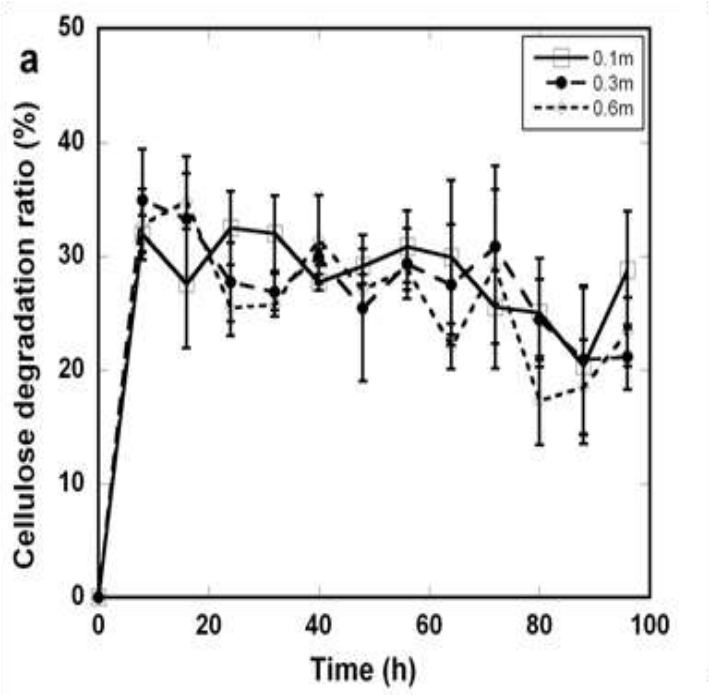

Figure 5.5 (a). Changes in the substrate average degradation ratio of cellulose at reactor heights of 0.1m, 0.3m and 0.6m in the reactor. Error bars represent standard deviations of three reactors.

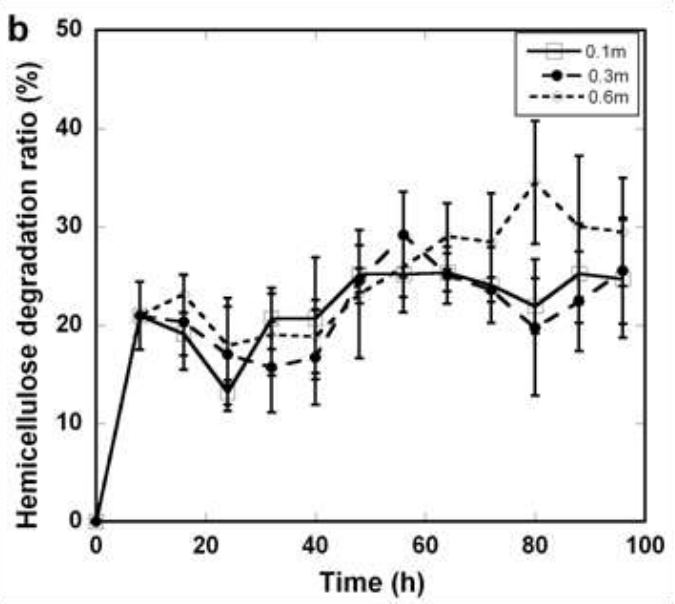

Figure 5.5(b). Changes in the substrate average degradation ratio of (b) hemicellulose at reactor heights of 0.1m, 0.3m and 0.6m in the reactor. Error bars represent standard deviations of three reactors.

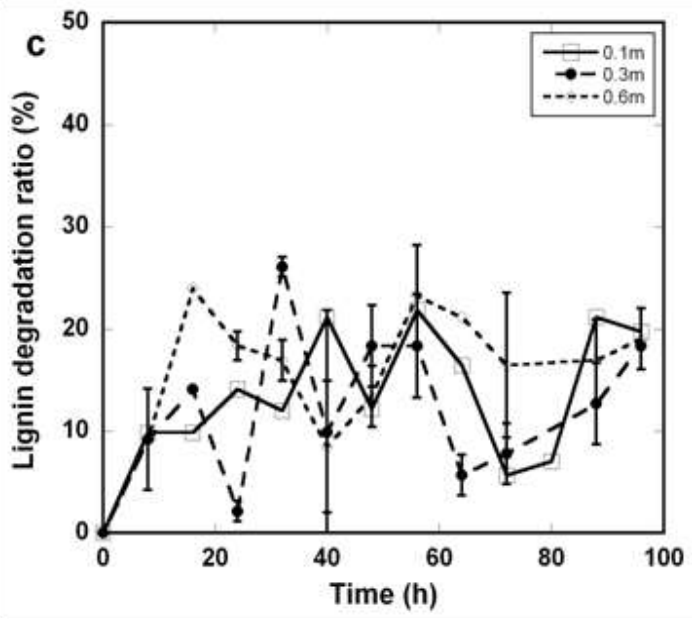

Figure 5.5(c). Changes in the substrate average degradation ratio of (c) lignin at reactor heights of 0.1m, 0.3m and 0.6m in the reactor. Error bars represent standard deviations of three reactors.

composting, switchgrass was incubated with green waste compost in a temperature controlled reactor for 31 days (Allgaier et al., 2010). At the end of that period, the authors found a 17% decrease in the original lignin content and a 28% decrease in the sugars associated with cellulose and hemicellulose. The extent of degradation found in these studies is numerically comparable to those obtained in this study, with the exception that these degradation rates were obtained within a fraction of the time of the other studies: 4 days versus 28 to 30 days. This is most likely due to the use of a direct nitrogen source as opposed to using other waste materials as this made the nitrogen more readily available during the composting process. This observation is supported by the carbon to nitrogen ratio, which was 30 for the rice straw mixture and 40 for the ryegrass mixture, compared to the low ratio of 16 used in this study.

Further observation of Figure 5.5 shows similar degradation patterns for the substrate components and indeed hemicellulose and cellulose degradation were positively correlated with each other ($p=0.002$) and lignin and cellulose degradation were correlated to each other ($p = 0.009$). This finding is comparable to another study which found that the degradation of hemicellulose and cellulose were positively correlated with each other and with lignin degradation (Huang et al., 2010). Changes in the degradation of all three substrate components were also commensurate with acetic acid concentration ($p =0.001$) and pH ($p < 0.0001$). Since switchgrass was the main carbon source, it follows that the decomposition of its main constituents would correlate with intermediary and final decomposition products.

The correlation between the lignocellulosic components and the microbial activity indicators of OCR and CER was also investigated. The results showed that cellulose degradation was positively correlated with OCR ($p=0.0001$) whereas both hemicellulose and lignin degradation were found to negatively correlate with CER ($p = 0.002$ and 0.018, respectively) while no significant correlation as found between

CO_2 concentration and cellulose degradation. It is often useful to obtain OCRand CER yield coefficients of the substrate in degradation studies because they are particularly useful for describing mass transfer through the reactors and for correlating substrate properties to microbial indicators.

The time rate of change of the substrate is also useful in biodegradation studies for extracting parameter kinetics that allow for the comparison of different substrates. This data is especially important in the development of mathematical models to describe microbial decomposition processes. Such substrate kinetic parameters are limited in the literature and only a few models of composting systems have incorporated substrate utilization kinetics (Fontenelle et al., Submitted; Kaiser, 1996; Sole-Mauri et al., 2007). Figure 5.6 shows the best fit curves for changes in the degradation ratio of the substrate components over time, assuming that substrate degradation follows the first order kinetics of: $dS/dt = kS$, where S represents the substrate and k is the first order decay kinetic constant. The plots in Figure 5.6 show that the hemicellulose degradation profile provided the best fit to the first order degradation model whereas the lignin degradation profile had the most scatter. The plots also show that the degradation kinetics of cellulose was different from that of hemicellulose and lignin in that the first order decay constant was negative for cellulose, but positive for hemicellulose and lignin. Overall, one would expect a continuous increase in degradation ratio if the process is carried out to completion; so the apparent decrease in the cellulose degradation ratio could most be due to an artifact of the method used to measure cellulose content in that it got easier to measure cellulose content as the degradation proceeded.

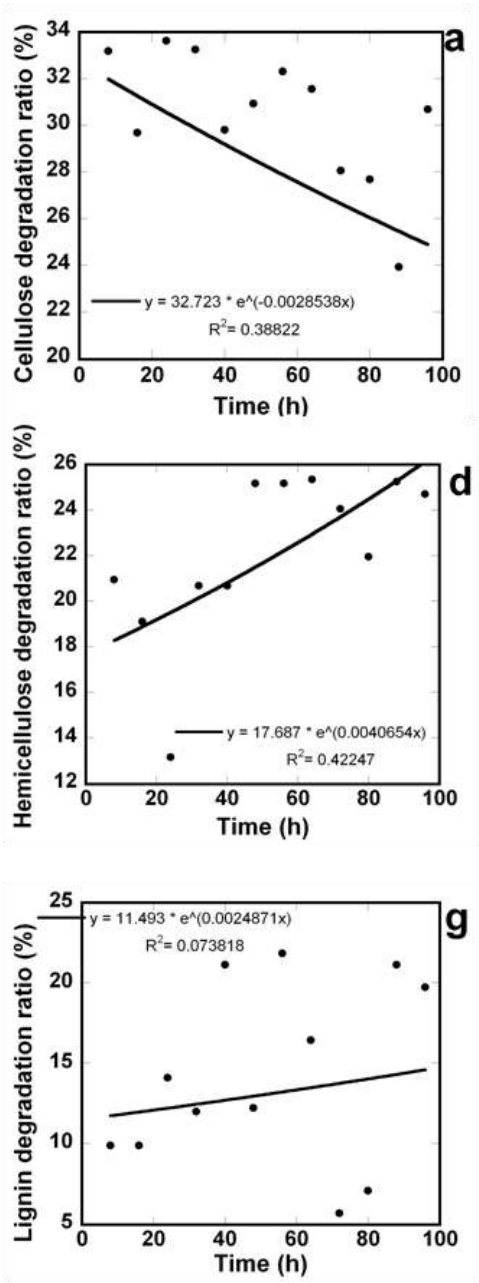

Figure 5.6 (a,g,h). Fitting of first order degradation model to lignocellulosic components featuring cellulose degradation ratio versus time at a height of (a) 0.1m, hemicellulose degradation ratio versus time at a height of (d) 0.1m, and lignin degradation ratio versus time at a height of (g) 0.1m.

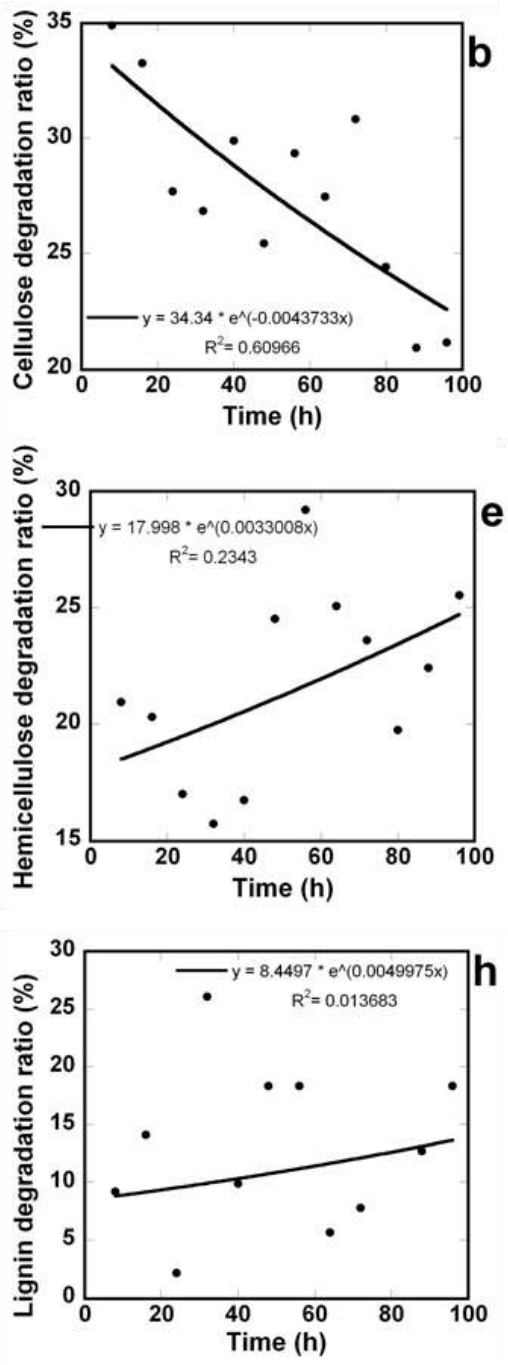

Figure 5.6 (b,e,h). Fitting of first order degradation model to lignocellulosic components featuring cellulose degradation ratio versus time at a height of (b) 0.3m, hemicellulose degradation ratio versus time at a height of (e) 0.3m; and lignin degradation ratio versus time at a height of (h) 0.3m.

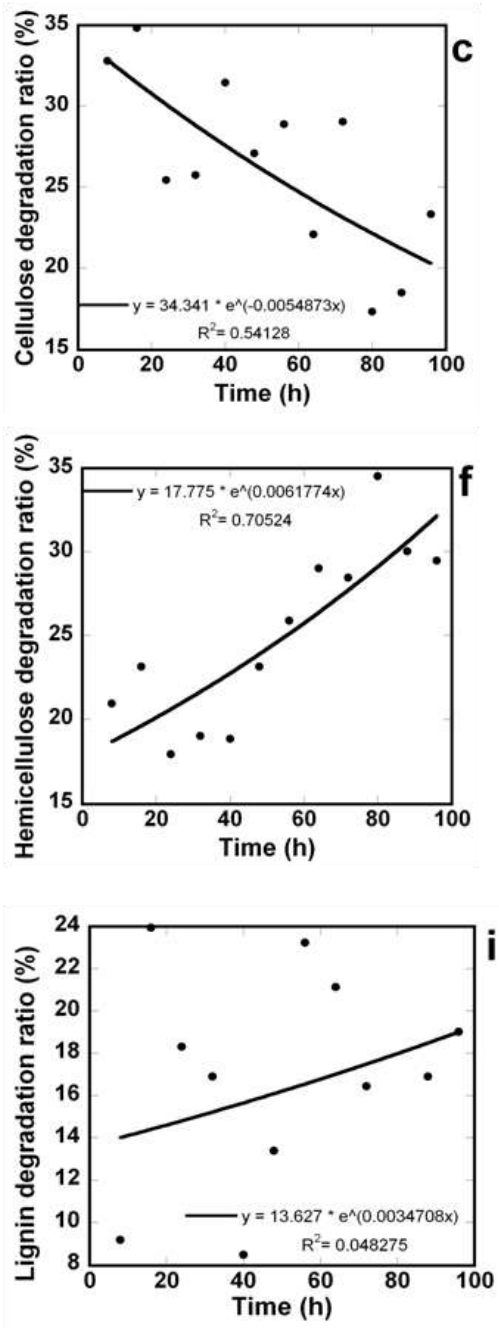

Figure 5.6(c,f,i). Fitting of first order degradation model to lignocellulosic components featuring cellulose degradation ratio versus time at a height of (c) 0.6m; hemicellulose degradation ratio versus time at a height of (f) 0.6m; and lignin degradation ratio versus time at a height of (i) 0.6m.

5.3.4 Microbial community dynamics

Microbial community succession during lignocellulosic composting is an attribute of aerobic composting. Typically, mesophilic bacteria and fungi dominate the initial stages of the process and metabolize easily degradable carbohydrates, followed by the activity of actinobacteria during the thermophilic phase to decompose the recalcitrant plant cell wall (Gajalakshmi & Abbasi, 2008; Ryckeboer et al., 2003). Subsequently another mesophilic community consisting mainly of fungi continue to break down the more complex components (Tuomela et al., 2000). Consistent with this generalized model of microbial succession and dynamics, Figures 5.7 to 5.10 show dramatic temporal changes in the 16S and 18S rRNA genes for universal and lactic acid bacteria and universal fungi and *Aspergillus spp.*, respectively as obtained via real time PCR. The high sensitivity of real time PCR in detecting small quantities makes it a valuable tool for monitoring even small changes in populations and may thus be used to assess changes in microbial composition of the organic matrix (Xu et al., 2009).

The data shows that of the four quantified populations, bacterial growth (Figure 5.7) was the highest for the majority of samples which is consistent with studies done using other molecular techniques (Chroni et al., 2009; Pedro et al., 2003; Schloss et al., 2005). Bacteria were detected at every sampled point and variations in the quantities show the succession of this population during the process. The single largest quantity of bacteria was observed at 8h at a height of 0.1m, and this coincides with the time at which peak temperatures were observed in the reactor. Comparison of the initial sample to the final sample revealed increases in the number of bacterial gene copies on the order of 99% at heights of 0.1 and 0.3m and 90% at a height of 0.6m. This further signifies that significant decomposition had occurred during the 96h period, to the point where the final samples were significantly differentiated from

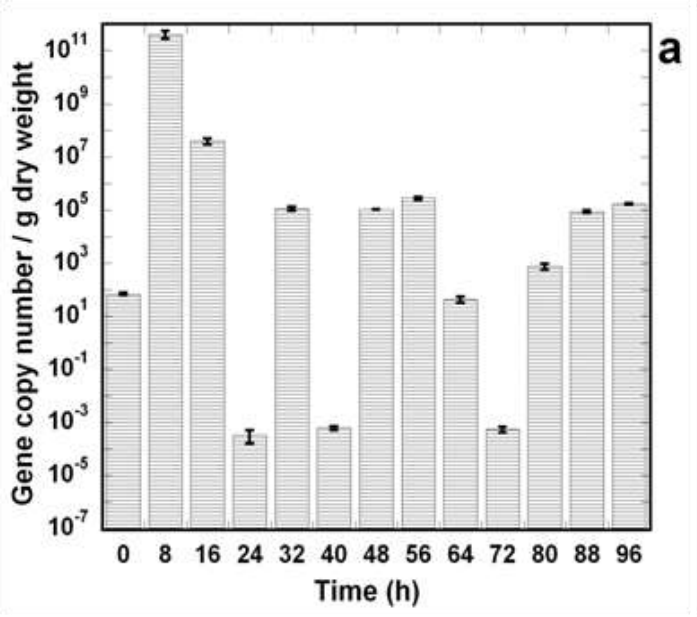

Figure 5.7(a). Real time PCR analyses of the population of 16S rRNA bacteria genes at a reactor height of (a) 0.1m. Error bars represent standard deviations of three reactors.

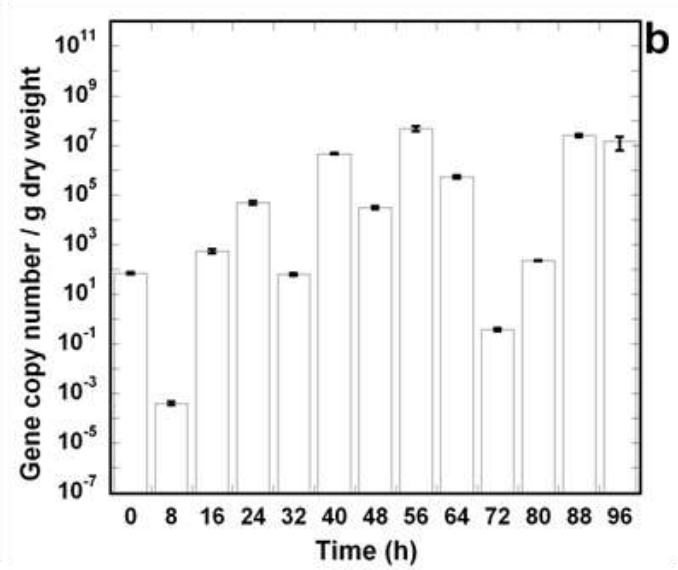

Figure 5.7(b). Real time PCR analyses of the population of 16S rRNA bacteria genes at a reactor height of (b) 0.3m. Error bars represent standard deviations of three reactors.

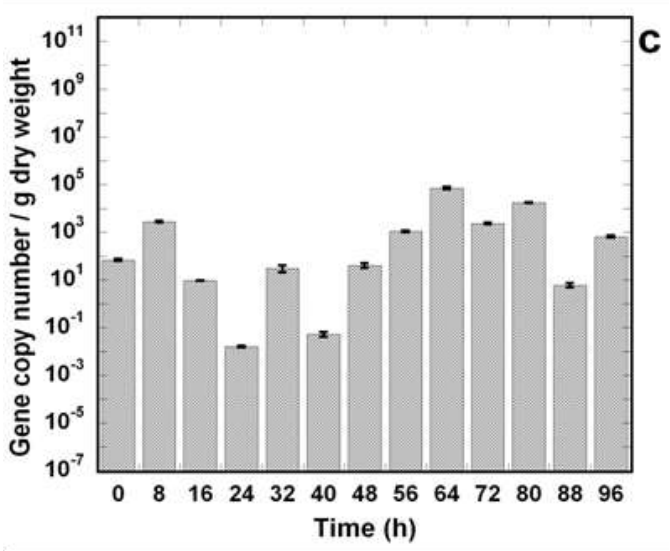

Figure 5.7(c). Real time PCR analyses of the population of 16S rRNA bacteria genes at a reactor height of (c) 0.6m. Error bars represent standard deviations of three reactors.

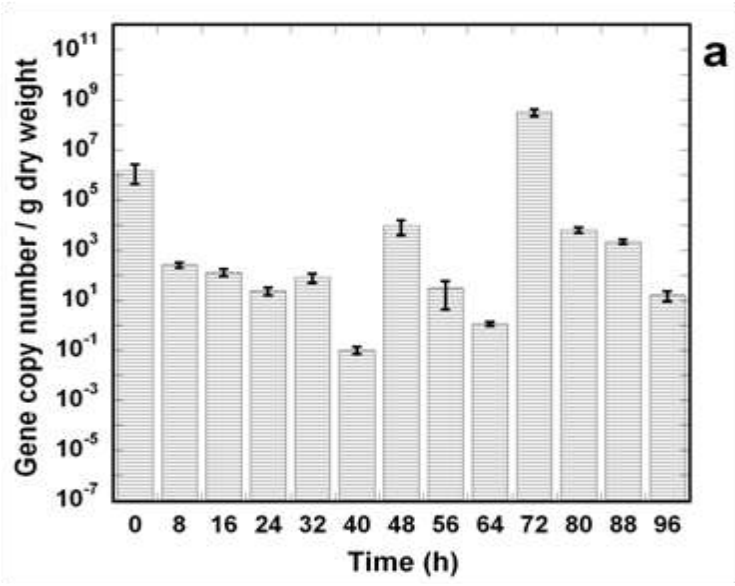

Figure 5.8(a). Real time PCR analyses of the population of 16S rRNA lactic acid bacteria genes at reactor heights of (a) 0.1m. Error bars represent standard deviations of three reactors.

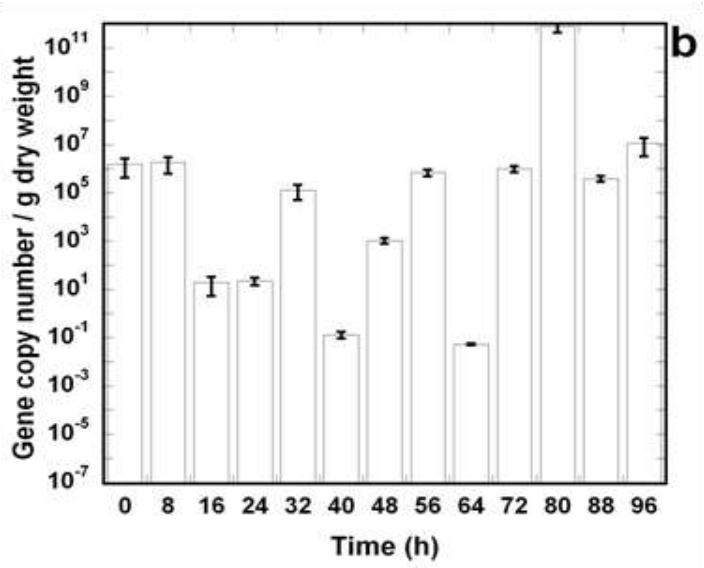

Figure 5.8(b). Real time PCR analyses of the population of 16S rRNA lactic acid bacteria genes at a reactor height of (b) 0.3m. Error bars represent standard deviations of three reactors.

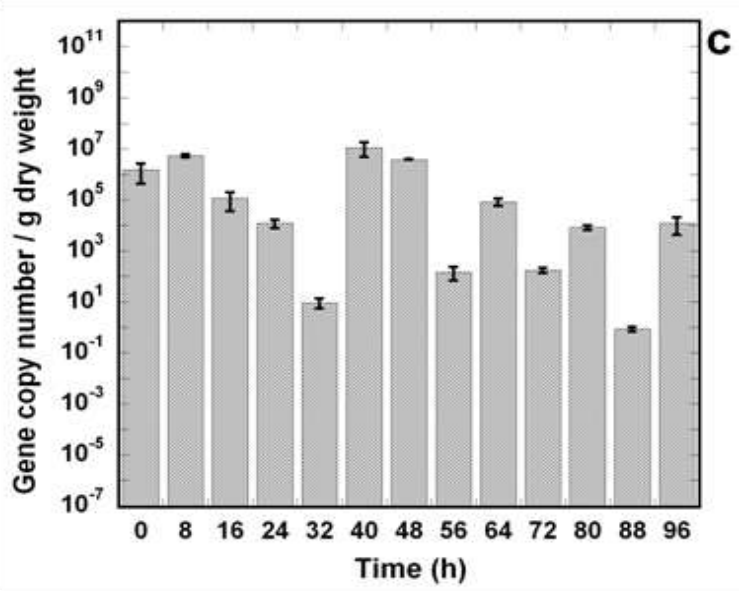

Figure 5.8(c). Real time PCR analyses of the population of 16S rRNA lactic acid bacteria genes at a reactor height of (c) 0.6m. Error bars represent standard deviations of three reactors.

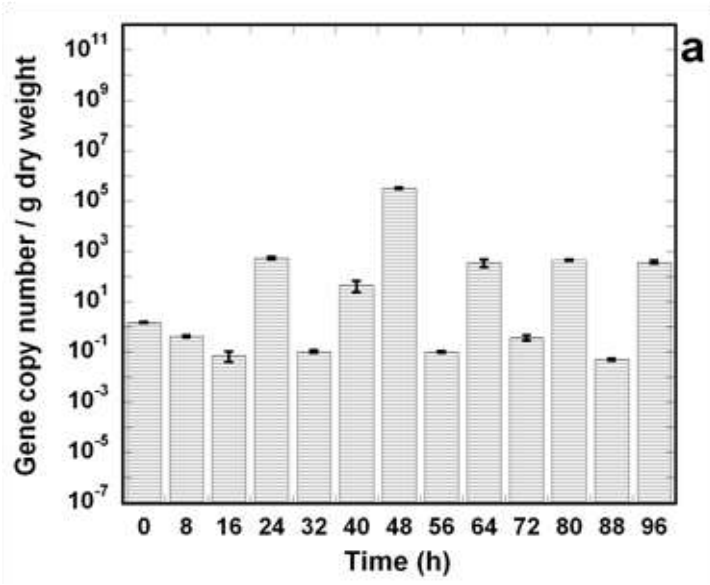

Figure 5.9(a). Real time PCR analyses of the population of 18S rRNA fungi genes at reactor heights of (a) 0.1m. Error bars represent standard deviations of three reactors.

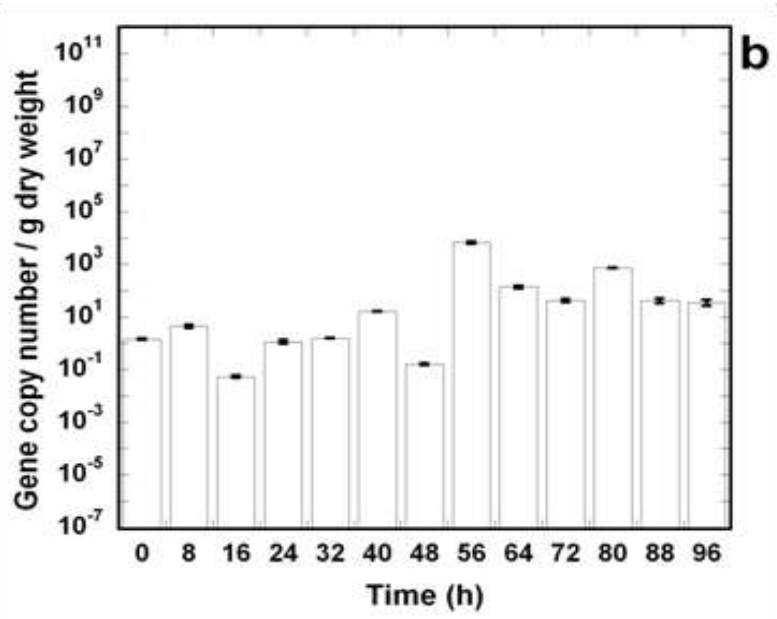

Figure 5.9(b). Real time PCR analyses of the population of 18S rRNA fungi genes at reactor heights of (b) 0.3m. Error bars represent standard deviations of three reactors.

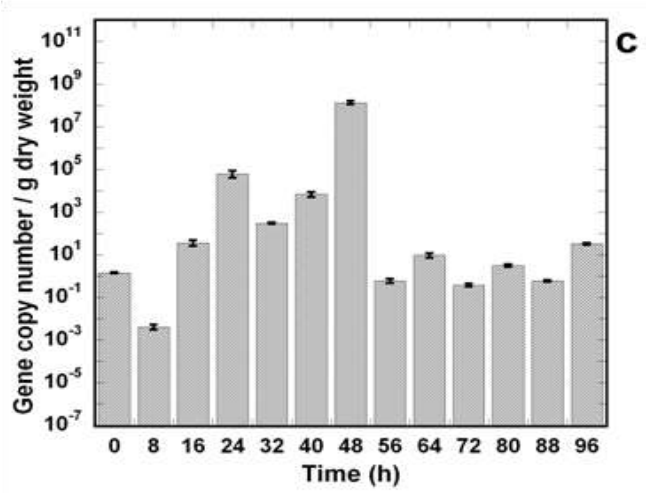

Figure 5.9(c). Real time PCR analyses of the population of 18S rRNA fungi genes at reactor heights of (c) 0.6m. Error bars represent standard deviations of three reactors.

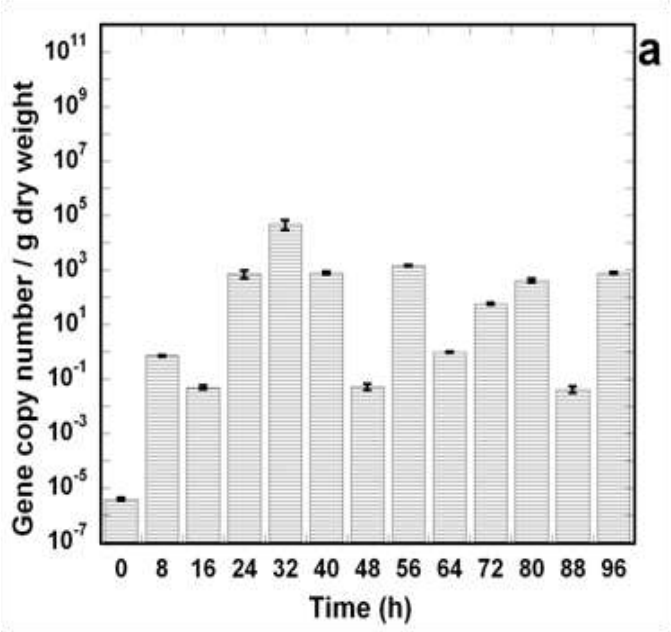

Figure 5.10(a). Real time PCR analyses of the population of 18S rRNA *Aspergillus spp.* genes at reactor heights of (a) 0.1m. Error bars represent standard deviations of three reactors.

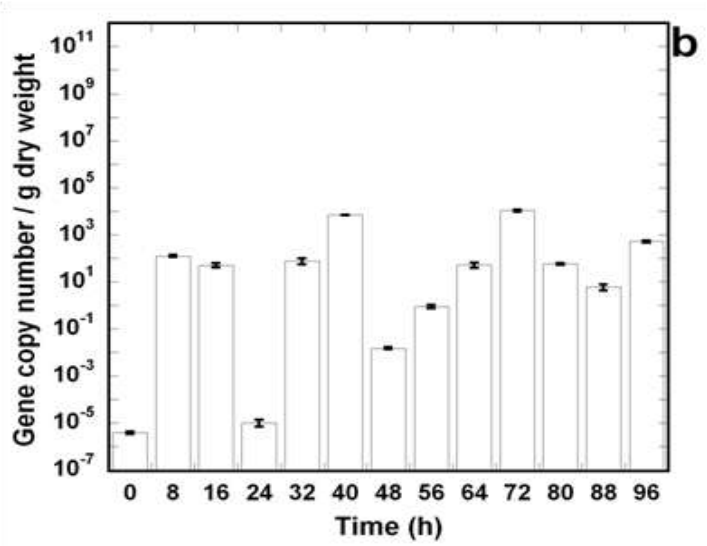

Figure 5.10(b). Real time PCR analyses of the population of 18S rRNA *Aspergillus spp.* genes at reactor heights of (b) 0.3m. Error bars represent standard deviations of three reactors.

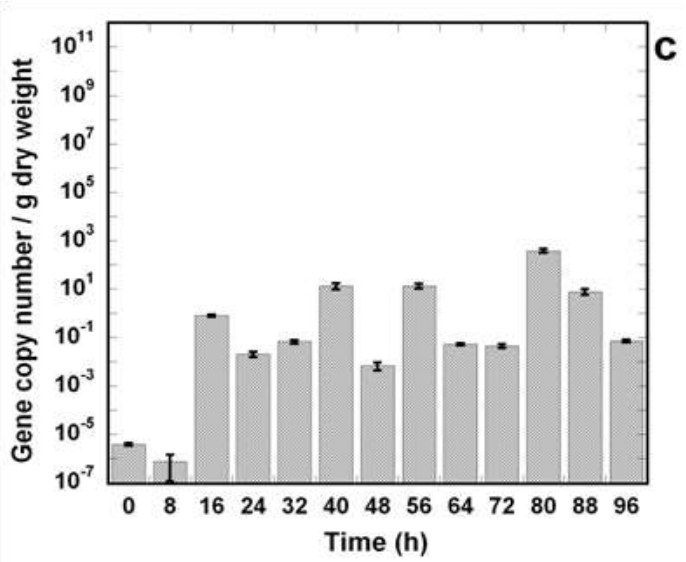

Figure 5.10(c). Real time PCR analyses of the population of 18S rRNA *Aspergillus spp.* genes at reactor heights of (c) 0.6m. Error bars represent standard deviations of three reactors.

the initial samples. This finding was confirmed by principal components analysis (data not shown). No significant correlations were found between the population of bacteria and the substrate components in this study, but Yu et al. (2007) found a strong correlation between the lignin degradation ratio and the group of quinones encoding for actinomycetes, including *Norcardia spp*., *Mycobacterium spp*., and *Cellulomonas spp*. whereas Huang et al. found that changes in that group of quinones correlated only with cellulose degradation when the composting process was carried out to completion.

Given that the production of organic acids is often attributed to the presence of lactic acid bacteria (Sundberg & Jonsson, 2008), it was anticipated that this group would dominate the initial microbial community and Figure 5.8 shows that this group was the most abundant at all reactor heights initially. The quantified lactic acid bacteria included *Lactobacillus, Pediococcus*, *Leuconostoc* and *Weisella* species which have been found to be most prominent in the composting of garbage (Hemmi et al., 2004). This group was quickly overshadowed at 0.1m by 8h, whereas they were only overtaken at 24h at the top of the reactor. This signifies a major shift in the microbial community from a dominance of lactic acid bacteria to general bacteria; however, there were no significant correlations between lactic acid bacteria gene copy numbers and the organic acid concentration.

As opposed to the somewhat dominant bacterial copy numbers, fungal copy numbers were noticeabley lower (Figure 5.9), but this is not surprising given that fungi usually play a more dominant role during the later stages of composting (Kornillowicz-Kowalska & Bohacz, 2010). Fungi were detected in all the reactor samples, but did dominate at any of the reactor heights. No significant correlations were found between fungi gene copy numbers and the degradation ratios of the lignocellulosic components although fungi are known to play an instrumental role in

degrading these complex substrates over longer periods of time (Gajalakshmi & Abbasi, 2008). *Aspergillus spp*. in particular have been identified as major fungal microorganisms during the degradation of lignocellulosics (Huang et al., 2010; Tuomela et al., 2000; Yu et al., 2007). The results for *Aspergillus spp* presented in Figure 5.10 include *Aspergillus niger, Aspergillus fumigatus, Aspergillus flavus* and *Aspergillus nidulans* species. The results show the largest *Aspergillus* copy numbers being found at the bottom of the reactor and that the number of copies for the most part increased after peak temperatures had been obtained. This was expected because fungi thrive at lower temperatures in the range of 25 to 30^{o}C (Tuomela et al., 2000).

5.4. Conclusions

Both spatial and temporal dynamics of physico-chemical and microbial properties of the early stage of switchgrass composting using a nitrogen fertilizer amendment were studied. Rapid increases in temperature, OCR and CER showed highly active microbial populations. Real time PCR was successfully applied to monitor microbial community dynamics and revealed a shift from a predominance of lactic acid bacteria to general bacteria and an increase in *Aspergillus spp*. after peak temperatures had been reached. Profiles of pH and acetic acid concentration were strongly correlated. Significant lignocellulosic degradation occurred during the study period, with 19% degradation in lignin, 24% degradation in cellulose and 26% degradation in hemicellulose content. Several correlations were found between biotic and abiotic variables, including between substrate degradation and the microbial activity indicators of OCR and CER; thereby providing some insight into some of the feedback loops that took place during the process. Overall, this study has provided valuable information about the dynamics and kinetics of microbial lignocellulosic

decomposition where switchgrass is the main carbon source and accomplished the goal of a rapid rate of degradation within 96h.

Acknowledgements

The authors gratefully acknowledge Lydia Contreras for providing and *E.coli* culture and Brian King for providing *Pleurotus Ostreatus* and *Aspergillus fumigatis* cultures.

REFERENCES

Adney, S., van der Lelie, D., Berry, A., M., H. 2008. *Biomass Recalcitrance*. John Wiley and Sons Incorporated.

Allgaier, M., Reddy, A., Park, J.I., Ivanova, N., D'Haeseleer, P., Lowry, S., Sapra, R., Hazen, T.C., Simmons, B.A., VanderGheynst, J.S., Hugenholtz, P. 2010. Targeted Discovery of Glycoside Hydrolases from a Switchgrass-Adapted Compost Community. *Plos One*, **5**(1).

Bueno, P., Tapias, R., Lopez, F., Diaz, M.J. 2008. Optimizing composting parameters for nitrogen conservation in composting. *Bioresource Technology*, **99**(11), 5069-5077.

Cen, P., Xia, L. 1999. Production of Cellulase by Solid-State Fermentation. *Advances in Biochemical Engineering/Biotechnology*, **65**.

Choi, M.H., Park, Y.H. 1998. The influence of yeast on thermophilic composting of food waste. *Letters in Applied Microbiology*, **26**(3), 175-178.

Chroni, C., Kyriacou, A., Georgaki, I., Manios, T., Kotsou, M., Lasaridi, K. 2009. Microbial characterization during composting of blowaste. *Waste Management*, **29**(5), 1520-1525.

Council, U.S.C. 2007. Test Methods for Evaluation of Compost and Composting.

Denning, D.W., Anderson, M.J., Turner, G., Latge, J.P., Bennett, J.W. 2002. Sequencing the Aspergillus fumigatus genome. *Lancet Infectious Diseases*, **2**(4), 251-253.

Einen, J., Thorseth, I.H., Ovreas, L. 2008. Enumeration of Archaea and Bacteria in seafloor basalt using real-time quantitative PCR and fluorescence microscopy. *Fems Microbiology Letters*, **282**(2), 182-187.

Fanaei, M.A., Vaziri, B.M. 2009. Modeling of temperature gradients in packed-bed solid-state bioreactors. *Chemical Engineering And Processing*, **48**(1), 446-451.

Fontenelle, L.T., Corgie, S.C., Walker, L.P. 2010. Abiotic and biotic dynamics during the initial stages of high-solids switchgrass degradation. *Environmental Technology*, **Accepted**.

Fontenelle, L.T., Corgie, S.C., Walker, L.P. Submitted. Integrating mixed microbial population dynamics into modeling energy transport during the initial stages of the aerobic composting of a switchgrass mixture. *Bioresource Technology*.

Gajalakshmi, S., Abbasi, S.A. 2008. Solid waste management by composting: State of the art. *Critical Reviews in Environmental Science and Technology*, **38**(5), 311-400.

Hemmi, H., Shimoyama, T., Nakayama, T., Hoshi, K., Nishino, T. 2004. Molecular biological analysis of microflora in a garbage treatment process under thermoacidophilic conditions. *Journal Of Bioscience And Bioengineering*, **97**(2), 119-126.

Holker, U., Lenz, J. 2005. Solid-state fermentation - are there any biotechnological advantages? *Current Opinion in Microbiology*, **8**(3), 301-306.

Horwath, W.R., Elliott, L.F. 1996. Ryegrass straw component decomposition during mesophilic and thermophilic incubations. *Biology And Fertility Of Soils*, **21**(4), 227-232.

Huang, D.-L., Zeng, G.-M., Feng, C.-L., Hu, S., Lai, C., Zhao, M.-H., Su, F.-F., Tang, L., Liu, H.-L. 2010. Changes of microbial population structure related to lignin degradation during lignocellulosic waste composting. *Bioresource Technology*, **101**(11), 4062.

Kaiser, J. 1996. Modelling composting as a microbial ecosystem: A simulation approach. *Ecological Modelling*, **91**(1-3), 25-37.

Koenig, R.T., Palmer, M.D., Miner, F.D., Miller, B.E., Harrison, J.D. 2005. Chemical amendments and process controls to reduce ammonia volatilization during in-house composting. *Compost Science & Utilization*, **13**(2), 141-149.

Kornillowicz-Kowalska, T., Bohacz, J. 2010. Dynamics of growth and succession of bacterial and fungal communities during composting of feather waste. *Bioresource Technology*, **101**(4), 1268-1276.

Larraya, L.M., Perez, G., Ritter, E., Pisabarro, A.G., Ramirez, L. 2000. Genetic linkage map of the edible basidiomycete Pleurotus ostreatus. *Applied And Environmental Microbiology*, **66**(12), 5290-5300.

Lee, S.H., Lee, H.J., Kim, S.J., Lee, H.M., Kang, H., Kim, Y.P. 2010. Identification of airborne bacterial and fungal community structures in an urban area by T-RFLP analysis and quantitative real-time PCR. *Science Of The Total Environment*, **408**(6), 1349-1357.

Liang, Y., Leonard, J.J., Feddes, J.J.R., McGill, W.B. 2006. Influence of carbon and buffer amendment on ammonia volatilization in composting. *Bioresource Technology*, **97**(5), 748-761.

Pedro, M.S., Haruta, S., Nakamura, K., Hazaka, M., Ishii, M., Igarashi, Y. 2003. Isolation and characterization of predominant microorganisms during decomposition of waste materials in a field-scale composter. *Journal of Bioscience and Bioengineering*, **95**(4), 368-373.

Peterson, J.D., Umayam, L.A., Dickinson, T., Hickey, E.K., White, O. 2001. The Comprehensive Microbial Resource. *Nucleic Acids Research*, **29**(1), 123-125.

Ramirez, M., Castro, C., Palomares, J.C., Torres, M.A.J., Aller, A.I., Ruiz, M., Aznar, J., Martin-Mazuelos, E. 2009. Molecular detection and identification of Aspergillus spp. from clinical samples using real-time PCR. *Mycoses*, **52**(2), 129-134.

Ryckeboer, J., Mergaert, J., Coosemans, J., Deprins, K., Swings, J. 2003. Microbiological aspects of biowaste during composting in a monitored compost bin. *Journal of Applied Microbiology*, **94**(1), 127-137.

Schloss, P.D., Hay, A.G., Wilson, D.B., Gossett, J.M., Walker, L.P. 2005. Quantifying bacterial population dynamics in compost using 16S rRNA gene probes. *Applied Microbiology and Biotechnology*, **66**(4), 457-463.

Simandi, P., Takayanagi, M., Inubushi, K. 2005. Changes in the pH of two different composts are dependent on the production of organic acids. *Soil Science and Plant Nutrition*, **51**(5), 771-774.

Sole-Mauri, F., Illa, J., Magri, A., Prenafeta-Boldu, F.X., Flotats, X. 2007. An integrated biochemical and physical model for the composting process. *Bioresource Technology*, **98**(17), 3278-3293.

Sundberg, C., Jonsson, H. 2008. Higher pH and faster decomposition in biowaste composting by increased aeration. *Waste Management*, **28**(3), 518-526.

Sundberg, C., Smars, S., Jonsson, H. 2004. Low pH as an inhibiting factor in the transition from mesophilic to thermophilic phase in composting. *Bioresource Technology*, **95**(2), 145-150.

Tengerdy, R.P., Szakacs, G. 2003. Bioconversion of lignocellulose in solid substrate fermentation. *Biochemical Engineering Journal*, **13**(2-3), 169-179.

Tilman, D., Socolow, R., Foley, J.A., Hill, J., Larson, E., Lynd, L., Pacala, S., Reilly, J., Searchinger, T., Somerville, C., Williams, R. 2009. Beneficial Biofuels-The Food, Energy, and Environment Trilemma. *Science*, **325**(5938), 270-271.

Tuomela, M., Vikman, M., Hatakka, A., Itavaara, M. 2000. Biodegradation of lignin in a compost environment: a review. *Bioresource Technology*, **72**(2), 169-183.

Wong, J.W.C., Fung, S.O., Selvam, A. 2009. Coal fly ash and lime addition enhances the rate and efficiency of decomposition of food waste during composting. *Bioresource Technology*, **100**(13), 3324-3331.

Xu, W.P., Reuter, T., Xu, Y.P., Alexander, T.W., Gilroyed, B., Jin, L.J., Stanford, K., Larney, F.J., McAllister, T.A. 2009. Use of Quantitative and Conventional PCR to Assess Biodegradation of Bovine and Plant DNA during Cattle Mortality Composting. *Environmental Science & Technology*, **43**(16), 6248-6255.

Yu, H., Zeng, G.M., Huang, H.L., Xi, X.M., Wang, R.Y., Huang, D.L., Huang, G.H., Li, J.B. 2007. Microbial community succession and lignocellulose degradation during agricultural waste composting. *Biodegradation*, **18**(6), 793-802.

CHAPTER 6

CONCLUSIONS

6.1 Summary of research

This dissertation represents extensive research on the characterization of the aerobic microbial degradation of switchgrass. Aerobic degradation of switchgrass is important for a number of reasons including understanding field and storage losses in feedstock logistical systems, and for understanding microbial interactions on recalcitrant cellulosic biomass. The overall goal of this work was to characterize the coupled abiotic and biotic interactions that occur during aerobic degradation in switchgrass with a particular focus on the temporal and spatial gradients in these interactions that occur during the early stages of the process. The systematic approaches and methods used for this characterization have been outlined in Chapters 3 through 5 and are summarized in the following sections.

6.1.1 Reactor performance and process reproducibility

The highly-instrumented reactor system designed in this study enabled us to capture the dynamics of biotic and abiotic phenomena during the early stages of biodegradation. In addition, high spatial and temporal resolution was achieved and this was important for the modeling research. Radial gradients were minimized through the use of insulation, allowing for the reactors to be modeled as one-dimensional systems. The system design also allowed for the capturing of axial gradients which were large, particularly for temperature, and MC across the reactors. Process reproducibility was established by the reproduction of similar profile results for all variables including temperature, pH, OCR and microbial population data when the reactors were run in triplicate. This resulted in relatively small standard deviations

on the measured variables. Overall this reactor system design provided a great framework for the spatial and temporal analysis of the dynamics of the biotic and abiotic parameters.

6.1.2 Effect of initial moisture content on composting process dynamics

Of the three moisture contents studied: 60%, 65% and 75% wet basis, the most activity was observed in the highest moisture content reactor. While all three moisture contents produced similar variable profiles, the 75% MC reactor produced the highest temperatures, the highest oxygen consumption rate, the highest carbon dioxide evolution rate, the highest rates of carbon degradation, and perhaps, most importantly, the highest bacterial populations. This suggests that for this system, increasing the initial moisture content increased the microbial activity and more specifically the bacterial population. Statistical analysis also showed that the 60% and 65% reactors were similar to each other in behavior, and that both of them were very different from the 75% reactor. These results suggest that the increased moisture in the 75% MC reactor had a significant impact on the performance and further suggests that this moisture content may be close to optimal for the substrate mixture used.

6.1.3 Effect of height on composting process variables

The study showed that temperature was the variable most influenced by reactor height, with temperatures at the bottom of the reactor being significantly lower than those at the top of the reactor. In fact, statistical analyses revealed that the reactors could be divided into three zones based on the temperature profile. The zones roughly divided into bottom, middle and top of the reactor. Moisture content of the reactors was also dependent on height, with samples near the top of the reactor containing more water than those at the bottom of the reactor. Surprisingly, neither the pH nor

the populations of bacteria, fungi and yeast varied significantly with reactor height. These results suggest that temperature and moisture content will be the major variables that need to be controlled in reactor scale up.

6.1.4 Correlation of abiotic and biotic phenomena during the early phases of composting

Many significant correlations were made between the different variables, with temperature having the most correlations. Temperature was highly positively correlated with pH, time, height, moisture content (60 and 65% reactors), bacteria population, carbon dioxide concentration and the extent of carbon degradation. Temperature was also highly negatively correlated with the oxygen concentration. The most revealing correlation was found between the bacterial population and the rate of carbon conversion which suggests that bacteria were the primary group responsible for the substrate degradation. The microbial population data obtained via probe hybridization also highlighted the role of yeasts as acid reducers in the initial stages of degradation. Principal components analysis was also completed to find patterns in the data and similarities among the variables. The principal component analysis revealed that time was the biggest factor in separating out the data, with samples at the end of the 64h period being significantly different from those at the beginning, leading to the conclusion that noticeable degradation had occurred within the time frame of the study. The second major component was reactor height, which suggests that there was also significant differentiation among the samples along the height of the reactors, which further suggests that temperature and moisture content played a big role in differentiating samples since these were the two variables that correlated with height.

6.1.5 Mathematical modeling of composting process

The ability to estimate microbial growth kinetics from experimental data was a key advancement for modeling this composting process because growth rates are highly dependent on environmental conditions such as temperature, other microbial populations, nutrient flow and moisture content. Having this extensive data set also facilitated modeling in both the temporal and spatial dimensions. Predictions made by the model of bacteria, fungi and yeast growth were in good agreement with experimental data. The integration of substrate degradation kinetics into the model also added another dimension to the model that is currently limited in the available literature. The incorporation of empirically derived kinetics led to model predictions of temperature and oxygen that were in good agreement with the experimental data.

6.1.6 Lignocellulosic degradation and impact of using nitrogen fertilizer as a nitrogen source on composting process dynamics and kinetics

The use of a nitrogen fertilizer resulted in very rapid increases in temperature and oxygen consumption rate; however these conditions were only sustained for only a few hours before returning to environmental conditions. This rise to thermophilic conditions occurred much quicker with the nitrogen fertilizer than when dog food was used as the nitrogen source in previous studies. This suggests that the use of a nitrogen fertilizer increased the rate of decomposition within the initial stages of composting. This was further confirmed by the substrate analysis which showed noticeable depreciation in the cellulose, hemicelluloses and lignin content. Within 96h, 19% of lignin, 24% of cellulose and 26% of hemicellulose had been degraded. Changes in the substrate content were also found to correlate with microbial activity indicators of oxygen and carbon dioxide concentration and degradation of the

substrate components was modeled using a first order decay model. Microbial succession of bacteria, fungi, lactic acid bacteria and *Aspergillus spp*., as revealed by real-time PCR was also well-documented.

6.1.7 Effect of organic acid concentration and microbial populations on pH

A number of C1 to C7 organic acids were detected throughout the process, with acetic acid being detected in the highest quantities. Isovaleric acid was the only volatile acid not detected in any of the samples. The total organic acid concentration was positively correlated with the oxygen concentration and negatively correlated with degradation ratios in cellulose, hemicellulose and lignin. This result suggests that the production of organic acids was due to microbial growth and activity. In addition to also being negatively correlated with the substrate components, the acetic acid concentration was also negatively correlated with temperature and pH. This relation with pH is expected because organic acids are known to decrease pH and the acetic acid concentration was the largest fraction of the total organic acid concentration. Profiles of the microbial populations show a shift from lactic acid bacteria to other types of bacteria in the reactors. This is commensurate with lower pH occurring at the beginning of the process. Interestingly, there was no statistical correlation between the organic acid concentration and the microbial population. This suggests that either the groups responsible for organic acid growth were not quantified of that those changes occurred at a qualitative rather than quantitative level and leaves room for more research in this area. This study was also the first to use real time PCR to analyze microbial population dynamics and its results which showed a dominance of the bacterial population was consistent with other studies on compost microbial communities using other techniques.

6.2 Suggestions for future research

Future research in this area harbors on obtaining more valuable data that can provide a more complete picture of the underlying mechanisms that drive the composting process. A key method that will greatly expand knowledge of microbial dynamics and succession is that of pyrosequencing. This sequencing technique will provide a comprehensive image of all the microbial groups present with the ability to classify this information at a number of different levels including the phylum, genus and species level. Such deep probing of microbial groups is essential because changes that may not apparent at the top levels, may be reflected at underlying levels. This stems from one of the advantages of pyrosequencing, which is the provision of sequences for all microorganisms present. Additionally, the state of the art technology, Fourier Transform Infrared Spectroscopy (FTIR) may be used to monitor changes in the substrate composition during the process.

Another beneficial direction for study would be to isolate cellulases from the composting process when switchgrass is used as a substrate. The successful extraction and isolation of cellulases will provide some key insights into some of the enzymes that will grow naturally to degrade switchgrass. The desired objective would be to obtain robust and efficient enzymes that were optimized for the metabolism of switchgrass. This information is critical for the conversion process of biomass to ethanol because the efficient enzymatic hydrolysis of pretreated biomass is a major bottleneck in the process. By prospecting for enzymes in self-propelled systems, such as composting, better enzymes may be obtained.

It would also be desirable to carry out the composting process to completion to see what impact increasing the initial rate would have on the overall process rate. This would extend the engineering design process to produce the final stable humic product

in a more efficient manner. Furthermore, experimentally capturing the full process can potentially lead to better simulation models for predicting the process.

APPENDIX A

MATLAB CODE FOR MODEL PRESENTED IN CHAPTER 3

The following code was used to obtain both the growth phase ("mesotemp") and the deceleration phase data ('thermotemp"). "Mesotemp" and "thermotemp" were written as two separate files containing the same code with the exception that the initial values used in "thermotemp" are the ending values from "mesotemp."

```
%This program is designed to describe the thermophilic phase of the
%degradation process

function f=mesotemp(t,y)

%%%% SPECIFY HEIGHT %%%%%%%%%%
z_initial = 0;
increment = 0.01;
z_final = 0.6;
Z = z_initial:increment:z_final;

Height_vector = [z_initial:increment:z_final];
% Total_Points = length(Height_vector)-1; % Height of 1D reactor
Height = length(Height_vector)-1; % Height of 1D reactor
Variable_Number = 9; % No. of variables

%Write out expressions for system of ODEs, NOW AT EVERY Z
for Point = 0:Height   % If Point is from 0 to 12, Height = 12
i.e.,(length of vector)-1;

    %Define the components of the variable y
    T=y(Point*Variable_Number+1,1); %Temperature
    s1=y(Point*Variable_Number+2,1); % Sugars and starch
    s2=y(Point*Variable_Number+3,1); % hemicellulose
    s3=y(Point*Variable_Number+4,1); % cellulose
    x1=y(Point*Variable_Number+5,1); % yeast
    x2=y(Point*Variable_Number+6,1); % bacteria
    x3=y(Point*Variable_Number+7,1); %fungi
    O2=y(Point*Variable_Number+8,1); %oxygen conc
    Q=y(Point*Variable_Number+9,1); %heat yield

%%%%%%%%%% CONSTANTS OF THE SYSTEM
%%%%%%%%%%%%%%%%%%%%%%%%%%%%%%%%%%%%%%%%%%%%

    %First define all parameters in the temperature equation
    q=11300; % Metabolic Heat yield; units = KJ/Kg biomass
```

```
   lambda=2250; % latent heat of vaporization of water; units = KJ/Kg
water
    ma=1.44; % mass flow rate of air; units = Kg air/hr
    Ga=19.74; % mass flux of dry air; units = Kg air/m^2 hr
    Vz=16.4; % superficial air velocity; units = m/h
    d=1.2102*10^-7; %curve fitting constant for latent heat; unit =
KJ/K
    m=0.056807;  %curve fitting constant for latent heat; unit = 1/K
    epsilon=0.4;
    Rd=287.05; %specific gas constant for air; units = J/KgK
    Patm=101325; %units = Pa
    rhoa=Patm/(Rd*T); % density of air; units = Kg/m^3
    cpa=1.0132; %specific heat of dry air; units = KJ/Kg air K
    cpv=1.8673; %specific heat of water vapor; units = KJ/Kg water K
    rhodb=160; % density of dry bulk/solids; units = Kg/m^3
    cps=2.0; %specific heat of dry solids; units = KJ/KgK
    cpw=4.1868; %specific heat of water; units = KJ/KgK
    V=0.05; %reactor volume; units = m^3
    Md=1.5; % moisture content on a dry basis

%     %Define growth rate constants
    %%%%%%%%%%%%%%%%%%%%%%%%%%%%%%%%%%%%%%%%%%%%%%%
    Actual_Height = z_initial + Point*increment;

    if (Actual_Height >= 0 && Actual_Height < 0.1)

        beta1 = 0.0 + (-0.203 - 0.0)/(0.1/increment)*(Point -
(0.0)/increment);   % Point*0.01+0.073;
        beta2 = 0.0 + (-0.438 - 0.0)/(0.1/increment)*(Point -
(0.0)/increment); %;Point*0.01+0.0736;
        beta3 = 0.0 + (-0.0352 - 0.0)/(0.1/increment)*(Point -
(0.0)/increment); %Point*0.01+0.08;

    elseif (Actual_Height >= 0.1 && Actual_Height < 0.2)

        beta1 = -0.203 + (-0.156 - -0.203)/(0.1/increment)*(Point -
(0.1)/increment);      % Point*0.01+0.073;
        beta2 = -0.438 + (-0.5 - -0.438)/(0.1/increment)*(Point -
(0.1)/increment);  %;Point*0.01+0.0736;
        beta3 = -0.0352 + (-0.115 - -0.0352)/(0.1/increment)*(Point -
(0.1)/increment); %Point*0.01+0.08;

    elseif (Actual_Height >= 0.2 && Actual_Height < 0.3)

        beta1 = -0.156 + (-0.125 - -0.156 )/(0.1/increment)*(Point -
(0.2)/increment);      % Point*0.01+0.073;
        beta2 = -0.5 + (-0.504 - -0.5 )/(0.1/increment)*(Point -
(0.2)/increment);  %;Point*0.01+0.0736;
        beta3 = -0.115 + (-0.072 - -0.115 )/(0.1/increment)*(Point -
(0.2)/increment); %Point*0.01+0.08;

    elseif (Actual_Height >= 0.3 && Actual_Height < 0.4)
```

```
        beta1 = -0.125 + (-0.121 - -0.125 )/(0.1/increment)*(Point -
(0.3)/increment);      % Point*0.01+0.073;
        beta2 = -0.504 + (-0.565 - -0.504 )/(0.1/increment)*(Point -
(0.3)/increment);  %;Point*0.01+0.0736;
        beta3 = -0.072 + (-0.0368 - -0.072 )/(0.1/increment)*(Point -
(0.3)/increment); %Point*0.01+0.08;

    elseif (Actual_Height >= 0.4 && Actual_Height < 0.5)

        beta1 = -0.121 + (-0.21 - -0.121)/(0.1/increment)*(Point -
(0.4)/increment);      % Point*0.01+0.073;
        beta2 = -0.565 + (-0.0902 - -0.565)/(0.1/increment)*(Point -
(0.4)/increment);  %;Point*0.01+0.0736;
        beta3 = -0.0368 + (-0.0285 - -0.0368)/(0.1/increment)*(Point
- (0.4)/increment); %Point*0.01+0.08;

    elseif (Actual_Height >= 0.5 && Actual_Height < 0.6)

        beta1 = -0.21 + (-0.057 - -0.21 )/(0.1/increment)*(Point -
(0.5)/increment);      % Point*0.01+0.073;
        beta2 = -0.0902 + (-0.0605 - -0.0902 )/(0.1/increment)*(Point
- (0.5)/increment);  %;Point*0.01+0.0736;
        beta3 = -0.0285 + (-0.0455 - -0.0285 )/(0.1/increment)*(Point
- (0.5)/increment); %Point*0.01+0.08;

    elseif (Actual_Height == 0.6)

        beta1 = -0.57;%use -0.057 for yeast data;
        beta2 = -0.5605;%-0.0605;
        beta3 = -0.0455;
    end

    %%%%%%%%%%%%%%%%%%%%%%%%%%%%%%%%%%%%%%%%%%%%%%%

    Ks1=0.06; %saturation constant of organism i; units=Kg yeast/Kg
composting material
    Ks2=0.08; %units= Kg bacteria/Kg composting material
    Ks3=0.08; % units = Kg fungi/ Kg composting material

    m2=6.0; %mass of composting material during mesophilic phase

    Y1=8; %yield constant for carbohydrates; units = Kg substrate/kg
organism
    Y2=8; % yield constant for hemicellulose; units =Kg substrate/kg
organism
    Y3=16; %yield constant for cellulose ; units = Kg substrate/kg
organism

    O2a=0.187; %concentration of ambient O2; units = %
    betaOx1=0.3; % specific oxygen uptake; units = kgO2/Kg yeast
    betaOx2=0.4; % units = KgO2/Kg bacteria
    betaOx3=0.3; %units = KgO2/Kg fungi
```

```
    %%%%%%% ALL CONSTANTS TILL HERE %%%%%%%%%%%%%%%%%%%%%%%%%%%%%%%%

    x1dot=beta1*x1*(s1/(Ks1+s1));
    x2dot=beta2*x2*((s1+s2+s3)/(Ks2+s1+s2+s3));
    x3dot=beta3*x3*((s1+s2+s3)/(Ks3+s1+s2+s3));
    s1dot=Y1*(s1*x1dot +(s1/(s1+s2+s3))*x2dot +
(s1/(s1+s2+s3))*(x3dot));
    s2dot=Y2*((s2/(s1+s2+s3))*x2dot + (s2/(s1+s2+s3))*(x3dot));
    s3dot=Y3*((s3/(s1+s2+s3))*x2dot + (s3/(s1+s2+s3))*x3dot);
    O2dot=(ma*(O2a - O2)-(m2*(betaOx1*x1 + betaOx2*x2 +
betaOx3*x3)))/(rhoa*V*epsilon);
    Qdot=q*(x1dot + x2dot + x3dot);

    %%%%%%%%%%%%%%%%%%%%%%%%%%%%%%%%%%%%%%%%%%%%%%%%%%%%%%%%%%%%%%%%%%%
    %Add the Del_T_by_Del_Z term

    if (Point == 0)
        Del_T_by_Del_Z = 0;

    if (Point ~= 0 && Point ~= Height)
        Del_T_by_Del_Z = ((y((Point+1)*Variable_Number+1,1) -
y((Point-1)*Variable_Number+1,1)))/(2*increment);
    end

    if (Point == Height)
        Del_T_by_Del_Z = 0;
    end
    %%%%%%%%%%%%%%%%%%%%%%%%%%%%%%%%%%%%%%%%%%%%%%%%%%%%%%%%%%%%%%%%%%%

    %Consolidate some other expressions
    M=V*rhoa*(cpa + d*exp(m*T))*Vz*Del_T_by_Del_Z; %M=V*rhoa*(cpa +
d*exp(m*T))*Vz*Del_T_by_Del_Z
    N=epsilon*rhoa*(cpa + cpv*(d*exp(m*T)));
    O=(1-epsilon)*rhodb*(cps + cpw*Md);

    P = V * (N + O);
    Tdot=(Q-M)/P;

    f(Point*Variable_Number+1,1) = Tdot;
    f(Point*Variable_Number+2,1) = s1dot;
    f(Point*Variable_Number+3,1) = s2dot;
    f(Point*Variable_Number+4,1) = s3dot;
    f(Point*Variable_Number+5,1) = x1dot;
    f(Point*Variable_Number+6,1) = x2dot;
    f(Point*Variable_Number+7,1) = x3dot;
    f(Point*Variable_Number+8,1) = O2dot;
    f(Point*Variable_Number+9,1) = Qdot;


end
```

The following code was then used to solve the system of equations presented in mesotemp or thermotemp.

```
% get the values from mesotemp or thermotemp
y0 = [299.0; 1.728; 1.4442; 1.6689; 7.45*10^-6; 3.89*10^-4; 6.65*10^-
5; 0.187; 0];


z_initial = 0;
increment = 0.01;
z_final = 0.6;
Z = z_initial:increment:z_final;

% Height_vector = [z_initial:increment:z_final];
% %Total_Points = length(Height_vector)-1; % Height of 1D reactor
% Height = length(Height_vector)-1; % Height of 1D reactor
% y_initial = zeros(length(Height_vector),1);
% Variable_Number = 9;


y_initial = [];
for i = 1:length(Z);
    y_initial = [y_initial; y0;];
end

 tspan1=0:0.01:38;
 options = odeset('RelTol',1e-2,'AbsTol',1e-3,'NormControl','off');
 [t_final1,y_final1]=ode45(@mesotemp,tspan1,y_initial,options);

For “thermotemp” only, the following was also included:
y_initial2 = transpose(y_final1(end,:));
 tspan2 = 0:0.01:26;

 %Solution using ODE 45

%options = odeset('RelTol',1e-1,'AbsTol',1e-1,'NormControl','off');
 [t_final y_final2] = ode45(@thermotemp,tspan2,y_initial2,options);
```

APPENDIX B

COMPLETE EXPERIMENTAL DATA SET

Degradation of switchgrass and dog food mixtures at initial moisture content of 60, 65 and 75%. All data presented are the averages over 3 reactor runs

Time (h)	Initial MC (%)	Height(m)	Temperature (^{o}C)	pH	MC(%)
0	75	0.1	24.33	5.50	75.77
0	75	0.2	22.77	5.50	75.77
0	75	0.3	23.64	5.50	75.77
0	75	0.4	22.67	5.50	75.77
0	75	0.5	23.03	5.50	75.77
0	75	0.6	22.70	5.50	75.77
8	75	0.1	23.35	4.94	73.78
8	75	0.2	24.79	4.94	72.26
8	75	0.3	24.21	4.90	72.95
8	75	0.4	29.64	4.87	72.47
8	75	0.5	31.51	4.87	71.41
8	75	0.6	32.71	4.84	72.65
14	75	0.1	23.64	5.68	72.11
14	75	0.2	27.29	5.32	71.61
14	75	0.3	25.96	5.77	72.65
14	75	0.4	36.19	5.12	71.56
14	75	0.5	38.01	5.14	71.16
14	75	0.6	39.46	4.95	72.30
20	75	0.1	24.20	6.82	70.36
20	75	0.2	33.07	6.84	70.39
20	75	0.3	29.09	6.99	73.21
20	75	0.4	42.63	6.66	71.24
20	75	0.5	44.55	5.38	72.57
20	75	0.6	44.93	5.34	70.64
26	75	0.1	26.68	7.31	70.19
26	75	0.2	35.45	7.63	71.14
26	75	0.3	40.94	6.20	71.94
26	75	0.4	48.23	6.75	72.75
26	75	0.5	50.62	5.56	70.57
26	75	0.6	50.52	5.63	71.74
32	75	0.1	23.40	7.46	71.88
32	75	0.2	33.57	7.17	70.85
32	75	0.3	31.99	7.91	73.51
32	75	0.4	52.41	7.32	70.64

Data continued for switchgrass/dog food mixture

Time (h)	Initial MC (%)	Height(m)	Temperature (^{o}C)	pH	MC(%)
32	75	0.5	55.16	6.88	70.89
32	75	0.6	57.07	7.23	71.91
38	75	0.1	22.07	7.84	70.74
38	75	0.2	31.48	7.61	69.30
38	75	0.3	30.76	8.59	71.56
38	75	0.4	48.46	8.32	72.32
38	75	0.5	52.44	8.01	75.44
38	75	0.6	55.48	8.31	76.24
44	75	0.1	24.00	7.96	71.92
44	75	0.2	32.61	8.41	71.19
44	75	0.3	36.40	8.62	74.57
44	75	0.4	47.02	8.50	72.06
44	75	0.5	51.37	7.93	73.12
44	75	0.6	54.50	7.74	74.43
50	75	0.1	25.46	8.25	69.78
50	75	0.2	32.91	8.30	67.23
50	75	0.3	32.17	8.65	66.32
50	75	0.4	46.73	8.70	73.05
50	75	0.5	51.18	8.10	73.39
50	75	0.6	54.11	8.32	76.49
58	75	0.1	23.22	8.21	67.94
58	75	0.2	29.90	8.72	64.33
58	75	0.3	29.71	8.73	65.32
58	75	0.4	45.32	8.47	61.01
58	75	0.5	48.52	8.48	70.55
58	75	0.6	51.16	8.66	73.36
64	75	0.1	23.93	8.72	67.41
64	75	0.2	28.67	8.71	64.77
64	75	0.3	28.88	8.71	66.44
64	75	0.4	43.10	8.61	75.12
64	75	0.5	47.73	8.76	74.00
64	75	0.6	50.07	8.17	78.24
0	65	0.1	21.32	5.52	65.45
0	65	0.2	21.19	5.52	65.45
0	65	0.3	21.08	5.52	65.45
0	65	0.4	20.60	5.52	65.45
0	65	0.5	20.59	5.52	65.45
0	65	0.6	20.20	5.52	65.45
8	65	0.1	20.68	4.86	65.95
8	65	0.2	22.14	4.77	66.27

Data continued for switchgrass/dog food mixture

Time (h)	Initial MC (%)	Height(m)	Temperature (^{o}C)	pH	MC(%)
8	65	0.3	23.66	4.74	65.74
8	65	0.4	24.71	4.76	67.39
8	65	0.5	25.91	4.68	66.81
8	65	0.6	26.52	4.74	73.48
14	65	0.1	22.82	4.82	65.94
14	65	0.2	25.89	4.77	66.61
14	65	0.3	28.72	4.79	68.86
14	65	0.4	30.00	4.75	66.64
14	65	0.5	31.15	4.72	68.78
14	65	0.6	31.31	4.70	68.07
20	65	0.1	24.58	4.90	65.70
20	65	0.2	29.31	5.26	67.47
20	65	0.3	34.25	5.30	67.42
20	65	0.4	36.17	5.40	66.64
20	65	0.5	37.70	4.83	66.04
20	65	0.6	38.13	5.01	68.30
26	65	0.1	25.84	5.15	64.64
26	65	0.2	30.97	5.43	65.54
26	65	0.3	38.10	5.36	64.90
26	65	0.4	40.28	5.26	67.39
26	65	0.5	41.99	5.67	67.56
26	65	0.6	42.70	5.28	67.16
32	65	0.1	27.78	5.46	66.38
32	65	0.2	32.53	5.50	62.61
32	65	0.3	40.77	5.55	67.25
32	65	0.4	43.11	5.58	65.98
32	65	0.5	44.95	5.57	66.82
32	65	0.6	45.78	5.39	67.38
38	65	0.1	30.43	5.25	64.74
38	65	0.2	33.98	5.25	64.33
38	65	0.3	41.45	6.57	64.67
38	65	0.4	43.73	5.84	66.28
38	65	0.5	45.69	5.93	66.37
38	65	0.6	46.66	5.90	68.63
44	65	0.1	29.51	6.42	61.85
44	65	0.2	33.74	6.72	63.58
44	65	0.3	40.76	6.97	67.81
44	65	0.4	43.40	6.46	67.18
44	65	0.5	45.47	6.12	66.72
44	65	0.6	46.39	6.03	69.98

Data continued for switchgrass/dog food mixture

Time (h)	Initial MC (%)	Height(m)	Temperature (^{o}C)	pH	MC(%)
50	65	0.1	28.77	7.43	59.19
50	65	0.2	32.75	6.99	59.95
50	65	0.3	39.96	7.46	68.39
50	65	0.4	43.01	7.14	70.73
50	65	0.5	44.78	6.35	71.74
50	65	0.6	45.57	6.25	72.95
58	65	0.1	28.12	7.43	55.05
58	65	0.2	32.90	7.62	51.78
58	65	0.3	42.25	7.79	66.22
58	65	0.4	44.55	6.79	71.68
58	65	0.5	46.27	7.09	72.42
58	65	0.6	47.00	6.20	73.28
64	65	0.1	27.06	7.50	47.84
64	65	0.2	31.95	7.67	52.92
64	65	0.3	39.30	8.34	60.75
64	65	0.4	42.76	7.88	68.20
64	65	0.5	44.90	7.30	68.41
64	65	0.6	45.62	7.26	75.05
0	60	0.1	23.46	5.46	61.13
0	60	0.2	22.04	5.46	61.13
0	60	0.3	21.95	5.46	61.13
0	60	0.4	21.79	5.46	61.13
0	60	0.5	22.37	5.46	61.13
0	60	0.6	22.19	5.46	61.13
8	60	0.1	23.89	4.91	60.99
8	60	0.2	20.81	4.88	60.12
8	60	0.3	22.39	4.84	61.51
8	60	0.4	23.16	4.77	62.34
8	60	0.5	26.67	4.79	60.52
8	60	0.6	27.88	4.76	61.48
14	60	0.1	24.75	4.81	59.02
14	60	0.2	24.28	4.82	60.70
14	60	0.3	27.06	4.84	60.86
14	60	0.4	28.12	4.83	63.58
14	60	0.5	31.57	5.02	63.30
14	60	0.6	32.40	4.71	62.73
20	60	0.1	23.30	5.29	60.83
20	60	0.2	27.87	4.96	60.66
20	60	0.3	32.49	4.94	61.23
20	60	0.4	33.47	5.16	61.97

Data continued for switchgrass/dog food mixture

Time (h)	Initial MC (%)	Height(m)	Temperature (^{o}C)	pH	MC(%)
20	60	0.5	37.99	5.22	63.56
20	60	0.6	38.62	4.97	63.95
26	60	0.1	25.44	5.54	62.62
26	60	0.2	32.29	5.80	59.70
26	60	0.3	35.91	5.68	61.59
26	60	0.4	40.55	5.44	61.05
26	60	0.5	44.60	5.34	63.86
26	60	0.6	45.38	5.37	63.62
32	60	0.1	27.01	5.79	59.46
32	60	0.2	33.77	5.70	61.97
32	60	0.3	40.21	5.99	59.40
32	60	0.4	43.17	5.48	59.30
32	60	0.5	47.08	5.97	60.20
32	60	0.6	48.09	5.87	63.91
38	60	0.1	25.81	5.92	58.24
38	60	0.2	33.34	6.42	57.31
38	60	0.3	39.33	6.29	59.40
38	60	0.4	41.87	6.01	59.44
38	60	0.5	47.70	6.46	62.66
38	60	0.6	49.24	6.13	66.75
44	60	0.1	24.65	6.65	53.72
44	60	0.2	31.65	7.01	58.47
44	60	0.3	37.41	7.03	56.99
44	60	0.4	38.81	7.25	64.27
44	60	0.5	45.83	7.12	64.41
44	60	0.6	47.85	7.04	68.11
50	60	0.1	24.57	6.29	51.97
50	60	0.2	30.23	7.32	57.10
50	60	0.3	35.06	6.93	51.54
50	60	0.4	36.17	7.00	58.90
50	60	0.5	43.12	6.73	63.49
50	60	0.6	45.34	7.02	65.22
58	60	0.1	22.57	7.02	44.14
58	60	0.2	28.14	7.04	46.17
58	60	0.3	33.33	7.05	48.50
58	60	0.4	32.40	7.17	57.08
58	60	0.5	39.70	7.21	59.63
58	60	0.6	41.86	7.42	64.18
64	60	0.1	22.74	7.82	44.72
64	60	0.2	26.53	7.31	47.27

Data continued for switchgrass/dog food mixture

Time (h)	Initial MC (%)	Height(m)	CO_2 (%)	O_2 (%)	% Conversion
64	60	0.3	29.23	7.27	51.94
64	60	0.4	28.88	7.35	58.95
64	60	0.5	35.30	7.21	62.46
64	60	0.6	37.20	7.64	64.95
0	75	0.1	0.148	19.009	0.000
0	75	0.2	0.148	19.009	0.000
0	75	0.3	0.148	19.009	0.000
0	75	0.4	0.148	19.009	0.000
0	75	0.5	0.148	19.009	0.000
0	75	0.6	0.148	19.009	0.000
8	75	0.1	0.628	18.746	1.437
8	75	0.2	0.628	18.746	1.437
8	75	0.3	0.628	18.746	1.437
8	75	0.4	0.628	18.746	1.437
8	75	0.5	0.628	18.746	1.437
8	75	0.6	0.628	18.746	1.437
14	75	0.1	1.329	18.319	5.206
14	75	0.2	1.329	18.319	5.206
14	75	0.3	1.329	18.319	5.206
14	75	0.4	1.329	18.319	5.206
14	75	0.5	1.329	18.319	5.206
14	75	0.6	1.329	18.319	5.206
20	75	0.1	1.595	18.111	8.773
20	75	0.2	1.595	18.111	8.773
20	75	0.3	1.595	18.111	8.773
20	75	0.4	1.595	18.111	8.773
20	75	0.5	1.595	18.111	8.773
20	75	0.6	1.595	18.111	8.773
26	75	0.1	2.185	17.947	15.356
26	75	0.2	2.185	17.947	15.356
26	75	0.3	2.185	17.947	15.356
26	75	0.4	2.185	17.947	15.356
26	75	0.5	2.185	17.947	15.356
26	75	0.6	2.185	17.947	15.356
32	75	0.1	2.427	17.695	20.573
32	75	0.2	2.427	17.695	20.573
32	75	0.3	2.427	17.695	20.573
32	75	0.4	2.427	17.695	20.573
32	75	0.5	2.427	17.695	20.573
32	75	0.6	2.427	17.695	20.573
38	75	0.1	2.296	17.787	23.224

Data continued for switchgrass/dog food mixture

Time (h)	Initial MC (%)	Height(m)	CO_2 (%)	O_2 (%)	% Conversion
38	75	0.2	2.296	17.787	23.224
38	75	0.3	2.296	17.787	23.224
38	75	0.4	2.296	17.787	23.224
38	75	0.5	2.296	17.787	23.224
38	75	0.6	2.296	17.787	23.224
44	75	0.1	2.120	17.810	24.904
44	75	0.2	2.120	17.810	24.904
44	75	0.3	2.120	17.810	24.904
44	75	0.4	2.120	17.810	24.904
44	75	0.5	2.120	17.810	24.904
44	75	0.6	2.120	17.810	24.904
50	75	0.1	2.068	17.817	27.633
50	75	0.2	2.068	17.817	27.633
50	75	0.3	2.068	17.817	27.633
50	75	0.4	2.068	17.817	27.633
50	75	0.5	2.068	17.817	27.633
50	75	0.6	2.068	17.817	27.633
58	75	0.1	1.761	17.846	27.544
58	75	0.2	1.761	17.846	27.544
58	75	0.3	1.761	17.846	27.544
58	75	0.4	1.761	17.846	27.544
58	75	0.5	1.761	17.846	27.544
58	75	0.6	1.761	17.846	27.544
64	75	0.1	1.551	18.041	26.859
64	75	0.2	1.551	18.041	26.859
64	75	0.3	1.551	18.041	26.859
64	75	0.4	1.551	18.041	26.859
64	75	0.5	1.551	18.041	26.859
64	75	0.6	1.551	18.041	26.859
0	65	0.1	0.182	18.999333	0
0	65	0.2	0.182	18.999333	0
0	65	0.3	0.182	18.999333	0
0	65	0.4	0.182	18.999333	0
0	65	0.5	0.182	18.999333	0
0	65	0.6	0.182	18.999333	0
8	65	0.1	0.4576667	18.857841	1.068783646
8	65	0.2	0.4576667	18.857841	1.068783646
8	65	0.3	0.4576667	18.857841	1.068783646
8	65	0.4	0.4576667	18.857841	1.068783646
8	65	0.5	0.4576667	18.857841	1.068783646
8	65	0.6	0.4576667	18.857841	1.068783646

Data continued for switchgrass/dog food mixture

Time (h)	Initial MC (%)	Height(m)	CO_2 (%)	O_2 (%)	% Conversion
14	65	0.1	0.6736667	18.675364	2.709829115
14	65	0.2	0.6736667	18.675364	2.709829115
14	65	0.3	0.6736667	18.675364	2.709829115
14	65	0.4	0.6736667	18.675364	2.709829115
14	65	0.5	0.6736667	18.675364	2.709829115
14	65	0.6	0.6736667	18.675364	2.709829115
20	65	0.1	1.185	18.4389527	6.660178616
20	65	0.2	1.185	18.4389527	6.660178616
20	65	0.3	1.185	18.4389527	6.660178616
20	65	0.4	1.185	18.4389527	6.660178616
20	65	0.5	1.185	18.4389527	6.660178616
20	65	0.6	1.185	18.4389527	6.660178616
26	65	0.1	1.4636667	18.001132	10.53954358
26	65	0.2	1.4636667	18.001132	10.53954358
26	65	0.3	1.4636667	18.001132	10.53954358
26	65	0.4	1.4636667	18.001132	10.53954358
26	65	0.5	1.4636667	18.001132	10.53954358
26	65	0.6	1.4636667	18.001132	10.53954358
32	65	0.1	1.5503333	17.8139373	13.6072062
32	65	0.2	1.5503333	17.8139373	13.6072062
32	65	0.3	1.5503333	17.8139373	13.6072062
32	65	0.4	1.5503333	17.8139373	13.6072062
32	65	0.5	1.5503333	17.8139373	13.6072062
32	65	0.6	1.5503333	17.8139373	13.6072062
38	65	0.1	1.5083333	17.8188987	15.67757744
38	65	0.2	1.5083333	17.8188987	15.67757744
38	65	0.3	1.5083333	17.8188987	15.67757744
38	65	0.4	1.5083333	17.8188987	15.67757744
38	65	0.5	1.5083333	17.8188987	15.67757744
38	65	0.6	1.5083333	17.8188987	15.67757744
44	65	0.1	1.349	17.7195493	16.24901048
44	65	0.2	1.349	17.7195493	16.24901048
44	65	0.3	1.349	17.7195493	16.24901048
44	65	0.4	1.349	17.7195493	16.24901048
44	65	0.5	1.349	17.7195493	16.24901048
44	65	0.6	1.349	17.7195493	16.24901048
50	65	0.1	1.4146667	17.976896	19.41363884
50	65	0.2	1.4146667	17.976896	19.41363884
50	65	0.3	1.4146667	17.976896	19.41363884
50	65	0.4	1.4146667	17.976896	19.41363884
50	65	0.5	1.4146667	17.976896	19.41363884

Data continued for switchgrass/dog food mixture

Time (h)	Initial MC (%)	Height(m)	CO_2 (%)	O_2 (%)	% Conversion
50	65	0.6	1.4146667	17.976896	19.41363884
58	65	0.1	1.4256667	17.899438	22.59357975
58	65	0.2	1.4256667	17.899438	22.59357975
58	65	0.3	1.4256667	17.899438	22.59357975
58	65	0.4	1.4256667	17.899438	22.59357975
58	65	0.5	1.4256667	17.899438	22.59357975
58	65	0.6	1.4256667	17.899438	22.59357975
64	65	0.1	1.2576667	17.931997	22.0880543
64	65	0.2	1.2576667	17.931997	22.0880543
64	65	0.3	1.2576667	17.931997	22.0880543
64	65	0.4	1.2576667	17.931997	22.0880543
64	65	0.5	1.2576667	17.931997	22.0880543
64	65	0.6	1.2576667	17.931997	22.0880543
0	60	0.1	0.1263333	18.892062	0
0	60	0.2	0.1263333	18.892062	0
0	60	0.3	0.1263333	18.892062	0
0	60	0.4	0.1263333	18.892062	0
0	60	0.5	0.1263333	18.892062	0
0	60	0.6	0.1263333	18.892062	0
8	60	0.1	0.4816667	18.787821	0.480457568
8	60	0.2	0.4816667	18.787821	0.480457568
8	60	0.3	0.4816667	18.787821	0.480457568
8	60	0.4	0.4816667	18.787821	0.480457568
8	60	0.5	0.4816667	18.787821	0.480457568
8	60	0.6	0.4816667	18.787821	0.480457568
14	60	0.1	0.783	18.583396	0.599892434
14	60	0.2	0.783	18.583396	0.599892434
14	60	0.3	0.783	18.583396	0.599892434
14	60	0.4	0.783	18.583396	0.599892434
14	60	0.5	0.783	18.583396	0.599892434
14	60	0.6	0.783	18.583396	0.599892434
20	60	0.1	1.2533333	18.293565	3.295933977
20	60	0.2	1.2533333	18.293565	3.295933977
20	60	0.3	1.2533333	18.293565	3.295933977
20	60	0.4	1.2533333	18.293565	3.295933977
20	60	0.5	1.2533333	18.293565	3.295933977
20	60	0.6	1.2533333	18.293565	3.295933977
26	60	0.1	1.469	17.865060	7.877911457
26	60	0.2	1.469	17.865060	7.877911457
26	60	0.3	1.469	17.865060	7.877911457
26	60	0.4	1.469	17.865060	7.877911457

Data continued for switchgrass/dog food mixture

Time (h)	Initial MC (%)	Height(m)	CO_2 (%)	O_2 (%)	% Conversion
26	60	0.5	1.469	17.865060	7.877911457
26	60	0.6	1.469	17.865060	7.877911457
32	60	0.1	1.5876667	17.701757	13.78520676
32	60	0.2	1.5876667	17.701757	13.78520676
32	60	0.3	1.5876667	17.701757	13.78520676
32	60	0.4	1.5876667	17.701757	13.78520676
32	60	0.5	1.5876667	17.701757	13.78520676
32	60	0.6	1.5876667	17.701757	13.78520676
38	60	0.1	1.548	17.71642167	18.70009781
38	60	0.2	1.548	17.71642167	18.70009781
38	60	0.3	1.548	17.71642167	18.70009781
38	60	0.4	1.548	17.71642167	18.70009781
38	60	0.5	1.548	17.71642167	18.70009781
38	60	0.6	1.548	17.71642167	18.70009781
44	60	0.1	1.328	17.83945467	21.15541977
44	60	0.2	1.328	17.83945467	21.15541977
44	60	0.3	1.328	17.83945467	21.15541977
44	60	0.4	1.328	17.83945467	21.15541977
44	60	0.5	1.328	17.83945467	21.15541977
44	60	0.6	1.328	17.83945467	21.15541977
50	60	0.1	1.134	17.99391133	20.18260176
50	60	0.2	1.134	17.99391133	20.18260176
50	60	0.3	1.134	17.99391133	20.18260176
50	60	0.4	1.134	17.99391133	20.18260176
50	60	0.5	1.134	17.99391133	20.18260176
50	60	0.6	1.134	17.99391133	20.18260176
58	60	0.1	0.85	18.19384833	18.73692342
58	60	0.2	0.85	18.19384833	18.73692342
58	60	0.3	0.85	18.19384833	18.73692342
58	60	0.4	0.85	18.19384833	18.73692342
58	60	0.5	0.85	18.19384833	18.73692342
58	60	0.6	0.85	18.19384833	18.73692342
64	60	0.1	0.605	18.55366833	12.53123999
64	60	0.2	0.605	18.55366833	12.53123999
64	60	0.3	0.605	18.55366833	12.53123999
64	60	0.4	0.605	18.55366833	12.53123999
64	60	0.5	0.605	18.55366833	12.53123999
64	60	0.6	0.605	18.55366833	12.53123999

Data continued for switchgrass/dog food mixture

Time (h)	Initial MC (%)	Height(m)	Bacteria (µg/µg substrate)	Yeast (µg/µg substrate)	Fungi (µg/µg substrate)
0	75	0.1	1.6444E-05	0.000205995	5.02987E-05
0	75	0.2	1.6444E-05	2.0600E-04	5.0299E-05
0	75	0.3	1.6444E-05	2.0600E-04	5.0299E-05
0	75	0.4	1.6444E-05	2.0600E-04	5.0299E-05
0	75	0.5	1.6444E-05	2.0600E-04	5.0299E-05
0	75	0.6	1.6444E-05	0.000205995	5.02987E-05
8	75	0.1	1.53908E-05	9.15698E-05	1.32715E-05
8	75	0.2	3.0368E-05	2.4392E-05	2.1409E-05
8	75	0.3	4.6206E-05	2.4574E-05	2.5962E-05
8	75	0.4	1.4754E-05	3.9340E-05	3.6294E-05
8	75	0.5	2.2382E-05	1.2376E-04	3.4343E-05
8	75	0.6	1.48895E-05	1.51663E-05	3.21939E-05
14	75	0.1	7.88744E-06	5.51807E-06	2.02866E-05
14	75	0.2	2.4629E-05	1.8351E-05	2.9505E-05
14	75	0.3	9.2721E-06	1.7256E-05	2.3058E-05
14	75	0.4	9.8805E-06	3.7464E-05	1.0924E-05
14	75	0.5	1.6335E-05	9.5496E-06	1.2848E-05
14	75	0.6	1.129E-05	2.01805E-05	1.67898E-05
20	75	0.1	1.33727E-05	0.000927487	2.05928E-05
20	75	0.2	1.2702E-05	2.2922E-04	2.2956E-05
20	75	0.3	9.2540E-06	1.2082E-05	2.4038E-05
20	75	0.4	1.5620E-05	3.2063E-05	1.8649E-05
20	75	0.5	6.8477E-06	5.0096E-05	2.6785E-05
20	75	0.6	1.5210E-05	0.000148416	1.0176E-05
26	75	0.1	7.44097E-06	0.000105806	1.39034E-05
26	75	0.2	2.5039E-05	4.8973E-05	1.3452E-05
26	75	0.3	7.1763E-05	3.9901E-05	1.8615E-05
26	75	0.4	6.0368E-04	1.1757E-05	1.6250E-05
26	75	0.5	2.4013E-04	6.2080E-05	7.6966E-05
26	75	0.6	2.1237E-04	1.32695E-05	1.6016E-05
32	75	0.1	2.8967E-05	0.000104966	1.3506E-05
32	75	0.2	4.2713E-05	2.7404E-05	3.6743E-06
32	75	0.3	1.3384E-04	5.3259E-07	1.4483E-05
32	75	0.4	5.7940E-04	1.0613E-05	3.5446E-05
32	75	0.5	3.3605E-04	1.6013E-05	7.1935E-06
32	75	0.6	2.4605E-04	1.7811E-05	1.6270E-05
38	75	0.1	7.5572E-06	8.45931E-06	3.5358E-06
38	75	0.2	3.1111E-05	1.7049E-06	1.7575E-06
38	75	0.3	4.3535E-05	1.1089E-06	1.3169E-06
38	75	0.4	6.6540E-05	1.0332E-05	1.5176E-06

Data continued for switchgrass/dog food mixture

Time (h)	Initial MC (%)	Height(m)	Bacteria (µg/µg substrate)	Yeast (µg/µg substrate)	Fungi (µg/µg substrate)
38	75	0.5	7.5879E-05	1.7313E-05	6.1396E-06
38	75	0.6	7.7146E-05	2.1164E-05	6.5629E-06
44	75	0.1	1.4107E-05	3.0446E-06	7.9067E-06
44	75	0.2	4.3873E-05	4.4512E-06	4.3024E-06
44	75	0.3	2.0173E-05	3.7325E-06	2.2791E-05
44	75	0.4	9.0607E-06	1.9720E-06	2.6134E-06
44	75	0.5	4.4491E-05	3.0813E-05	2.3000E-05
44	75	0.6	1.4507E-04	2.6105E-05	1.6161E-05
50	75	0.1	4.2595E-05	1.65841E-05	1.0815E-05
50	75	0.2	2.4199E-05	1.2885E-05	3.1051E-06
50	75	0.3	7.8662E-05	2.4303E-05	7.7177E-06
50	75	0.4	1.9801E-04	1.5551E-05	8.4519E-06
50	75	0.5	4.6987E-05	3.3419E-05	1.4634E-05
50	75	0.6	1.5619E-05	1.2820E-04	3.6372E-05
58	75	0.1	5.5384E-05	4.07869E-05	2.4475E-05
58	75	0.2	6.0651E-05	1.9084E-05	1.0578E-05
58	75	0.3	1.5003E-04	1.7244E-05	4.9625E-05
58	75	0.4	2.2276E-04	2.9364E-05	2.9501E-05
58	75	0.5	3.3079E-04	3.6579E-04	4.2737E-05
58	75	0.6	6.6384E-04	1.2232E-04	8.4899E-05
64	75	0.1	4.0205E-05	1.36393E-05	3.9811E-06
64	75	0.2	3.3199E-05	3.7080E-05	2.5700E-06
64	75	0.3	8.3135E-05	2.7312E-05	2.8683E-06
64	75	0.4	5.4248E-05	8.9065E-06	7.1216E-06
64	75	0.5	3.1890E-04	1.5413E-04	1.1058E-05
64	75	0.6	8.2368E-05	7.8013E-05	2.6466E-05
0	65	0.1	1.74905E-05	0.00017808	2.0269E-05
0	65	0.2	1.74905E-05	0.00017808	2.0269E-05
0	65	0.3	1.74905E-05	0.00017808	2.0269E-05
0	65	0.4	1.74905E-05	0.00017808	2.0269E-05
0	65	0.5	1.7491E-05	1.7808E-04	2.0269E-05
0	65	0.6	9.11259E-06	0.00017808	2.0269E-05
8	65	0.1	1.38264E-05	8.3001E-05	2.5067E-05
8	65	0.2	1.5827E-05	0.00011847	3.2447E-05
8	65	0.3	1.80798E-05	0.00013532	2.2059E-05
8	65	0.4	1.85126E-05	0.00019031	3.5236E-05
8	65	0.5	2.1557E-05	1.5411E-04	8.2383E-05
8	65	0.6	1.22879E-05	0.00022507	4.9388E-05
14	65	0.1	9.88218E-06	0.00014468	2.9124E-05
14	65	0.2	1.07671E-05	2.006E-05	1.2424E-05

Data continued for switchgrass/dog food mixture

Time (h)	Initial MC (%)	Height(m)	Bacteria (µg/µg substrate)	Yeast (µg/µg substrate)	Fungi (µg/µg substrate)
14	65	0.3	1.67041E-05	0.00025359	1.9277E-05
14	65	0.4	1.34227E-05	0.00014191	1.6734E-05
14	65	0.5	1.2280E-05	1.3768E-04	2.5135E-05
14	65	0.6	5.99374E-06	0.00019608	1.8622E-05
20	65	0.1	1.87939E-05	0.00015286	1.8159E-05
20	65	0.2	1.59856E-05	8.4654E-05	1.5871E-05
20	65	0.3	1.62743E-05	0.00019763	2.2455E-05
20	65	0.4	1.26864E-05	0.00015872	2.5591E-05
20	65	0.5	2.3543E-05	6.6965E-05	2.0773E-05
20	65	0.6	9.66187E-06	0.00013988	2.0868E-05
26	65	0.1	1.03228E-05	6.8067E-05	1.1421E-05
26	65	0.2	1.5763E-05	4.4533E-05	1.2364E-05
26	65	0.3	7.88745E-06	5.8309E-05	1.589E-05
26	65	0.4	9.81514E-06	6.4595E-05	1.526E-05
26	65	0.5	3.5408E-05	5.6154E-05	2.2157E-05
26	65	0.6	2.1784E-05	5.1493E-05	2.0634E-05
32	65	0.1	3.62342E-05	3.2492E-05	2.9304E-05
32	65	0.2	3.6834E-05	0.00011549	2.6212E-05
32	65	0.3	2.23118E-05	8.2661E-05	8.2027E-06
32	65	0.4	2.67028E-05	9.3865E-05	1.327E-05
32	65	0.5	2.2467E-05	9.8934E-05	9.7340E-05
32	65	0.6	4.72757E-05	0.00014101	3.1692E-05
38	65	0.1	2.7668E-05	7.2482E-05	1.551E-05
38	65	0.2	3.35624E-05	8.4884E-05	1.2023E-05
38	65	0.3	1.71352E-05	0.00015439	5.0322E-06
38	65	0.4	1.50126E-05	2.8766E-05	3.9396E-06
38	65	0.5	2.4495E-05	4.3461E-05	1.2659E-05
38	65	0.6	1.19338E-05	1.614E-05	3.196E-05
44	65	0.1	2.03292E-05	0.00012587	6.0615E-05
44	65	0.2	1.61375E-05	9.3992E-06	9.8551E-06
44	65	0.3	8.081E-06	0.00020224	1.1682E-05
44	65	0.4	1.41015E-05	0.00015273	2.562E-05
44	65	0.5	7.2156E-05	3.7046E-05	2.1599E-05
44	65	0.6	5.75885E-06	2.223E-05	1.9789E-05
50	65	0.1	9.46813E-06	7.2851E-06	1.7632E-05
50	65	0.2	7.9785E-06	3.4056E-05	1.2225E-05
50	65	0.3	4.22366E-06	1.9666E-05	1.5033E-05
50	65	0.4	3.77541E-05	1.8212E-05	3.0334E-05
50	65	0.5	3.0064E-05	7.2149E-05	2.6342E-05
50	65	0.6	1.31335E-05	2.4155E-05	2.0167E-05

Data continued for switchgrass/dog food mixture

Time (h)	Initial MC (%)	Height(m)	Bacteria (µg/µg substrate)	Yeast (µg/µg substrate)	Fungi (µg/µg substrate)
58	65	0.1	4.8861E-04	2.5707E-04	5.3027E-06
58	65	0.2	4.6753E-05	1.9406E-03	1.8952E-05
58	65	0.3	3.8602E-05	4.0048E-05	1.5757E-05
58	65	0.4	5.0960E-05	1.4151E-04	1.4243E-05
58	65	0.5	5.5417E-05	1.4207E-05	1.5191E-05
58	65	0.6	1.86975E-05	1.9275E-05	2.3663E-05
64	65	0.1	2.46475E-06	4.7995E-06	8.5985E-06
64	65	0.2	4.15599E-06	0.00014707	7.8173E-06
64	65	0.3	3.5786E-05	6.2527E-05	1.0079E-05
64	65	0.4	0.000100434	0.00015709	2.199E-05
64	65	0.5	2.5602E-05	1.5074E-04	4.1797E-05
64	65	0.6	8.71397E-05	3.5374E-05	3.1693E-05
0	60	0.1	7.47225E-06	0.000272578	3.50641E-05
0	60	0.2	7.47225E-06	0.000272578	3.50641E-05
0	60	0.3	7.47225E-06	0.000272578	3.50641E-05
0	60	0.4	7.47225E-06	0.000272578	3.50641E-05
0	60	0.5	7.47225E-06	0.000272578	3.50641E-05
0	60	0.6	7.47225E-06	0.000272578	3.50641E-05
8	60	0.1	2.47628E-05	6.08098E-05	2.67811E-05
8	60	0.2	1.82366E-05	0.000174206	2.92431E-05
8	60	0.3	1.6584E-05	0.000235286	6.71491E-05
8	60	0.4	1.79615E-05	0.000182956	5.7162E-05
8	60	0.5	2.13149E-05	0.000131686	4.30622E-05
8	60	0.6	1.2498E-05	0.000150757	1.37264E-05
14	60	0.1	1.8015E-05	0.000140129	4.10791E-05
14	60	0.2	1.15008E-05	0.000140797	1.94903E-05
14	60	0.3	2.08069E-05	3.46113E-05	3.05719E-05
14	60	0.4	8.48452E-06	4.76019E-05	2.69045E-05
14	60	0.5	9.38593E-06	6.3297E-05	1.66417E-05
14	60	0.6	1.46236E-05	3.26552E-05	1.26713E-05
20	60	0.1	1.81111E-05	0.00022322	1.86385E-05
20	60	0.2	1.19888E-05	0.000119562	1.01195E-05
20	60	0.3	1.16956E-05	6.66294E-05	1.38021E-05
20	60	0.4	2.03278E-05	4.72897E-05	1.09427E-05
20	60	0.5	1.62146E-05	2.69576E-05	1.09453E-05
20	60	0.6	1.19868E-05	2.07595E-05	1.91365E-05
26	60	0.1	2.40816E-05	5.54719E-05	9.79577E-06
26	60	0.2	3.16218E-05	0.000156075	4.25939E-06
26	60	0.3	3.2056E-05	4.74719E-05	1.23051E-05
26	60	0.4	1.42442E-05	1.70418E-05	9.61672E-06

Data continued for switchgrass/dog food mixture

Time (h)	Initial MC (%)	Height(m)	Bacteria (µg/µg substrate)	Yeast (µg/µg substrate)	Fungi (µg/µg substrate)
26	60	0.5	1.64685E-05	2.11631E-05	1.70783E-05
26	60	0.6	1.27198E-05	1.2245E-05	1.36531E-05
32	60	0.1	1.79016E-05	0.000163493	1.31623E-05
32	60	0.2	1.34773E-05	3.94352E-05	1.39987E-05
32	60	0.3	3.69088E-05	1.73536E-05	1.00502E-05
32	60	0.4	2.40586E-05	1.93374E-05	5.61569E-06
32	60	0.5	3.31182E-05	2.92458E-05	9.20926E-06
32	60	0.6	4.05055E-05	2.98409E-05	4.34065E-06
38	60	0.1	2.40512E-05	0.00025169	1.96719E-05
38	60	0.2	1.67198E-05	0.00041341	2.19314E-05
38	60	0.3	2.13355E-05	0.001313092	2.86866E-05
38	60	0.4	1.70056E-05	0.000159305	2.10277E-05
38	60	0.5	2.53229E-05	6.46559E-05	5.59141E-05
38	60	0.6	3.0583E-05	8.5623E-06	4.26936E-05
44	60	0.1	1.83798E-05	0.000103511	2.72284E-05
44	60	0.2	1.81584E-05	0.000222968	2.1635E-05
44	60	0.3	1.20051E-05	0.000359266	2.59037E-05
44	60	0.4	1.30349E-05	3.75445E-05	2.08561E-05
44	60	0.5	1.94728E-05	0.000127422	1.73735E-05
44	60	0.6	4.0742E-05	9.1305E-06	2.29474E-05
50	60	0.1	1.72799E-05	4.47047E-05	3.27859E-05
50	60	0.2	1.03666E-05	9.00198E-05	2.4314E-05
50	60	0.3	3.3500E-05	2.3050E-05	3.6576E-05
50	60	0.4	5.2449E-05	2.0297E-05	2.6597E-05
50	60	0.5	1.0017E-04	7.1326E-05	3.4149E-05
50	60	0.6	1.7051E-04	8.3547E-05	2.66733E-05
58	60	0.1	2.9468E-05	5.1414E-05	1.8499E-05
58	60	0.2	3.3769E-05	2.7209E-05	7.4973E-06
58	60	0.3	6.5151E-05	3.8895E-05	7.6086E-05
58	60	0.4	6.4195E-05	1.6257E-05	1.6199E-05
58	60	0.5	1.0636E-04	1.0663E-04	2.6856E-05
58	60	0.6	8.5116E-05	1.9629E-05	2.6446E-05
64	60	0.1	4.95952E-06	0.000447969	2.37853E-05
64	60	0.2	1.14967E-05	0.00013248	1.96551E-05
64	60	0.3	1.99101E-05	0.000778551	2.41028E-05
64	60	0.4	5.4552E-05	1.2179E-04	1.1907E-05
64	60	0.5	5.2701E-05	9.5640E-05	1.9047E-05
64	60	0.6	2.80825E-05	1.99672E-05	2.07875E-05

Data for switchgrass/nitrogen fertilizer mixture which had an initial moisture content of 63%

Time (h)	Height(m)	Temperature (^{o}C)	pH	MC (%)	O_2 (%)	CO_2 (%)
0	0.1	22.504	6.57	63.56	18.65	1.15
0	0.3	20.891	6.57	63.56	18.65	1.15
0	0.6	24.045	6.57	63.56	18.65	1.15
8	0.1	29.339	8.24	62.07	17.30	1.91
8	0.3	41.562	8.46	63.16	17.30	1.91
8	0.6	62.537	8.52	63.56	17.30	1.91
16	0.1	25.321	8.74	61.02	17.33	1.70
16	0.3	36.241	8.91	61.66	17.33	1.70
16	0.6	57.753	8.86	64.26	17.33	1.70
24	0.1	25.067	8.23	61.20	17.96	1.03
24	0.3	32.363	8.66	60.69	17.96	1.03
24	0.6	50.104	8.77	63.20	17.96	1.03
32	0.1	24.928	8.70	58.84	18.27	0.75
32	0.3	30.836	9.02	58.78	18.27	0.75
32	0.6	45.071	9.04	60.93	18.27	0.75
40	0.1	23.835	8.87	59.95	18.50	0.61
40	0.3	28.695	9.01	63.36	18.50	0.61
40	0.6	41.837	8.94	64.07	18.50	0.61
48	0.1	23.026	8.90	60.43	18.53	0.52
48	0.3	26.801	9.10	60.58	18.53	0.52
48	0.6	38.951	9.29	65.46	18.53	0.52
56	0.1	22.424	8.95	59.25	18.65	0.47
56	0.3	25.827	9.11	60.27	18.65	0.47
56	0.6	36.519	9.07	54.07	18.65	0.47
64	0.1	22.078	8.88	57.81	18.73	0.43
64	0.3	25.056	9.08	59.63	18.73	0.43
64	0.6	35.018	9.16	66.65	18.73	0.43
72	0.1	21.149	8.97	58.91	18.72	0.24
72	0.3	23.331	8.97	61.64	18.72	0.24
72	0.6	32.722	8.98	65.29	18.72	0.24
80	0.1	20.942	9.31	59.35	18.84	0.20
80	0.3	22.598	9.20	62.37	18.84	0.20
80	0.6	30.231	9.37	64.02	18.84	0.20
88	0.1	20.811	9.11	56.65	18.83	0.17
88	0.3	22.234	9.29	58.90	18.83	0.17
88	0.6	29.081	9.30	62.49	18.83	0.17
96	0.1	20.804	8.90	57.51	18.86	0.18
96	0.3	22.145	8.88	58.68	18.86	0.18
96	0.6	28.402	9.06	64.45	18.86	0.18

Data continued for switchgrass/nitrogen fertilizer mixture

Time (h)	Height(m)	Cellulose degradation ratio (%)	Hemicellulose degradation ratio (%)	Lignin degradation ratio (%)
0	0.1	0	0	0
0	0.3	0	0	0
0	0.6	0	0	0
8	0.1	31.22065728	24.51790634	5.633802817
8	0.3	31.22065728	24.51790634	5.633802817
8	0.6	31.22065728	24.51790634	5.633802817
16	0.1	28.87323944	16.80440771	14.08450704
16	0.3	34.27230047	14.87603306	2.816901408
16	0.6	33.56807512	20.93663912	2.816901408
24	0.1	28.87323944	22.58953168	11.26760563
24	0.3	34.50704225	18.18181818	38.02816901
24	0.6	32.86384977	19.00826446	16.90140845
32	0.1	27.69953052	26.99724518	16.90140845
32	0.3	24.64788732	20.66115702	25.35211268
32	0.6	28.16901408	19.55922865	18.30985915
40	0.1	30.51643192	26.99724518	
40	0.3	25.58685446	25.34435262	
40	0.6	25.82159624	19.28374656	
48	0.1	27.23004695	27.27272727	36.61971831
48	0.3	30.51643192	30.85399449	42.25352113
48	0.6	35.91549296	25.34435262	15.49295775
56	0.1	22.0657277	23.96694215	22.53521127
56	0.3	27.23004695	22.31404959	23.94366197
56	0.6	28.16901408	25.34435262	26.76056338
64	0.1	22.53521127	20.11019284	
64	0.3	26.5258216	23.69146006	
64	0.6	30.98591549	23.41597796	
72	0.1	30.51643192	21.21212121	
72	0.3	21.59624413	24.79338843	32.3943662
72	0.6	20.18779343	39.66942149	23.94366197
80	0.1	23.70892019	22.58953168	
80	0.3	28.16901408	20.66115702	
80	0.6	19.48356808	30.02754821	
88	0.1	23.00469484	25.8953168	35.21126761
88	0.3	21.12676056	30.85399449	23.94366197
88	0.6	17.6056338	30.85399449	19.71830986
96	0.1	28.63849765	25.06887052	19.71830986
96	0.3	18.07511737	26.99724518	18.30985915
96	0.6	21.12676056	38.01652893	16.90140845

Data continued for switchgrass/nitrogen fertilizer mixture. Microbial data in the following table has units of **copy number / g dry weight compost**

Time (h)	**Height(m)**	**Bacteria**	**Fungi**	***Aspergillus spp.***	**Lactic acid bacteria**
0	0.1	6.91E+01	1.42E+00	3.73415E-06	1.53E+06
0	0.3	6.91E+01	1.42E+00	3.73415E-06	1.53E+06
0	0.6	6.91E+01	1.42E+00	3.73415E-06	1.53E+06
8	0.1		4.00E-01	6.95E-01	2.60E+02
8	0.3	3.94E-04	4.34E+00	1.25E+02	1.83E+06
8	0.6	2.75E+03	4.12E-03	7.47E-07	5.36E+06
16	0.1	3.95E+07	6.81E-02	4.89E-02	1.29E+02
16	0.3	5.41E+02	5.35E-02	5.12E+01	1.92E+01
16	0.6	9.39E+00	3.63E+01	7.86E-01	1.16E+05
24	0.1	3.36E-04	5.21E+02	7.24E+02	2.34E+01
24	0.3	4.90E+04	1.14E+00	1.00E-05	2.26E+01
24	0.6	1.60E-02	6.30E+04	2.02E-02	1.23E+04
32	0.1	1.13E+05	9.94E-02	n/a	7.99E+01
32	0.3	6.22E+01	1.54E+00	7.66E+01	1.29E+05
32	0.6	3.05E+01	2.99E+02	6.65E-02	9.29E+00
40	0.1	6.17E-04	4.40E+01	7.78E+02	1.01E-01
40	0.3	4.64E+06	1.61E+01	6.95E+03	1.31E-01
40	0.6	5.26E-02	6.87E+03	1.32E+01	1.13E+07
48	0.1	1.04E+05	3.10E+05	5.21E-02	9.61E+03
48	0.3	3.11E+04	1.61E-01	1.49E-02	1.04E+03
48	0.6	4.12E+01	n/a	6.68E-03	3.76E+06
56	0.1	2.79E+05	9.63E-02	1.43E+03	3.00E+01
56	0.3	4.71E+07	6.71E+03	8.75E-01	6.94E+05
56	0.6	1.09E+03	6.00E-01	1.32E+01	1.48E+02
64	0.1	4.24E+01	3.43E+02	9.45E-01	1.13E+00
64	0.3	5.36E+05	1.37E+02	5.23E+01	5.24E-02
64	0.6	7.07E+04	9.56E+00	5.25E-02	8.38E+04
72	0.1	5.38E-04	3.58E-01	5.77E+01	n/a
72	0.3	3.74E-01	4.19E+01	1.08E+04	9.99E+05
72	0.6	2.32E+03	3.76E-01	4.43E-02	1.70E+02
80	0.1	7.56E+02	4.32E+02	4.06E+02	6.34E+03
80	0.3	2.24E+02	7.22E+02	5.77E+01	7.94E+11
80	0.6	1.71E+04	3.12E+00	3.79E+02	8.22E+03
88	0.1	8.70E+04	4.76E-02	4.11E-02	2.17E+03
88	0.3	2.47E+07	4.18E+01	5.91E+00	3.89E+05
88	0.6	6.01E+00	5.87E-01	7.79E+00	8.61E-01
96	0.1	1.71E+05	3.62E+02	7.78E+02	1.56E+01
96	0.3	1.25E+07	3.47E+01	5.19E+02	1.11E+07
96	0.6	6.58E+02	3.25E+01	7.12E-02	1.24E+04

Data continued for switchgrass/nitrogen fertilizer mixture

Time (h)	Height(m)	Acetic acid conc. (mM)	Propionic acid (mM)	Isobutyric acid (mM)	Butyric acid (mM)
0	0.1	0.373	0.002	0.000	0.000
0	0.3	0.373	0.002	0.000	0.000
0	0.6	0.373	0.002	0.000	0.000
8	0.1	0.093	0.000	0.000	0.000
8	0.3	0.062	0.000	0.000	0.000
8	0.6	0.047	0.000	0.000	0.000
16	0.1	0.107	0.000	0.000	0.000
16	0.3	0.053	0.000	0.000	0.000
16	0.6	0.007	0.000	0.000	0.000
24	0.1	0.258	0.066	0.000	0.009
24	0.3	0.166	0.049	0.000	0.001
24	0.6	0.119	0.037	0.000	0.000
32	0.1	0.129	0.015	0.000	0.000
32	0.3	0.147	0.004	0.000	0.000
32	0.6	0.000	0.000	0.000	0.000
40	0.1	0.066	0.000	0.000	0.000
40	0.3	0.078	0.000	0.000	0.000
40	0.6	0.000	0.000	0.000	0.000
48	0.1	0.063	0.000	0.000	0.045
48	0.3	0.051	0.000	0.000	0.039
48	0.6	0.019	0.000	0.000	0.039
56	0.1	0.127	0.130	0.087	0.189
56	0.3	0.188	0.151	0.070	0.173
56	0.6	0.181	0.096	0.053	0.186
64	0.1	0.443	0.061	0.000	0.094
64	0.3	0.427	0.067	0.000	0.088
64	0.6	0.310	0.058	0.000	0.124
72	0.1	0.210	0.046	0.000	0.039
72	0.3	0.245	0.025	0.000	0.031
72	0.6	0.184	0.036	0.000	0.067
80	0.1	0.056	0.074	0.000	0.097
80	0.3	n/a	n/a	n/a	n/a
80	0.6	n/a	n/a	n/a	n/a
88	0.1	0.007	0.000	0.000	0.000
88	0.3	0.049	0.000	0.000	0.000
88	0.6	0.060	0.000	0.000	0.000
96	0.1	0.000	0.001	0.000	0.000
96	0.3	0.046	0.000	0.000	0.000
96	0.6	0.000	0.000	0.000	0.000

Data continued for switchgrass/nitrogen fertilizer mixture

Time (h)	Height(m)	Isovaleric acid conc. (mM)	Valeric acid (mM)	Isocaproic acid (mM)	Caproic acid (mM)
0	0.1	0.000	0.000	0.000	0.000
0	0.3	0.000	0.000	0.000	0.000
0	0.6	0.000	0.000	0.000	0.000
8	0.1	0.000	0.000	0.000	0.000
8	0.3	0.000	0.000	0.000	0.000
8	0.6	0.000	0.000	0.000	0.000
16	0.1	0.000	0.000	0.000	0.000
16	0.3	0.000	0.000	0.000	0.000
16	0.6	0.000	0.000	0.000	0.000
24	0.1	0.000	0.001	0.002	0.000
24	0.3	0.000	0.000	0.000	0.000
24	0.6	0.000	0.000	0.000	0.000
32	0.1	0.000	0.000	0.000	0.000
32	0.3	0.000	0.000	0.000	0.000
32	0.6	0.000	0.000	0.000	0.000
40	0.1	0.000	0.000	0.000	0.000
40	0.3	0.000	0.000	0.000	0.000
40	0.6	0.000	0.000	0.000	0.000
48	0.1	0.000	0.020	0.104	0.009
48	0.3	0.000	0.014	0.098	0.003
48	0.6	0.000	0.011	0.101	0.000
56	0.1	0.000	0.071	0.046	0.086
56	0.3	0.000	0.101	0.041	0.054
56	0.6	0.000	0.075	0.036	0.117
64	0.1	0.000	0.050	0.041	0.016
64	0.3	0.000	0.025	0.007	0.028
64	0.6	0.000	0.037	0.005	0.018
72	0.1	0.000	0.002	0.000	0.012
72	0.3	0.000	0.002	0.000	0.013
72	0.6	0.000	0.007	0.000	0.022
80	0.1	0.000	0.028	0.091	0.001
80	0.3	n/a	n/a	n/a	n/a
80	0.6	n/a	n/a	n/a	n/a
88	0.1	0.000	0.000	0.000	0.000
88	0.3	0.000	0.000	0.000	0.000
88	0.6	0.000	0.000	0.000	0.000
96	0.1	0.000	0.000	0.000	0.000
96	0.3	0.000	0.000	0.000	0.000
96	0.6	0.000	0.000	0.000	0.000

Data continued for switchgrass/nitrogen fertilizer mixture

Time (h)	Height(m)	Heptanoic acid conc. (mM)	Extracted DNA conce. (µg/ml)
0	0.1	0.000	321.333
0	0.3	0.000	321.333
0	0.6	0.000	321.333
8	0.1	0.000	784.250
8	0.3	0.000	356.000
8	0.6	0.000	208.000
16	0.1	0.000	349.500
16	0.3	0.000	334.000
16	0.6	0.000	195.250
24	0.1	0.019	817.500
24	0.3	0.011	546.250
24	0.6	0.006	401.250
32	0.1	0.000	646.250
32	0.3	0.000	336.750
32	0.6	0.000	394.500
40	0.1	0.000	601.667
40	0.3	0.000	405.167
40	0.6	0.000	416.000
48	0.1	0.191	684.750
48	0.3	0.077	414.333
48	0.6	0.026	331.750
56	0.1	0.081	659.667
56	0.3	0.081	401.833
56	0.6	0.073	327.250
64	0.1	0.063	717.250
64	0.3	0.047	1026.250
64	0.6	0.065	557.000
72	0.1	0.048	430.000
72	0.3	0.043	665.500
72	0.6	0.042	481.833
80	0.1	0.048	841.250
80	0.3	n/a	326.250
80	0.6	n/a	769.750
88	0.1	0.000	1476.500
88	0.3	0.000	271.750
88	0.6	0.000	425.167
96	0.1	0.000	548.000
96	0.3	0.000	532.500
96	0.6	0.000	1151.000